Electric Technology U.S.S.R.

ЭЛЕКТРИЧЕСТВО

Volume 2, April, 1959

Selected papers from *Elektrichestvo* Nos. 5 and 6, 1958

Published by

PERGAMON PRESS N

or Pergamon Institute, New York and

ELECTRIC TECHNOLOGY, U.S.S.R.

PERGAMON INSTITUTE

A NON-PROFIT FOUNDATION FOR THE FURTHERANCE
AND DISSEMINATION OF SCIENTIFIC KNOWLEDGE

President of the Board of Governors:

Sir Robert Robinson, O.M., F.R.S.

Executive Director: Captain I. R. Maxwell

4 & 5 Fitzroy Square, London W.1
122 East 55th Street, New York 22, N.Y.

Pergamon Institute can occasionally use additional translators for science and engineering material to assist with this programme of translation from Russian and other Slavonic languages.

Scientists and engineers who have a knowledge of Russian, and who are willing to assist with this work, should apply to the Administrative Secretary of the Institute. They should write to either New York or London for rates of payment and other details.

Financial assistance has also been received from A.S.E.A., Sweden

---

Four volumes per annum. Approximately 700 pages per annum.
Annual Subscription Rate £20 ($56).
Single volumes may be purchased for £6 ($14).

Orders should be sent to the distributors at either of the following addresses

4 & 5 Fitzroy Square, London W.1

122 East 55th Street, New York 22, N.Y.

PUBLISHED BY

PERGAMON PRESS LTD.
LONDON · NEW YORK · PARIS · LOS ANGELES

April 1959

THE HIGH-POWER HIGH-VOLTAGE RECTIFIER*

F.I. BUTAEV, N.S. KLIMOV, M.F. KOSTROV and A.A. SAKOVICH

All-Union Lenin Electrotechnical Institute

(Received 5 November 1957)

Directives of the XXth congress of the Communist Party of the Soviet Union envisage power transmission at high direct voltage; for this purpose during the next five years the d.c. transmission line between Stalingrad Hydro-Electric Station and the Donbas should be put into operation. The electrical industry should develop and manufacture the equipment for this line. Putting into effect this decision of the Party, the Board of the All-Union Lenin Electrotechnical Institute (VEI) has developed a high-power high-voltage rectifier for the converter substations of the d.c. transmission line.

Work on the development of high-voltage rectifiers began long ago in the U.S.S.R. and abroad.

In Sweden, work on the development of high-voltage rectifiers has been carried out since 1929. A rectifier with two parallel-working anodes, each anode designed for a maximum current of 100 A and a voltage of 65 kV, has been constructed.

In Germany the AEG and Siemens Cos. have been working for a long time on the development of high-voltage rectifiers. The AEG Co. has developed a rectifier for a voltage of 120 kV and a maximum current of 150 A, and the Siemens Co. has developed rectifiers for a still higher voltage but for the same current. The former rectifiers were to be connected, three in series, into an arm of a 220 kV bridge and the latter were to be connected two-in series into an arm of a bridge of the same type.

High-voltage rectifiers of a multianode construction have been designed by the B.B.C. but the work of this firm resulted in no practical solution.

In other foreign countries the achievements in the development of high-voltage rectifiers are even less significant.

In the Soviet Union before the war, work was carried out on these rectifiers

* *Elektrichestvo* No. 5, 1-7, 1958.

in the VEI laboratories (Larionov and Krauz in 1937, Klimov in 1938-39 and Galdin in 1940). The result of this work led to the development and testing of the following devices: a rotary d.c. machine for 80 kV, 5 kW, an ionic-mechanical convertor for 10 kV, 100 kW and a six-anode mercury rectifier for 25 kV, 100 A, with an intermediate electrode, a shield in the anode assembly and also aluminium seals.

Large scale work on the development of high-power high-voltage rectifiers began in our country after the war.

During the first years after the war, high-voltage rectifiers and control gears were developed for the first experimental d.c. transmission line from Kashira HEPS* to Moscow. This work started and to a considerable extent was accomplished by the scientific and technical office of the former Ministry of the Electrical Industry, with the co-operation of prominent German experts (Dobke, Chelters and others). In addition, the following investigations on models were performed in this office: a system of control from the earth potential of all rectifiers of the substation with the use of a double impulse; a d.c. transformer; substation protection with a pick-up device and the use of a shunting rectifier. Investigations were also carried out on the method of damping spurious oscillation processes.

Numerous investigations and tests of rectifiers were performed on various test benches and installations of the VEI.

As a result of this work a batch of 30 rectifiers of the VR-1 (which passed the tests) and their control panels were made by the scientific and technical office, and partly by the experimental factory of the VEI; in the second half of 1950 they were delivered to the Ministry of Power Stations for the substation equipment of the experimental transmission line.

During the adjustment of the experimental d.c. transmission line, the VEI jointly with the Institute of Direct Current carried out tests on rectifiers under normal service conditions.

On an equivalent circuit in the VEI, where normal conditions for rectifiers are produced, the probability of backfires was determined: on the average one backfire in 24 hours occurred. The recovery time of the controlling capacity of the grid was equal to 2 el deg. at a cooling-oil temperature of 16°, and a rise in the anode voltage of 70 kV.

The investigation of the flashover and the anode insulator showed, that the distribution of the potential along the external part of the insulator was uniform: In the case of flashover between the intermediate electrodes (between all or a part of them) the distribution of the potential outside becomes very irregular, and this brings about an increase in the field intensity which causes flashover along

* Hydro-electric Power Station.

the insulator. This probably happens owing to the fact that the speed of discharge formation in vacuum is considerably smaller than the corresponding speed in air.

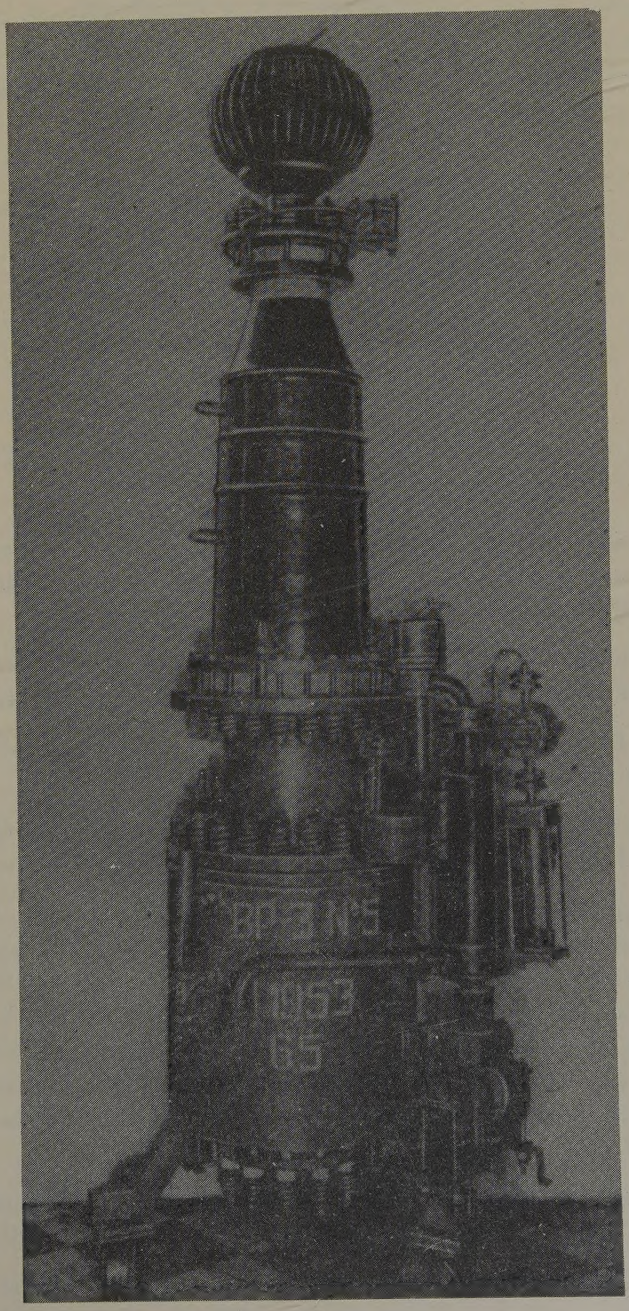

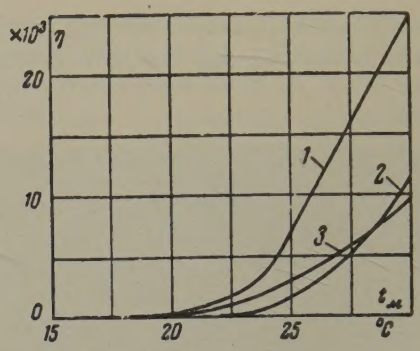

FIG. 2. The relationship between the arcing back frequency and the valve cooling temperature, revealed by the pulse counter (Gorev and Kingdon-Lawton circuit).
1 – valve VR-1 ($\frac{di}{dt} = 2.10^6$ A/sec, U_{pr} 150 kV);
2 – valve VR-3 ($\frac{di}{dt} = 1.27.10^7$ A/sec, $U_{pr} = 160$ kV); valve VR-9.

In the case of ignition failure, when one of the intermediate electrodes begins acting as a grid, a violent distortion of the potential distribution takes place on the insulator, which may cause the insulator flashover.

The problem of the possibility of breaking a small anode current (up to 0.5 A) by a grid was investigated and it was found that such a possibility existed.

In 1950-51 work was performed in the VEI in order to increase the power of rectifiers for the experimental transmission line.

The rectifier (Type VR-3) for maximum current 300 A and maximum voltage 130 kV was developed (Fig. 1). Twelve of these rectifiers were constructed.

Investigations and tests showed that these rectifiers have a considerably greater electric strength than the first rectifiers for the experimental transmission line, with ratings: maximum current 150 A and maximum voltage 120 kV. Thus a static electric strength of this rectifier without ageing was 160 kV of the effective value, and in the case when the external ohmic potential divider was connected, this voltage was increased to 205 kV, which corresponds to a maximum voltage of 290 kV. High peak inverse anode voltage of this rectifier can be seen from curve (2) in Fig. 2.

Operation of high power rectifiers in the experimental transmission line network showed that sputtering in the anode assembly is insignificant.

In 1952 work was begun in the VEI on the development of high-power high-voltage rectifiers with a maximum voltage of 130 kV and a maximum current of

rectifier), 5, 4, 3, 2 and 1 (Andree's design) intermediate electrodes were built and tested under varying conditions.

These investigations have shown that with an increased number of intermediate electrodes, the peak inverse anode voltage and the electric strength increase; the sputtering and poisoning of the anode decrease, but the losses also increase and arcing is hampered. With a decreased number of intermediate

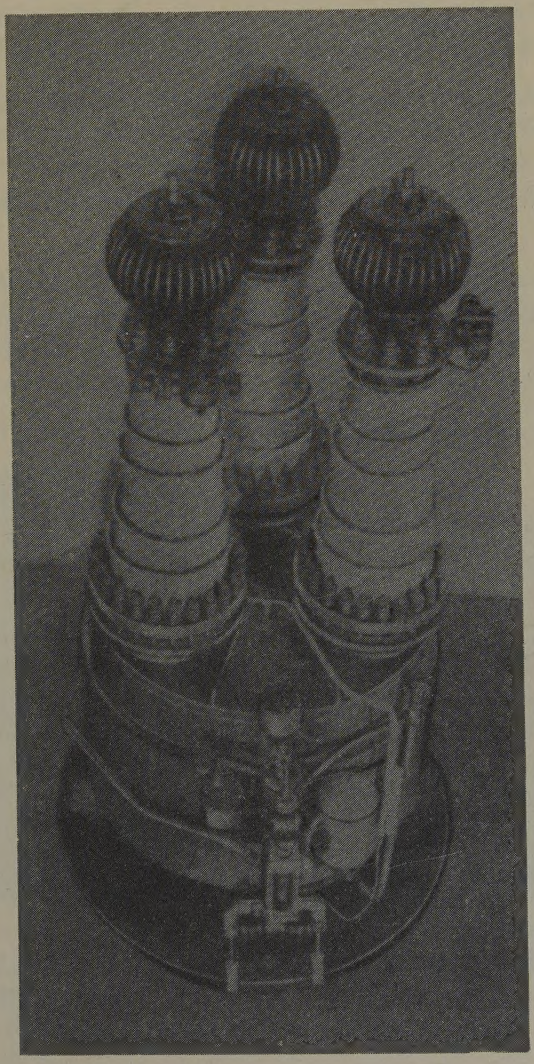

FIG. 3.

900 A, which had to be connected in series into an arm of a bridge circuit. To develop such a rectifier, suitable for industrial transmission, it was necessary to perform exhaustive research work and to answer many major problems.

It was necessary to decide whether the rectifier had to be a single-anode or multi-anode one. Many experts in our country and abroad denied the possibility of obtaining high power in a single anode because of a danger of concentrating a discharge on a small section, which may disturb the working of the rectifier. It was difficult to give a single well-founded answer to this question solely on a theoretical basis. Therefore, work was carried out in the VEI on the development of single-anode and multi-anode rectifiers, and experimental models were made.

Fig. 3 shows a three-anode rectifier for maximum voltage of 130 kV and a maximum current of 750 A made in 1952. A current divider between the three parallel working anodes was developed and made for this rectifier. The rectifier proved to be very cumbersome, unwieldy in assembling, handling and rather unreliable.

The comparison of the designs of three-anode and single-anode rectifiers showed the incontestable superiority of the latter. Nevertheless, it remained to be proved that the difficulties connected with the concentration of discharge on a small section could be overcome.

For this purpose, the current distribution on the anode and grid surfaces was investigated.

The current distribution proved relatively uniform on an anode with a diameter of a few hundred millimetres. Edges of the anode were less loaded.

Fig. 4 shows a typical curve of the mean distribution of the current on the anode (ion current on probe, measured by a magneto-electric device). The distribution of the instantaneous current (Fig. 5) shows that the arc column moves from place to place with a considerable speed. This speed increases with the increase of current. At every given point the current varies within wide limits, and these oscillations increase from the centre of the anode towards its periphery.

Investigations on the current distribution have shown that:

(a) the whole end surface of the anode works, although not quite uniformly;
(b) the whole surface of the anode is heated;
(c) the drop in the current density is smaller in the anode of a larger diameter than in the smaller one. Therefore, if it is desirable to increase the rectifier current, it is advisable to increase the anode diameter.

On the basis of these investigations a single-anode rectifier was adopted.

It was decided to determine the optimum number of intermediate electrodes for the anode assembly. Experimental models of rectifiers with 15 (Kesaev's

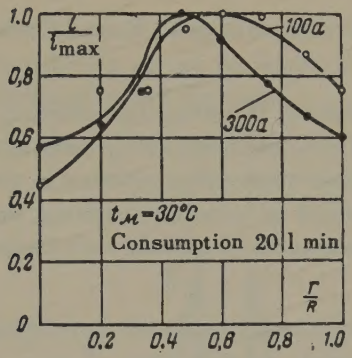

FIG. 4

electrodes, the inverse phenomena are observed. The number of intermediate electrodes was chosen to obtain the maximum advantage and the fewest possible defects.

The next important problem was the choice of the geometrical shape and the distribution of intermediate electrodes. The ring-shaped, shutter-type, conical, overlapping, radial, grid and other electrodes were considered. On the basis of the experiments performed, the electrodes that showed the best results were used on the majority of rectifiers.

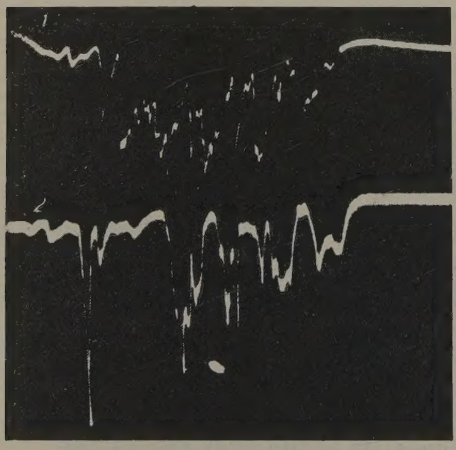

FIG. 5. Oscillograms of current distribution over the anode (ionic current on a sonde) 1 – in the centre (R = 0); 2 – at the edge (R = 1).

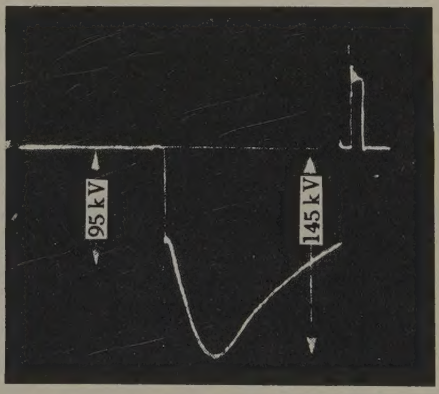

FIG. 6

Operational experience will enable us to choose the best geometrical shape of the intermediate electrodes.

Extensive work was performed in testing the materials used in the manufacture of high-voltage rectifiers, and particularly materials for the main and control electrodes, and for other components situated in the discharge zone. Materials were tested with regard to backfires, gassing, sputtering and other properties. As a result of these tests, materials were chosen for the various rectifier components.

Special vacuum technical installations were developed, constructed and put into operation in 1951-52; namely vacuum ovens of large capacity, benches for technical finishing and vacuum testing of the individual assembles of the rectifier, special heaters, etc.

Special test installations were built: an equivalent circuit, which allows rectifiers to be tested at the maximum current of 1000 A and maximum voltage of 160 kV (the shape of the curve for the anode-cathode potential is shown on Fig. 6); an impulse installation for 350 kV; benches for the low tension tests and others. For the overload tests the shock circuit of the high tension section of the VEI was used; this circuit was designed for testing air circuit-breakers.

The construction of high-power high-voltage rectifiers differs considerably from the construction of rectifiers that are normally used in industry and traction.

Fig. 7 shows a diagramatical section of such a rectifier (Type VR-9/3) for maximum current 900 A and maximum voltage 130 kV. The main parts of the rectifier are: the anode, which is cooled by a special cooler; the anode insulator with auxiliary inleads; the tank with a cooling jacket; the cathode; the anode high-voltage assembly, the low-voltage assembly and the cooled cathode cap.

The heat developed in the rectifier is partly carried away by the cooling liquid, and is partly dissipated in air by the cooling fins of the tank and of the cooler, and also by the insulator surface. The heat of the anode head is carried away towards the cooler surface by the mercury vapour, which is formed inside the vacuum chamber of the cooler.

The intermediate electrodes are situated between the anode and the low-voltage assembly. The low-voltage assembly consists of two grids and a filter. The excitation anodes also form a part of this assembly. On the cathode, which is filled with mercury, two quarts baffles and the slot ignitor are situated.

Although the cathode is liquid cooled, natural air cooling is also sufficient The rectifier tank is provided with a cooling jacket with a directing spiral. To increase the cooling surface one model of the rectifier was provided with a spiral tube. A cooled cathode cap is used for the following purpose: to increase

cooling, to decrease the pressure of mercury vapour and to ensure its uniformity, to improve the current distribution across the anode and grid assemblies. The cooling liquid (oil) is circulated round the cap.

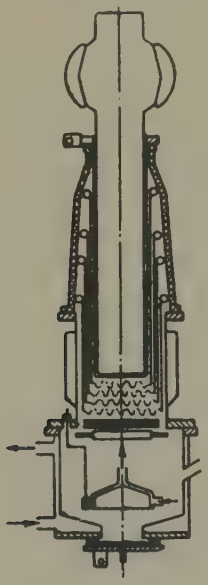

FIG. 7.

The rectifier is evacuated by an oil and a mercury pump. A high-vacuum electromagnetic tap, remote controlled electrically, is situated on the exhaust pipe. Fig. 8 shows a general view of the rectifier.

The control panel is provided with many improvements (remote control, light control), which increases the service reliability at high voltage and facilitate the operation of the installation.

The design of the control panel and some other problems are not discussed in this article, because they will be discussed separately.

Since 1952, 25 models of high-power rectifiers of different types and varieties have been constructed. These rectifiers underwent exhaustive investigations and tests. Some results of these tests are discussed later.

The electric strength of the rectifier is sufficiently high. During the static tests it withstands the effective voltage of 140-160 kV without the external divider. The use of the external divider increases the electric strength.

The peak inverse anode voltage of this rectifier is higher than that of rectifiers used in the experimental transmission installation. The results of one of the tests of the peak inverse anode voltage of a high-power rectifier, recorded

on an impulse installation, are shown on Fig. 2 (curve 3).

The density of the mercury vapour and the vapour dynamics are of great importance for the operation of the rectifier. To obtain the necessary density of mercury vapour was a very difficult problem. The investigation of the state of the mercury vapour was carried out by the probe methods developed in the gas discharge laboratories of the VEI. It has been shown that with oil cooling the density of the mercury vapour did not correspond to the temperature of the outcoming oil and that there was a difference between the temperature, corresponding to the vapour density, and the temperature of the outcoming oil. With different methods of oil cooling this temperature difference may vary from plus a few tens of degrees to minus a few degrees. For example, Fig. 9 shows curves of the variation in the temperature differences in relation to the current load of the rectifier for two different systems of cooling: the tank with a spiral tube (curve 1) and the tank with a spiral tube and a cooled cathode cap (curve 2). On comparing these curves the very strong influence of the cooled cathode cap on the vapour pressure in the rectifier becomes apparent.

Electrical tests at full current and voltage values were performed on the equivalent circuit made in the VEI for maximum current up to 1000 A and maximum voltage up to 160 kV. These tests provided very valuable information.

It was found that the occurence of backfires at the maximum back-voltage of about 135 kV and maximum current 900 A is less than one backfire every 24 hr. The rate of current decrease was 1×10^6 A/sec, the jump in the back voltage was 90 kV, and the voltage increased at a rate of 40 kV/°C.

The investigations have shown that besides loss of the control action of the grids, direct breakdown also occurred. By direct breakdown we mean such a phenomenon, when, in the pressure of a positive anode potential, a cathode spot appears on the upper grid and the current flows towards the cathode, avoiding the discharge gap the upper grid (cathode). The frequency of direct breakdown does not exceed the frequency of back-fires.

The stability of the excitation arc plays a very important role in rectifier operation. It has been found that the principal causes of the extinction of the excitation arc are: short circuiting of the tank with the cathode by mercury streams; the presence of insulating particles at the bottom of the tank; the low-quality mercury wetting considerable portions of the tank surface; and excessive oscillations of the mercury vapour pressure in the region of the excitation anodes. Different measures have been applied to avoid these disadvantages and steady arcing of the excitation arc has been achieved.

An unusual phenomenon has been observed in the high-voltage rectifiers; namely, with the positive anode potential and normal working of all excitation anodes and grids, no ignition of the main anode occurs, i.e. the ignition fails.

FIG. 8.

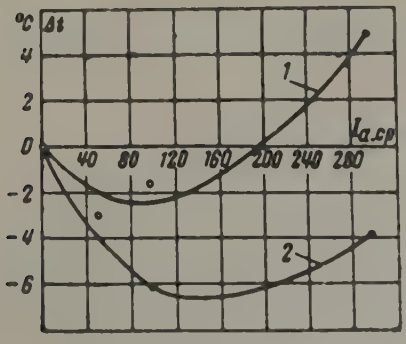

FIG. 9.

This happens only at high voltage and occurs more often when the value of the voltages increases. This phenomenon does not occur at low voltages.

The cause of the ignition failures according to our explanation is the appearance on the auxiliary electrodes of negative potential, which may be due to different causes. Thus, the problem of ignition failures is overcome by the suppression of these negative potentials.

During the development of high-power rectifiers it has been found that failures in the ignition of auxiliary electrodes may be caused by the presence of the condensed mercury vapour in the grid region, which brings about "splashes" in the vapour pressure and the cascade arcing of one of the grids. The ignition dispersion may also be connected with intermittent contacts of the auxiliary electrodes with the tank.

After modification, the failures in the auxiliary electrodes ignition ceased. The tests showed that the probability of flashover on the insulator is considerably less with the high-power rectifiers than with the rectifiers on the experimental transmission installation.

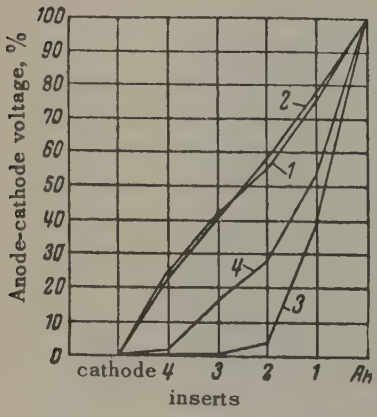

FIG. 10. Voltage distribution curves on inserts in a VR-9 valve, taken on an equivalent circuit ($U_{max.\ test.}$ = 140 kV, U_{sk} = 80 kV, I_{sr} = 280-300 A, $t_{oil\ outlet}$ = 25° C)
1 – inverter regime – jump; 2 – same regime – maximum value; 3 – rectifying regime – jump; 4 – the same, maximum value.

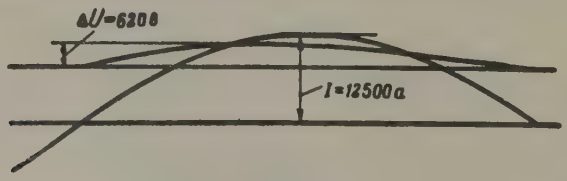

FIG. 11.

The tests showed that the potential distribution on the intermediate electrodes is very irregular owing to the influence of the remaining plasma, and maximum irregularity occurs at the beginning of deionization. The greatest potential drop takes place during the conversion period in the gap between the anode and the first insert and during the inversion period in the gap between the last intermediate electrode and the grid. After some lapse of time from the begin-

ning of deionization the potential distribution improves.

Fig. 10 shows curves of the potential distribution on the intermediate electrodes of the VR-9 high-power rectifier; they were recorded on the equivalent circuit. These curves show that during the inversion operation, in which direct potential is applied at the end of deionization, the negative potential jump is absent; the distribution of the positive potential is practically uniform both for the jump and for the maximum value. In the conversion action, the potential distribution is irregular. The maximum irregularity in distribution occurs during the jump, since in this case phenomena take place during the period of deionization. The maximum potential value is divided more uniformly than the jump value, since the maximum value is attained considerably later, after the completion of deionization.

The use of the external divider, for example, with resistances, in practice brings about a sufficiently quick equalization in potential dividing.

The overload capacity of high-voltage rectifiers differs considerably from the overload capacity of low-voltage rectifiers owing to the lower density of the mercury vapour. Tests of high-voltage rectifiers at low-voltage (220 V) show that a relatively small increase in the anode current brings about a break of the current with all its consequences (overvoltages etc). Thus, in the VR-9 high-power rectifier with a nominal value of maximum current 900A breaks occur in the current at 3500 A at an anode voltage of 220V.

Investigations of the overload capacity of the high-power rectifiers at the high voltages (50-100 kV) showed — as the authors of this article had anticipated — that the current breaks did not occur even at the currents of 15,000 A within the range of operating temperatures. The voltage arc-drop in this case reaches a value of 700-800V.

Fig. 11 shows the anode current oscillogram and the arc-drop of a high-power high-voltage rectifier recorded on the power circuit at a maximum anode voltage of about 50 kV.

The tests showed that the potential distribution along the discharge gap was rectilinear contrary to our expectations. This can probably be explained by the arc contracting to the cross-section, whose area is several times smaller than the area of the intermediate electrodes.

For power tests on high-power high-voltage rectifiers 120 MVA test plant has been installed in the Institute of Direct Current, in Moscow. Rectifiers may be tested under short-circuit conditions and on the "closed loop circuit" with a conversion and inversion group of rectifiers.

In this plant tests were made under short-circuit conditions at full current and two values of reverse voltage, 50 and 90 kV. Fig. 12 shows the shape of the reverse voltage curve.

The rate of increase of the reverse voltage at an anode voltage of 50 kV was 24 kV/degree, and 44 kV/el. degree at an anode voltage of 90 kV.

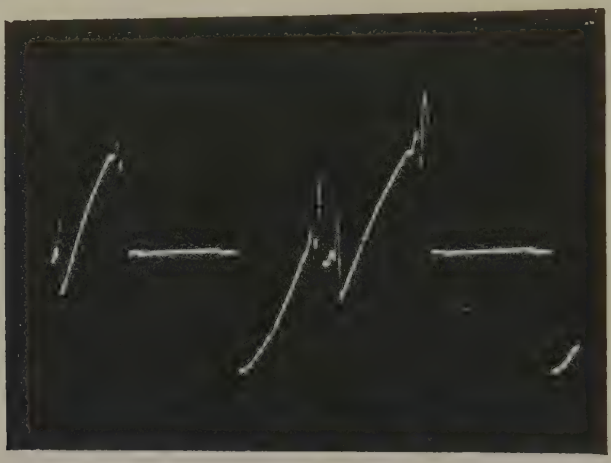

FIG. 12. Oscillogram of anode–cathode voltage on the bench with the valves working on regime 3 (U_{pr} = 77 kV, U_{obr} = 100 kV).

The results of the series of tests showed that at a current of 900 A and a reverse voltage jump of 50 kV, the rectifiers do not suffer from irregularities (back-fires, direct breakdowns, extinctions of excitation). At a current of 900 A and a reverse voltage jump of 90 kV no extinction of the excitation arc occurs in the rectifiers; the number of backfires is considerably less than one backfire in 24 hr.

If we take into consideration that rectifiers are to be series-connected into the bridge arm, we must conclude that such a performance is satisfactory. Tests of the operation of these rectifiers under more severe conditions and their further adjustment are continuing.

For the transmission line from Stalingrad HEPS to the Donbos (potential difference between poles 800 kV and line current 900 A), the VEI proposed an eight-bridge circuit. Voltage across each bridge was 100 kV. This plan has been approved by the Commission of Experts. In this circuit two rectifiers are series connected into the bridge arm.

According to data issued by the Institute of Direct Current, the normal ratings of the rectifier in this circuit are: the maximum reverse voltage 61 kV, the reverse voltage jump 34 kV, maximum current value 900 A. It is understood that under service conditions, particularly in cases of emergency, the rectifiers will operate under much heavier conditions, but these conditions will be of a transitory nature. To secure the operational reliability of the rectifiers, automatic control

and protective gear has been provided in the transmission network. A short – circuiting valve has been provided in particular.

The rational solution of the power transmission network in conjuction with automatic and special protective devices will contribute greatly to the successful operation of high-power high-voltage rectifiers and will speed up the practical realization of long distance power transmission at high direct voltages.

The results of the first series of bench tests show that the high-power rectifier developed by the VEI will be able to work singly in the bridge arm, provided rational power circuits are developed to limit currents and voltages under emergency conditions.

The rectifier design permits a great variety of modifications for different operating conditions by changing the parameters of the high- and low-voltage assemblies.

The high-power high-voltage rectifier can ensure the reliable operation of the transmission line between Stalingrad HEPS and the Donbos in the network designed for it.

The work discussed in this article has been carried out for several years in the high-voltage rectifier laboratories of the VEI in co-operation with the laboratories for gas discharge apparatus and physical research of the same institute. The rectifier models were made by the experimental electromechanical factory of the VEI.

The porcelain and ceramic parts were developed and manufactured by the porcelain factory "Izoliator" and the Institute GIEKI.

The investigations on the rectifiers and the tests on the test power installation were carried out jointly with the Institute of Direct Current.

The following persons took direct and active part in this work: N.P. Stepanov, N. P. Savin, N.M. Maslennikov, I.D. Shkolin, A.A. Pertsev, V.S. Grigor´ev, A.A. Timofeev, R.I. Grigor´eva, V.V. Bazhenov, I.V. Blond, A.A.Ivanov, E.P. Shmarina, and others.

Translated by S. Szymanski

THE PROBLEM OF THE APPROXIMATE ANALYTICAL SOLUTION OF OSCILLATIONS OF A SYNCHRONOUS MACHINE*

B.L. KONSTANTINOV

Bulgaria, Sofia

(Received 2 February 1957)

If a synchronous generator works whilst connected to the bus-bars of a constant voltage then if working conditions are changed, the differential equation of the motion of the rotor, after certain simplifications, can be written:

$$M\frac{d^2\delta}{dt^2} = P_0 - P_m \sin\delta, \tag{1}$$

where M – the inertial constant of the machine;

δ – the angle between the vectors of an axial e.m.f. and the voltage of the system;

P_0 – the power of the prime mover;

P_m – the maximum value of the power characteristic under the new conditions.

The substitution:

$$d\delta/dt = \phi(\delta)$$

lowers the order of the differential equation:

$$\frac{d\delta}{dt} = \sqrt{\frac{2P_0}{M}}\sqrt{\delta - \delta_0 \frac{P_m}{P_0}(\cos\delta_0 - \cos\delta)} \tag{2}$$

To make clear the character of the rotor motion (oscillations or continuous acceleration) it is necessary to analyse the function:

$$y = \delta - \delta_0 - \frac{P_m}{P_0}(\cos\delta_0 - \cos\delta). \tag{3}$$

**Elektrichestvo* No. 5, 24-26, 1958.

If the equation $y = 0$ has no other root except δ_0 then the machine breaks out of synchronism; the presence of the two roots is evidence of the ordinary oscillatory process.

The analysis of the first and second derivative of function (3), and also of the equation $y = 0$ (Kepler's equation of the type $\delta = \text{psin}\,\delta + \alpha$), shows that for the existence of the second root the condition $P_m / P_0 > 1$ should be satisfied. In so far as this condition is not connected with the initial angle δ_0, it cannot be considered as a criterion, which determines the character of the rotor motion. In order to find an approximate criterion determining the relationship between the values P_0, δ_0 and P_m, it is necessary to make use of the condition of the preservation of the stability, which is based on the principle of the comparison of areas.

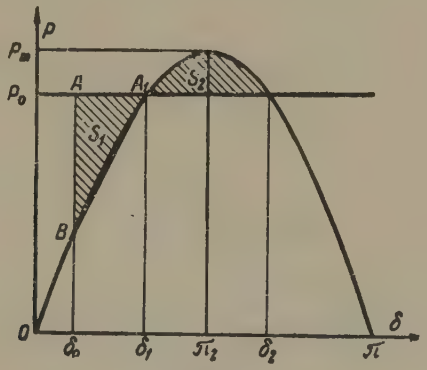

FIG. 1

If with the change of working conditions the parallel working remains undisturbed, then the area S_1 is smaller than the area S_2 (see Fig.) In further discussion, in order to make the analysis easier, we shall assume that the power characteristic under the new conditions may be represented by a parabola [1]

$$P = P_m\left[1 - \frac{4}{\pi^2}\left(\frac{\pi}{2} - \delta\right)^2\right], \tag{4}$$

which passes through the points (0,0), $(\frac{\pi}{2}, P_m)$ and $(\pi, 0)$. Such an approximation, which is permissible within the interval $0 < \delta < \pi$, does not alter the result substantially.

In this case:

$$S_2 = \int_{\delta_1}^{\delta_2} P_m\left[1 - \frac{4}{\pi^2}\left(\frac{\pi}{2} - \delta\right)^2\right] d\delta - P_0(\delta_2 - \delta_1),$$

and the values of δ_1 and δ_2 are found from:

$$P_0 = P_m\left[1 - \frac{4}{\pi^2}\left(\frac{\pi}{2} - \delta_{1,2}\right)^2\right],$$

i.e.

$$\delta_{1,2} = \frac{\pi}{2}\left(1 \mp \sqrt{1 - \frac{P_0}{P_m}}\right).$$

Thus, as a final result we get:

$$S_2 = \frac{2}{3}\pi P_m\left(1 - \frac{P_0}{P_m}\right)^{3/2}.$$

Without making any great mistake we may assume that the area S_1 is equal to the difference of the areas of the rectangle $\delta_0\, AA_1\, \delta$ and trapezium $\delta_0\, BA_1\, \delta_1$, i.e.

$$S_1 \approx P_0(\delta_1 - \delta_0) - \frac{P_0 + P_m\left[1 - \frac{4}{\pi^2}\left(\frac{\pi}{2} - \delta_0\right)^2\right]}{2}(\delta_1 - \delta).$$

Substituting the value of δ_1 obtained above, after certain rearrangements, we get:

$$S_1 \approx \frac{1}{4}\pi P_m\left(1 - \frac{P_0}{P_m}\right)^{3/2}(z^2 - 1)(z - 1),$$

where

$$z = \frac{2}{\pi}\frac{\frac{\pi}{2} - \delta_0}{\sqrt{1 - \frac{P_0}{P_m}}}.$$

Taking into account the condition $S_1 < S_2$, we get the inequality

$$(z^2 - 1)(z - 1) < \frac{8}{3},$$

which is satisfied for $Z > 1.951$.

Consequently:

$$\frac{1}{\pi}\frac{\frac{\pi}{2} - \delta_0}{\sqrt{1 - \frac{P_0}{P_m}}} < 0.9755$$

or

$$\frac{P_m}{P_0} > \frac{1}{1 - 1.051\left(\frac{1}{2} - \frac{\delta_0}{\pi}\right)^2}. \qquad (5)\ *$$

It is necessary to point out that a similar result is obtained by the analysis of the solution of equation (4-58), which is given in [1, p.123]. The analysis shows that:

$$\frac{P_m}{P_0} > \frac{1}{1 - \left(\frac{1}{2} - \frac{\delta_0}{\pi}\right)^2}. \qquad (6)$$

The difference between the right-hand sides of equations (5) and (6) is less than 1.7 per cent even for $\delta = 0$, i.e. in the case which is impossible in practice. By using an exact value of S_1 we may expect that this value will be equal to zero.

* If we introduce a more accurate value of S_1, the preservation of stability is also possible for a smaller value of P.

Therefore, in the further discussion we shall consider the inequality (6) as a criterion for the preservation of stability. We substitute into equation (2)

$$\delta = \frac{\pi}{2} - x \text{ and } \delta_0 = \frac{\pi}{2} - x$$

and by using equation (4), we get an approximate solution of equation (1) within the interval $0 < \delta < \pi$

$$t = \sqrt{\frac{\pi^2 M}{8P_m}} \left[\frac{\pi}{2} - \arcsin \frac{\pi^2 P_0 - 8P_m \delta}{\pi^2 P_0 - 8P_m \delta_0} \right]. \tag{7}$$

Solving (7) with respect to δ we get:

$$\delta = \delta_0 + \left(\frac{\pi}{4} \cdot \frac{P_0}{P_m} - 2\delta_0 \right) \sin^2 \left[t \sqrt{\frac{2P_m}{\pi^2 M}} \right], \tag{8}$$

from which we determine at once the initial interval of oscillations.

$$\delta_0 \leqslant \delta \leqslant \frac{\pi}{4} \frac{P_0}{P_m} - \delta_0,$$

and also a "half-period" of this interval.

$$T = \frac{\pi^2}{2} \sqrt{\frac{M}{2P_m}}$$

It is understood that the relationship (8) and the values of δ_0 and T, that we obtained, have a meaning if the inequality (6) is satisfied.

If the inequality (6) is not satisfied then, substituting into (7) instead of angle δ the value of the limiting permissible angle δ_{lim}, we obtain the maximum permissible time of the cutting-out of the short-circuit. Obviously, the formula for this case, due to its simplicity, has a considerable advantage in comparison with the method of successive intervals.

If δ_{lim} does not exceed 60° we can by solving equation (2) make use of the expansion of cos δ into the series:

$$\cos \delta = 1 - \frac{\delta^2}{2!} + \frac{\delta^4}{4!}.$$

In this case the solution of equation (2) leads to the Abel's elliptical integral. Without discussing the solution itself we shall give only the final results. The limiting time of the cutting-out of the short-circuit is determined by the following relationship.

$$t = \left[\frac{M}{2P_m k_1 \sqrt{2\alpha^2 + c}} \right]^{1/2} \int_0^{\varphi} \frac{d\varphi}{\sqrt{1 - k^2 \sin \varphi}}, \tag{9}$$

where

$$k = \frac{P_0}{P_m} - \delta_0 + \frac{\delta_0^3}{3};$$

α – a real root of the cubic equation $u^3 + pu + q = 0$, in which:

$$r=\frac{\delta_0}{6k_1}-3a^2;\quad q=\frac{a\cdot\delta_0+0{,}25}{6k_1}-2a^3 \text{ and } a=\frac{2-\delta_0^2}{12k_1};$$

$$c=-\frac{q}{a};\quad k^2=\frac{1}{2}\left(1-\frac{3}{2}\,\frac{a}{\sqrt{2a^2+c}}\right);$$

$$\varphi=2\operatorname{arctg}\left[\frac{\sqrt{2r^2+c}}{\dfrac{1}{\delta_{np}-\delta_0}-(a+a)}\right]^{1/2}.$$

Three real roots $\alpha_1\ \beta_1\ \gamma$ ($\alpha>\beta>\gamma$) of the cubic equation $u^3+pu+q=0$ correspond to the conditions of the machine oscillations. Therefore the formulae for t, k^2 and ϕ assume another form:

$$t=\left[\frac{M}{2P_m k_1(\alpha-\gamma)}\right]^{1/2}\int_0^{\varphi}\frac{d\varphi}{\sqrt{1-k^2\sin\varphi}};$$

$$k^2=\frac{\beta-\gamma}{\alpha-\gamma}\quad\text{и}\quad\varphi=\arcsin\left[\frac{\alpha-\gamma}{1-(\alpha+\gamma)(\delta-\delta_0)}\right]^{1/2}. \tag{10}$$

Let us remark that these formulae can also be used for $\delta>60°$. Thus, for example, formula (9) gives the same results as the solution by the method of successive intervals even for $\delta=90\text{-}100°$.

The solutions of two concrete problems, which were obtained by formulae (7) and (9), are given below; for comparison the results obtained by the method of successive intervals are also shown.

TABLE 1

References in which problems are solved	Initial conditions	Limiting time of cutting-out of the short-circuit, sec.		
		By formula 7	By formula 8	By the method of successive intervals
[2] pp. 122-127]	$S=\frac{300}{220}$; $T_j=6$ sec, $P_0=1$; $\delta_0=0{,}6026$ rad, $P_m=0{,}502$; $\delta=1{,}0943$ rad. (62.7°)	0.189	0.193	0.193**
[3 p.95]	$S_n=1{,}3$; $T_j=6$ sec; $P_0=0{,}9$; $\delta_0=0{,}422$ rad; $P_m=0{,}66$; $\delta=1.593$ rad (91.3°)	0.321	0.330	0.330

$$M=\frac{S_n T_g}{\omega_0}$$

** In the book the third decimal figure is omitted; this can be seen from Fig. 5-14

As can be seen from these data, the time calculated by formula (9) is exactly the same as that calculated by the method of successive intervals, although the angle δ is greater than 90°. This is explained by the relatively small influence of $\cos\delta$, which appears in the square root sign of equation, (2), for angles of tripping of about 90°.

It is necessary to point out that formula (9) can be successfully used in the case of the parallel operation of two stations of a comparable power under the same limitations concerning the variation of the angle δ.

Since in this case equation (1) can be written in the following form:

$$\frac{d^2(\delta+\mu)}{dt} = P_0' - P_m' \sin(\delta+\mu),$$

where

$$P_0' = \frac{1}{M_1}\left(P_{01} - \frac{E_1^2}{z_{11}}\sin\alpha_{11}\right) -$$

$$-\frac{1}{M_2}\left(P_{02} - \frac{E_2^2}{z_{22}}\sin\alpha_{22}\right);$$

$$P_m = \left(\frac{1}{M_1}+\frac{1}{M_2}\right)\frac{E_1E_2}{z_{12}}\frac{\cos\alpha_{12}}{\cos\mu}$$

and

$$\operatorname{tg}\mu = \frac{M_1 - M_2}{M_1 + M_2}\operatorname{tg}\alpha_{12},$$

then we have to substitute into formula (9) unity instead of M, because M_1 and M_2 appear in P_0 and P_m. For the numerical example given in [2, pp. 134-142] the limiting time of tripping the short-circuit obtained by this method was 0.278 sec. Solution by the method of successive intervals gave this time equal to 0.277 sec.

Translated by S. Szymanski

REFERENCES

1. V.A. Vyenikov and L.A. Zhukov; *Perekhodnyye protsessy v elektricheskikh sistemakh (Transient processes in electrical systems)*, Gozenergoizdat (1953).
2. P.S. Zhdanov; *Ustoichivost'elektricheskikh sistem (Stability of* electrical systems), Gozenergoizdat (1948).
3. K. Bogatev; *Parallelna rabota na elektricheskite tsentrali (Parallel operation in a power station), Izd. "Nauka i Izkustvo"*, Sofia (1951).

THE INFLUENCE OF THE LAW OF THE EXCITATION CONTROL ON THE DAMPING OF OSCILLATIONS OF A SYNCHRONOUS MACHINE*

V.M. MATIUKHIN

Krzhizhanovski Power Institute, U.S.S.R. Academy of Sciences

(Received 29 June 1957)

Knowledge of the roots of a characteristic equation of a synchronous machine is important for a quantitative characterization of the degree of stability of the machine for small oscillations, and for an approximate evaluation of the speed of damping of a transient process for finite disturbances. The analysis of the roots enables us to compare different laws of control in this respect and, as far as possible, to choose the best.

We know from experience that the cause of disturbance of the stability of a synchronous generator connected with the automatic excitation control is usually the tendency of the rotor towards self-oscillation. Therefore, the roots related to the frequency and degree of damping of the rotor fundamental oscillations are of major interest.

In this article the influence of different laws of control on the damping and frequency of the machine oscillations are discussed using as an example the fourth-order system.

Differential and characteristic equations of a synchronous machine for automatic control of excitation

Assuming that the voltage of the receiving system remains constant, and also neglecting transient processes in the stator and the influence of the damping winding, we write the equations of a synchronous machine for a small disturbance in the following form:

$$Jp^2\Delta\delta + \frac{\partial P}{\partial \delta}\Delta\delta + \frac{\partial P}{\partial E_d}\Delta E_d = 0; \quad \Delta E_d (1 + T'_d p) - Cp\Delta\delta = \frac{\Delta U_c}{1 + T_1 p} = \Delta U_f; \tag{1}$$

$$\Delta U_c = k\Delta R_1 + (k'p + k''p^2)\Delta R_2,$$

where J is the mechanical constant of the rotor; P is its power; E_d the e.m.f. of the

* *Elektrichestvo*, No.5, 27 – 31 1958.

no-load run; U_c the control device output voltage; U_f the voltage on the rotor rings; T_d the time constant of the rotor winding during closing of the line on the bus-bars of the receiving system; T_1 the time constant of the exciter; R_1 and R_2 respectively: a parameter by which a basic excitation control is carried out; and a parameter which is used for stabilizing the control process (as R_1 and R_2: voltage U, the stator current I or angle δ may be used); k k' k'' control coefficients.

Constant C_1 if we neglect the ohmic resistance of the line and generator and assume $x_q = x_d$, is given by the following formula [1]:

$$C = T_{d0} U_0 \frac{x_d - x'_d}{x_d} \sin\delta,$$

where x_d and x_q are synchronous and transient reactances of the generator and the line taken together; T_{d0} the time constant of the rotor for the open stator winding. To the set of equations (1) there corresponds the characteristic equation:

$$\begin{aligned} &J\left(T_1 T'_d - \frac{\partial R_2}{\partial E_d} k''\right) p^4 + J\left(T_1 + T'_d - \frac{\partial R_2}{\partial E_d} k'\right) p^3 + \\ &+ \left[J\left(1 - \frac{\partial R_1}{\partial E_d} k\right) + T_1\left(\frac{\partial P}{\partial E_d} C + \frac{\partial P}{\partial \delta} T'_d\right) - \left(\frac{\partial P}{\partial \delta}\frac{\partial R_2}{\partial E_d} - \frac{\partial P}{\partial E_d}\frac{\partial R_2}{\partial \delta}\right) k''\right] p^2 + \\ &+ \left[\frac{\partial P}{\partial \delta}(T_1 + T'_d) + \frac{\partial P}{\partial E_d} C - \left(\frac{\partial P}{\partial \delta}\cdot\frac{\partial R_2}{\partial E_d} - \frac{\partial P}{\partial E_d}\cdot\frac{\partial R_2}{\partial \delta}\right) k'\right] p + \\ &+ \left[\frac{\partial P}{\partial \delta} - \left(\frac{\partial P}{\partial \delta}\cdot\frac{\partial R_1}{\partial E_d} - \frac{\partial P}{\partial E_d}\frac{\partial R_1}{\partial \delta}\right) k\right] = 0. \end{aligned} \tag{2}$$

General analysis of the fourth-order equation

According to the Hurvitz criterion it is necessary for the stability of a fourth-order system that the coefficients of the characteristic equation should be positive

$$a_4 p^4 + a_3 p^3 + a_2 p^2 + a_1 p + a_0 = 0 \tag{3}$$

and that the following inequality should be satisfied:

$$a_1 a_2 a_3 - a_1^2 a_4 - a_3^2 a_0 > 0. \tag{4}$$

From this inequality we may draw certain conclusions.

It is obvious that the increase of a_2 can never bring a stable system into an unstable state. On the contrary, the increase of a_2 makes the inequality more marked and, consequently, should increase the margin of stability. Furthermore, it is seen that a_0 and a_4 are contained in the inequality only with a minus sign, i.e. their increase may upset the stability of the system. But we have no influence on a_0, since it depends on amplification factors, which are determined by static characteristics (static conditions of the generator voltage or conditions of normal and emergency states). Therefore the only thing we may consider is to try to make the coefficient a_4 as small as possible.

So far as values a_1 and a_3 are concerned, condition (4) shows that their increase

is possible only up to a certain limit. It is necessary to try to vary the coefficients of the characteristic equation in the desired sense by introducing into the control device derivatives of this or another quantity. The characteristic equation has four roots, of which two, usually conjugate complex roots, determine the basic motion of the rotor; let us call them conventionally "mechanical" roots. We shall call the two remaining roots, which strongly depend on time constants T_1 and T_d, "electrical" roots.

When the damping of the rotor oscillations is insignificant and the constant T_1 is not very small, the frequency of the rotor oscillations and the damping ratio may be expressed approximately by formulae (see Appendix):

$$\omega^2 \approx \frac{a_2}{2} + \sqrt{\left(\frac{a_2}{2}\right)^2 - a_0}\,; \tag{5}$$

$$\alpha \approx \frac{1}{2}\left(a_3 - \frac{a_1}{\omega^2}\right). \tag{6}$$

In these formulae it is assumed, for the sake of brevity, that the coefficient of the highest-degree term in equation (3) is unity. This obviously does not impair the general character of our considerations.

Although formulae (5) and (6) are valid only near the limit of stability of the system, nevertheless they permit, as can be seen from the examples given below, a correct estimate of the values of various coefficients of the equation; these values can be varied by means of the control device. From expressions (5) and (6) it follows that to increase the damping moment it is necessary to increase the value of a_2. This agrees with the deduction about the importance of the value of a_2 for the stability of the system, which is obtained from the Hurvitz criterion. The increase in a_2 means, in conformity with expression (5), an increase in the frequency of the rotor oscillations. Thus,if by the action of the control device, only the value of a_2 is increased, then the increase in damping will be accompanied by an increase in the frequency of the rotor oscillations.

From expression (6) it follows that to improve the action of damping it is also desirable to increase the value of a_3 and decrease a_1. The Hurvitz criterion does not allow such a categorical conclusion in this respect, but this criterion deals with arbitrary values of the equation coefficients, whereas in the case under consideration they are restricted by the relatively small values of electrical roots.

Investigation of the fourth order system for various methods of control

Let us first consider the excitation control of a generator by the angle and its derivatives. In this case, in the characteristic equation (2), we have to assume that:

$$R_1 = R_2 = \delta,$$

i.e.

$$\frac{\partial R_1}{\partial E_d} = \frac{\partial R_2}{\partial E_d} = 0; \quad \frac{\partial R_1}{\partial \delta} = \frac{\partial R_2}{\partial \delta} = 1.$$

Let us also denote

$$k = k_\delta;\ k' = k'_\delta;\ k'' = k''_\delta.$$

The subscripts of factors k, k', k'', indicate the quantity by means of which the

control is exerted.

The factor of control, k''_δ, by the second derivative of the angle, affects only the value of a_2; i.e. the coefficient of the second degree of p in equation (2). According to the above considerations a sufficiently large value of k''_δ will ensure good damping of the rotor oscillations. With the increase of k''_δ and a_2 the frequency of rotor oscillations will also increase, as follows from formula (5).

The control factor k_δ affects only the value of a_1, and therefore, in accordance with formula (6), it should weaken the action of damping.

For the numerical examples given below the parameters of the long range transmission line are chosen; they correspond approximately to the parameters of the preliminary project of the Kuibyshev-Moscow transmission line:

$J = 16$ sec; $T_d = 3.85$ sec; $\delta = 68°$, $E_d = 1.28$; $C = 1.08$, $x_{\text{d.gen}} = 0.5$, $x_1 = 0.8$; $x'_{\text{d.gen}} = 0.2$, $\cos \phi_n = 0.92$.

Table 1 shows the influence of the control factors k''_δ and k'_δ on the frequency of rotor oscillations and the damping ratio. The time constant of the exciter was $T_1 = 0.3$ sec and the static factor of the angle control $k_\delta = 0.5$.

TABLE 1.

k'_δ	k''_δ	$p_{1,2}$: "mechanical" roots	$p_{3,4}$: "electrical" roots
0	0	$+0.025 \pm j\,3.32$	$-0.34 \quad -3.26$
0	1	$-0.88 \pm j\,4.45$	$-0.43 \quad -1.41$
0	2	$-1.24 \pm j\,5.7$	$-0.56 \pm j\,0.234$
0	4	$-1.48 \pm j\,7.6$	$-0.32 \pm j\,0.33$
1	2	$-1.06 \pm j\,5.7$	$-0.31 \quad 1.26$

From Table 1 it follows that the second derivative of the angle control ensures good damping of the rotor oscillations. For example, for $k''_\delta = 2$ and $k' = 0$, for the frequency of oscillations $f = 5.7/2\pi = 0.9$ c/s, the amplitude of oscillations decreases in 1 sec to the value $\exp(-1.24) = 0.29$ of the initial value. The frequency of the rotor oscillations increases with the increase of k''_δ.

The introduction of the first derivative of the angle control decreases the damping ratio of the rotor oscillations, as can be expected from the general analysis. Without the first derivative of the angle control the system is unstable, and it is characteristic that this instability manifests itself in a self-oscillation of the rotor, since the "electrical" roots remain negative. If the control applied is only the second derivative control, then for a sufficiently large value of k''_δ the "electrical" roots remain a conjugate complex, and the frequency of electrical oscillations is low.

Table 2 shows the influence of the time constant T_1 for control factors

$k_\delta = 0.5$; $k'_\delta = 1$; $k''_\delta = 2$.

TABLE 2.

T_1	$p_{1,2}$ — "mechanical" roots	$p_{3,4}$ — "electrical" roots
1	$-0.17 \pm j\ 4.3$	-0.36; -0.56
0.3	$-1.06 \pm j\ 5.7$	-0.31; -1.2
0.1	$-4.03 \pm j\ 7.32$	-0.29; -1.85
0.02	-6.50; -2.40	-0.29; -41.4

From Table 2 it follows that the decrease in the value of time constant T_1 leads to the increase in damping of the rotor oscillations. For a very small value of $T_1 = 0.02$ sec the motion of the rotor becomes aperiodic. However, it does not follow from this that in a simple system we should try at all costs to obtain a very small value of T_1 since already for $T_1 = 0.3$ sec the damping is good and can be still increased by increasing the factor k''_δ. The increase in the damping ratio is accompanied by an increase in the rotor oscillations, as long as the rotor motion preserves its oscillatory character.

For the control by the stator current and by its derivatives we have to assume in the characteristic equation (2):

$$R_1 = R_2 = I,$$

i.e.

$$\frac{\partial R_1}{\partial E_d} = \frac{\partial R_2}{\partial E_d} = \frac{\partial I}{\partial E_d}; \qquad \frac{\partial R_1}{\partial \delta} = \frac{\partial R_2}{\partial \delta} = \frac{\partial I}{\partial \delta},$$

and also

$$k = k_1;\ k' = k_1';\ k'' = k_1''.$$

The analysis of equation (2), for the control stability derivatives of the stator current, leads to the following conclusions:

Factors of the derivative control k_1', and k_1'' are limited above because if they are sufficiently large, coefficients a_3 and a_4 of the characteristic equation become negative, and this means instability of the system. The main problem of getting a stable and well-damped system consists in increasing the coefficient a_2 and decreasing a_4; this problem can be solved by a proper choice of the factor of the second derivative of the stator current control.

According to the conditions of control stability and of good damping there is no need in the first derivative of the stator current control, since in this case the coefficient of p^3 decreases and the coefficient of p increases, and this is, according to formula (6), undesirable. However, the first derivative control may be used to force the exciter voltage. This general analysis of the characteristic equation (2) is confirmed by the examples given in Table 3. The evaluation of roots was performed for

$T_1 = 0.3$ sec and $k_1 = 0.5$.

TABLE 3.

k_1'	k_1''	$p_{1,2}$ — "mechanical" roots	$p_{3,4}$ — "electrical" roots
0	0	$-0.05 \pm j\ 3.32$	-0.24; -3.28
0	0.5	$-0.57 \pm j\ 3.7$	-0.25; -3.31
0	1	$-1.6 \pm j\ 4.2$	-0.26; -3.24
0	1.5	$-4.15 \pm j\ 4.4$	-0.26; -3.04
1	1	$-1.15 \pm j\ 4.65$	-0.22; -3.28

As follows from this table, the second derivative of the stator current control produces a strong damping moment of a synchronous machine, which arises when the departures from synchronous running occur. In this case, as in the case of the second derivative of the angle control, the increase in damping is accompanied by an increase in frequency of the rotor oscillations.

The addition of the first derivative of the current control weakens the damping action of the control. When the derivatives of the current are zero the system is on the verge of stability, because the damping of mechanical oscillations falls almost to zero. The "electrical" roots are separated, and

$$p_3 \approx -\frac{1}{T_d'}; \quad p_4 \approx -\frac{1}{T_1}.$$

Stabilizing the process of the control by introducing the derivatives of the stator current also has, as is known from [2], a certain disadvantage; this consists in that for a considerable variation in the parameters of a transmission line, a change in the setting of the control device may be needed in order to preserve the stability of operation. Moreover, as has already been said, the derivatives of the stator current are limited above for the sake of stability, which has significance, for example, in the excitation control by voltage.

Let us now consider voltage control and control by its two derivatives. Into the characteristic equation (2) we have to substitute:

$$R_1 = R_2 = U,$$

i.e.

$$\frac{\partial R_1}{\partial \delta} = \frac{\partial R_2}{\partial \delta} = \frac{\partial U}{\partial \delta}; \quad \frac{\partial R_1}{\partial E_d} = \frac{\partial R_2}{\partial E_d} = \frac{dU}{\partial \delta},$$

and also

$$k = -k_U; \quad k' = -k_U'; \quad k'' = -k_U''.$$

Then, on the basis of equation (2) we may draw the following conclusions.

The increase of the coefficient a_2 by introducing the second derivative of the

current control cannot produce the same effect as the second derivative of the angle or stator current control, since in this case coefficient a_4 increases simultaneously, and this has an unfavourable influence on the stability. At the same time the increase a_3 (the first derivative of voltage control) will not always produce the required effect, since the value of a_1 increases simultaneously, and this, according to formula (6), acts unfavourably on the damping of mechanical oscillations. Thus, only certain optimum values of the factors k'_u and k''_u can be obtained.

Table 4 confirms these general considerations. Roots are calculated for $T_1 = 0.3$ sec and $k_u = 20$.

TABLE 4.

k'_U	k''_U	$p_{1,2}$ — "mechanical" roots	$p_{3,4}$ — "electrical" roots
5	10	$-0.045 \pm j\ 3.7$	$-0.46 \pm j\ 1.26$
5	30	$-0.024 \pm j\ 3.77$	$-0.166 \pm j\ 0.8$
20	10	$-0.195 \pm j\ 3.56$	$-0.93 \pm j\ 1.0$
40	10	$+0.015 \pm j\ 3.72$	$-3.42;\ -0.51$

The increase in the factor of the second derivative control from 10 to 30 has decreased the already weak damping of the rotor oscillations (for $k'_u = 5$). The best result is obtained for $k'_u = 20$ and $k''_u = 10$. But even in this case the damping ratio is equal to 0.195, i.e. is considerably smaller than for the second derivative of the angle or stator current control. The increase of k'_u acts favourably only up to a certain limit; for $k'_u = 40$ the motion of a generator becomes unstable.

A radical method for the increase in damping of the rotor oscillations for the excitation control by the stator voltage consists in introducing into the means of control derivatives of the angle instead of derivatives of the voltage.

$$\frac{\partial R_1}{\partial \delta} = \frac{\partial U}{\partial \delta};\ \frac{\partial R_1}{\partial E_d} = \frac{\partial U}{\partial E_d};\ \frac{\partial R_2}{\partial \delta} = 1;\ \frac{\partial R_2}{\partial E_d} = 0;$$

$$k = -k_U;\ k' = k'_\delta;\ k'' = k''_\delta.$$

Substituting these values into equation (2) we may draw conclusions about the favourable influence of the second derivative of the angle control.

Table 5 gives the values of roots for the case in question for $T_1 = 0.3$ sec., $k_u = 20$, $k'_\delta = 1$.

TABLE 5.

k''_δ	$p_{1,2}$ — "mechanical" roots	$p_{3,4}$ — "electrical" roots
2	$-1.27 \pm j\ 6.2$	$-0.54 \pm j\ 1.85$
4	$-1.44 \pm j\ 8.05$	$-0.36 \pm j\ 1.4$

From these data it follows that the damping of mechanical oscillations has sharply increased after the introduction of the second derivative of the angle control. The first derivative of the angle control will be significant, as in the previous cases, only for forcing excitation.

Thus, in a fourth-order system, irrespective of parameters by which the basic control is exerted, the second derivative of the angle control always ensures a good damping of the rotor oscillations.

Conclusions

1. The damping of the rotor oscillations depends upon the e.m.f.'s applied to the control device, these e.m.f.'s being proportional to the derivatives of current, voltage or angle.

2. By using the second derivative of the angle control in a fourth-order system we may ensure strong damping. The first derivative control on the contrary lowers the damping ratio of the rotor oscillations. The second derivative of the stator current control also gives strong damping for the excitation control by the stator current. However, the value of the second derivative of the stator current is limited above for the sake of stability, and this is significant for basic control by the voltage.

3. The improvement of damping, when using the second derivative of the angle and stator current control, depends on the increase in frequency of the rotor oscillations.

4. For the derivative of voltage control both derivatives should be used. However, in this case, in principle, no strong damping can be ensured. The examples given above show that in this case the damping is much weaker than in the case of the second derivative of the angle control.

Appendix

Let us consider the equation:

$$p^4 = a_3 p^3 + a_2 p^2 + a_1 p + a_0 = 0. \qquad (I,1)$$

Let us assume that equation (I,1) has two conjugate complex roots with a small real part. Then we may assume:

$$p^2 \approx -\omega^2, \qquad (I,2)$$

where ω is the coefficient of the imaginary parts of the root. Thus, the equation (I,1) may be written:

$$p^2 + \left(a_3 - \frac{a_1}{\omega^2}\right) p + \left(a_2 - \frac{a_0}{\omega^2}\right) = 0. \qquad (I,3)$$

Let us find out on what conditions in this equation the coefficient of p, taken with the opposite sign, is equal to the sum of the real parts of the roots in question. The Viette formula gives:

$$a_3 = -(p_1 + p_2) - (p_3 + p_4); \quad a_1 = -p_1 p_2 (p_3 + p_4) - p_3 p_4 (p_1 + p_2).$$

Let p_1 and p_2 be the complex roots with which we are concerned. According to condition (I,2),

$$p_1 p_2 \approx \omega^2. \tag{I,4}$$

Using the Viette formula and condition (I,4) we get:

$$a_3 - \frac{a_1}{\omega^2} = -(p_1 + p_2) + \frac{p_3 p_4 (p_1 + p_2)}{\omega^2}. \tag{I,5}$$

Therefore, in order that the coefficient of p in equation (I,3) should give the modulus of the sum of the real parts of the complex roots, it is necessary that the product of the two other roots $p_3 p_4$ be small in comparison with ω^2. In powerful synchronous generators one of the roots connected with T'_d (say p_3) is usually small, so as a rough approximation we can write $p_3 = -1/T_d$. On the other hand, with frequency of the rotor oscillations 1 c/s, $\omega^2 \approx 36$. Therefore, if the second constant T_1 is not very small, i.e. if the root p_4 is not large, then the condition $p_3 p_4 \ll \omega^2$ is fulfilled and, consequently, near the limit of stability we shall have

$$\alpha \approx \frac{1}{2}\left(a_3 - \frac{a_1}{\omega^2}\right),$$

where α is the damping ratio of the rotor oscillations.

Let us determine further on what conditions the free term of equation (I,3) is equal to the square of the frequency.

By the Viette formula we have:

$$a_2 = p_1 p_2 + p_3 p_4 + (p_1 + p_2)(p_3 + p_4); \qquad a_0 = p_1 p_2 p_3 p_4.$$

Therefore, for the condition assumed (I,4) we get:

$$a_2 - \frac{a_0}{\omega^2} \approx p_1 p_2 + (p_1 + p_2)(p_3 + p_4).$$

Since the sum $p_1 + p_2$ is assumed small, p_3 is of comparatively small magnitude; then again, if the constant T_1 is not too small, we get:

$$a_2 - \frac{a_0}{\omega^2} \approx p_1 p_2 = \omega^2.$$

Therefore, the frequency of the rotor oscillations is:

$$\omega^2 \approx \frac{a_2}{2} + \sqrt{\left(\frac{a_2}{2}\right)^2 - a_0}.$$

Thus the principal conditions for using equation (I,3) to find the mechanical roots p_1 and p_2 are as follows: the real part of these roots should be small in comparison with the imaginary one and every one of the two other roots should be small in comparison with ω.

After finding the mechanical roots, the "electrical" roots p_3 and p_4 can be found. The better the conditions discussed above are fulfilled, the more accurately the roots are determined. If the roots p_3 and p_4 are real, they can be easily determined exactly

by applying the Horner method for the evaluation of polynomials, after which the more accurate values of the roots p_1 and p_2 can be found.

Another method of solving the fourth order equation for widely differing roots is described in [3].

Equation (I,3) has been used in this work not so much for solving the fourth-order equation, as for a qualitative investigation of the influence of different coefficients on the damping of the rotor oscillations; and this was done in this article.

The calculation of roots in this work was carried out by one of the processes of the iteration method, discussed in [4]. Only in the case when the system was on the verge of stability were calculations made by the method discussed in this appendix. In all cases the accuracy of the solutions can be verified by the Viette formulae given here.

Translated by S. Szymanski

REFERENCES

1. V.M. Matiukhin; Uravneniia i strukturnaia skhema sinkhronnogo generatora pri avtomaticheshom regulirovanii vozbuzhdeniia (Equations and a block diagram of a synchronous generator for automatic excitation control), *Izv. Akad. Nauk SSSR, otd. tekh. nauk*, No. 9 (1952).
2. V.A. Venikov and I.V. Litkens; *Elektrichestvo*, No. 11 (1955).
3. V.S. Vyedrov; *Dinamicheskaia ustoichivost' samoleta (Dynamical stability of an aircraft)*, Oborongiz (1938).
4. E.V. Popov; *Dinamika sistem avtomaticheskogo regulirovoiniia (Dynamics of automatic control systems)* (1954).

ARTIFICIAL METHODS OF OBTAINING HIGH POWER FOR THE INVESTIGATION OF ARC EXTINCTION DEVICES*

M.M. AKODIS

Sverdlovsk

(Received 24 February 1957)

The principle of designing of artificial networks† which was proposed in 1940, allows a correct reproduction of operational conditions of circuit breakers and ionic rectifiers. In these networks (Fig. 1, 2) the full voltage is applied from charged capacitors (of circuit II) to the point of junction of two series connected pieces of apparatus. Circuit I acts as a source of current. The networks designed on this principle allow an arbitrary choice of the resistance of the high-tension circuit; this enables a correct reproduction of the real conditions of operation of both circuit-breakers and rectifiers, [1 and 2].

A network for testing circuit-breakers

In testing circuit-breakers it is necessary to ensure a time of arcing not less than 1.5 - 2 half-cycles and even more. In the network in Fig.1 the time of arcing, due to the lower voltage in the circuit of the current at cut-off will be, as a rule, shorter, than in the circuit of the full voltage. In this arrangement the high-tension circuit cannot increase the time of arcing, since the arc can be restruck only in one of the two pieces of apparatus, which are series connected in the circuit of the current at cut-off. Thus this network, which has already found a wide application, does not permit the conducting of exhaustive tests of the great majority of existing circuit breakers.

To ensure the necessary time of arcing the network should be supplemented by one or more circuits III Fig.2, which are added to restrike the arc in both circuit-breakers. In most cases it is advisable to design this network in such a way that the full voltage of the circuit III, striking the arc, should be applied to circuit breakers, before the current to be cut-off reaches its zero value. This

* *Elektrichestvo* No. 5, 42-47, 1957.

† M.M. Akodis. Author's certificate No. 85, 166 of 25 March 1940, *Bulletin of inventions*, No.8, 1951.

allows restriking of the arc in both circuit breakers by using a comparatively small voltage in circuit III. After the action of the arc restriking circuits III, of which there may be 2-3 and more, has ceased, the recovery voltage from the capacitors of the circuit is applied to the circuit-breakers.

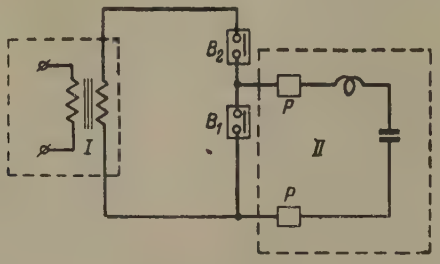

FIG.1. An artificial network without a restriking circuit. I- circuit of the current to be cut off; II- circuit of the recovery voltage; B_1 and B_2 - apparatus on test and auxiliary; P - separation and synchronizing device.

To ensure reliable striking and maintaining of the arc in both circuit breakers it is necessary that the circuit III should be connected slightly before the current reaches its zero value; that is, when the conductance of the arc gaps is sufficiently high (moment of time t_1 in Fig.3). In this case the current from circuit III increases in both circuit breakers at a greater rate and is directed towards the current to be

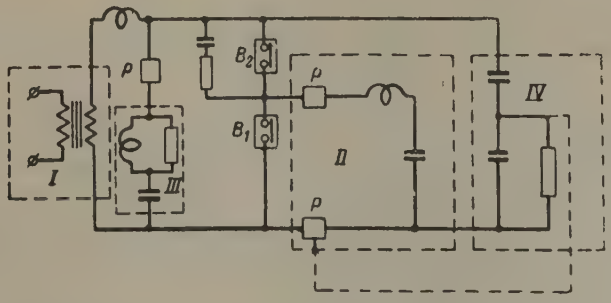

FIG.2. An artificial network with a restriking circuit. I- circuit of the current to be cut off; II- circuit of the recovery voltage; III- circuit of the arc restriking; IV- voltage divider; B_1 and B_2 apparatus on test and auxiliary; P - separation and synchronizing device.

cut-off. Due to a very quick decrease of the full current in both circuit-breakers, after circuit III has been connected, the conductance of the arc gaps, at a moment

of the zero value of the currents, will still be high, and this will ensure the flow of the pulse current i_3 (from circuit III) in the reverse direction. During the time of flow of the current i_3 in the circuit-breakers the current at cut-off reverses its direction and continues to flow through the circuit breakers, and this ensures one more half-period of arcing. Using several arc-striking circuits III, it is possible to increase the time of arcing in the low voltage circuit, through which the current to be cut-off flows, by a few half-periods. After the action of striking circuits has ceased, the circuit breakers come under the influence of the recovery voltage from the capacitors of circuit II.

By varying the extent of the influence of circuits III, we may find the critical length of the arc, for which the circuit-breaker can withstand the recovery voltage of the circuit II, and consequently we may determine the limiting rupturing capacity of the circuit breaker.

The current pulse from the arc igniting circuit should be of a sufficient duration since its quick damping may bring about the suppression of the current at cut-off off immediately after the firing pulse has stopped.

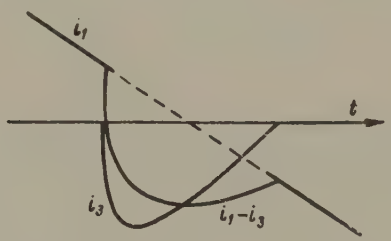

FIG.3. Current variation in the circuit breaker on test. i_1 - current at cut-off; i_3 - current pulse of the restriking circuit.

Investigations of the operation of the igniting network* have shown that normal arc igniting may be secured by means of a capacitance, which is discharged into the arc through parallel connected inductance and resistance, and by a circuit, which is designed as a chain network with inductances of the first links shunted by resistances.

The operation of such a network is illustrated by the oscillograms shown in Fig.4. Since the capacitance of the arc igniting circuit is considerable, it is necessary to separate it after discharge from the network of the cut-off current by protectors.

Another alternative, which is also possible for the operation of the network, is shown in Fig.2. At first, the recovery voltage from circuit II is applied to the

* Investigations were carried out by V.M. Rudnyi

circuit-breakers. If after this a restriking occurs in the circuit-breaker on test, then the synchronizing devices will cause circuit III to operate, and this will send a voltage sufficient for restriking the arc in the second circuit-breaker. At the end of the arcing half-period, high voltage is applied from the circuit II (or from the same circuit, which in the meantime has been recharged, or from a doubling circuit). If the circuit-breaker on test does not extinguish the arc, the process is repeated, but, if the circuit-breaker on test withstands the recovery voltage, then the experiment is finished. Such an arrangement of the network enables us to reduce the number of experiments, which are needed for determination of rupturing capacity of a circuit-breaker, but requires either a stronger insulation of the interrupted circuit, or installing of a protective reactor in this circuit.

The rupturing capacity of a modern circuit-breaker should be determined in a cycle of automatic reclosure (AR). The artificial network under consideration enables us to carry out tests on an arbitrary cycle of AR, and to do this it is sufficient only to provide a certain number of circuits II and III.

In modern circuit breakers, operating in the AR cycle, the arc extinction capacity decreases with each cut-off, therefore it is sufficient to verify the arc-extinction capacity, when applying voltage from circuit II, only for the last half-cycle of the last cut-off in the AR cycle.

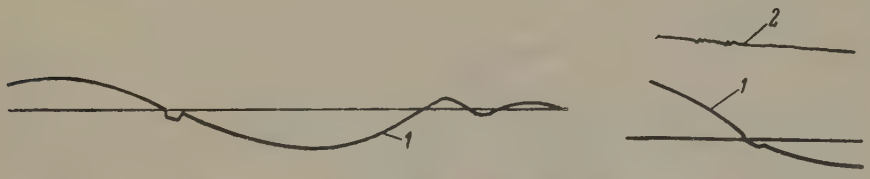

FIG. 4. Oscillograms of tests of an experimental arc extinction device of a tank oil circuit-breaker for 110 kV. a - arc ignition for a current of 10.8 kA; b - arc ignition for a current of 19 kA; 1 - current i_1; 2 - recovery voltage of a frequency 17,000 c/s.

In all previous switching-off tests, our action may be restricted to securing the necessary time of arcing, fixed in advance, by means of arc igniting circuits III.

Such a design of a network allows a considerable simplification of the installation and lowering of its cost, while preserving the full validity of the tests.

Voltage recovery in the circuit-breaker on test

The circuit of the recovery voltage may be connected in different ways.

If in the networks of Figs. 1 and 2 the apparatus on test is the circuit breaker B_2 then the recovery voltage from circuit II should be opposite in polarity to that of the tripping circuit I, in so far as they act on the opposite sides of the apparatus on test. In this case the recovery voltage on the circuit breakers on test is equal

to the sum of voltages of both circuits, but only the voltage of circuit II acts on the second (protective) circuit-breaker.

If in the network under consideration the recovery voltage is applied at the mid point between the two series connected circuit-breakers, it appears as a recovery (reverse) voltage only for one piece of apparatus, (i.e. for that on test B_2), but for the second, protective B_1 it has the polarity of the arc voltage before extinction. If we change the polarity, i.e. shift by 180°, the phase of the circuit of the recovery voltage or of the circuit of the current being cut-off, then the voltage of circuit II will be equivalent to the recovery voltage for the second apparatus B_1 and to the arc voltage for the first B_2. In other words, the circuit-breaker on test and the protective one will interchange their roles. In the last case, only the voltage of circuit II will be applied to the circuit-breaker on test B_1, and the difference of the circuit voltages will be applied to the protective B_2.

The circuit of the recovery voltage II may be connected to the network either before the cut-off of the current in the circuit-breaker on test, or at the moment of its cut-off, In applying a high voltage to the circuit-breaker on test, when the current reaches its zero value, we should ensure the exact synchronization of the action of the circuits. In this case, the synchronizing network must ensure the switching on of circuit II with great precision, a few micro seconds before the current being switched off reaches its zero value. For synchronizing the action of

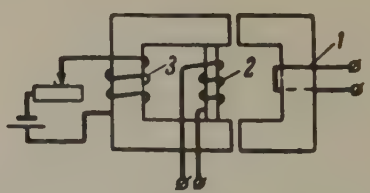

FIG.5. A peak transformer for the circuit synchronization. 1 - primary winding; 2 - secondary winding; 3 - d.c. winding.

circuits a special three-bar peak transformer may be used (Fig.5). The presence on the additional bar of a winding, shifting the voltage peak, and the presence of an air-gap in the core ensure the elimination of the influence of the strong primary current on this winding at the moment of reversal of the magnetic polarity. Investigations have shown that such a transformer, with a sufficiently small dispersal, can reproduce the voltage peak with an advance of a few microseconds.

In testing circuit breakers with a small residual conductance of the arc gap we may have a somewhat increased inductance of the recovery voltage circuit and a corresponding decrease in the capacitance of the network, which brings about a reduction of its cost. In this case the requirements concerning the accuracy of

synchronization may be considerably lowered, if the network is designed in such a way that, from the first moment after the current passes through zero, and till the rupture of the separating gap P of the circuit II, the recovery voltage of the circuit in which the current is being switched off, should be applied to the circuit-breaker on test. In this case we may considerably simplify the synchronizing device, using for the connecting of circuit II a part of the recovery voltage of circuit I [3], through the divider IV, (Fig.2).

It is necessary to take into consideration that the use of the increased inductance in the circuit of the recovery voltage requires in each particular case a verification of the absence of the influence of the arc residual conductance of the operation of the circuit-breaker.

In switching on the recovery voltage circuit, before the moment of dying out of the current in the circuit-breaker on test, the arc extinction in the auxiliary circuit-breaker and the reclosing of the circuit-breaker on test into the circuit of the full voltage may occur before the cessation of the current in the circuit-breaker on test.

In other networks, in which the exact reproduction of the inductance in the recovery voltage circuit was impossible, this procedure always brought about inadmissible distortion of the current at cut-off [4].

So far as the inductance of the network under discussion may be reproduced with a required degree of accuracy, we may in principle avoid the distortion of the current to be disconnected, when connecting the recovery voltage circuit shortly before the arc extinction in the circuit-breaker on test. At the instant of connection of circuit II, before the cut-off current has died out the capacitor of this circuit starts discharging through this circuit-breaker, which is connected into the discharge circuit, provided arcing still persists in this circuit. After one half-period of the natural oscillations of this circuit its current again assumes the zero value, and the voltage across the capacitance assumes the amplitude value of the reverse polarity.

If the circuit of the recovery voltage is switched on before the current in circuit I reaches its zero value (approximately at a time a half-period of its natural frequency oscillations earlier) and if the polarity of circuit II is so chosen, that in the circuit-breaker in the discharge circuit of circuit II the current is directed against the current which is cut-off, then the current in this circuit-breaker will die out a little earlier (moment of time t_2 in Fig.6), than in the circuit-breaker on test (moment of time t_3). Because of this, at the end of the half-period of arcing, circuits I and II become connected in series with the circuit-breaker on test which from this moment on will be under the influence of the sum of voltages of both circuits.

Such a connexion may somewhat decrease the distortion of the curve of the current at cut-off at the end of a half-period, particularly if a voltage peak occurs on the arc immediately before its extinction, which apparently is possible in

certain circuit-breakers even when heavy currents are interrupted. For this connexion it is more difficult to ensure the exact synchronization of circuits, since the switching-on of circuit II should be done 1000 - 2000 μsec before the current being interrupted reaches its zero value, nevertheless for such closing rather large variations of the moment of switching on are permissible. It is necessary to keep in

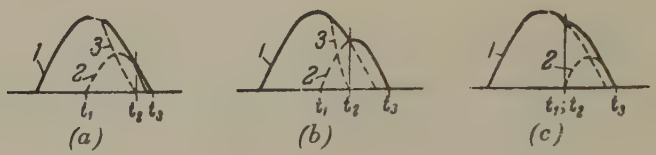

FIG.6 Graphs showing the relationship between the shape of the current at cut-off and the moment of connecting the circuit of the recovery voltage 1 - current from the circuit I, 2 - current from the circuit II, 3 - current in the auxiliary circuit-breaker after the connexion of circuit II. t_1 -connexion of the recovery voltage circuit; t_2 - the moment of arc extinction in the auxiliary apparatus; t_3 - the moment when the current at cut-off reaches zero value.

mind that an excessive advance in arc extinction in the auxiliary circuit-breaker will bring about a discontinuity in the curve of the current through the circuit-breaker, and the interruption of the current will occur with an excessive delay, (Fig. 6b).

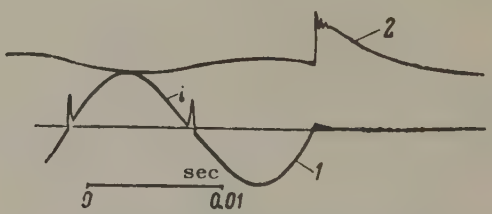

FIG.7 Oscillogram illustrating the operation of the network during the tests of an air circuit-breaker with isolating nozzles. 1 - current at cut-off; 2 - recovery voltage.

The artificial increase in the lapse of time between the moment of current dying out and the moment of its amplitude value, which occurs in this case, may in certain arc extinction devices considerably facilitate the arc extinction, and in others make it more difficult. As experiments have shown a peak transformer enables us to choose the moment, when the peak of the restriking voltage appears with a sufficient accuracy, even when the circuit of the recovery voltage is switched on long before the current reaches its zero value. If for such a connexion of circuit II we choose the voltage polarity on the capacitor in such a way, that in the circuit-breaker of the discharge circuit of circuit II both currents flow in the same

direction, then this circuit-breaker becomes the one on test, on which after the arc extinction the voltage of the required polarity will be restored. For such a choice of polarity of circuit II, which has been made by Biermans [5], the current from circuit II in the circuit-breaker on test is superimposed on the current flowing in the same direction from circuit I thus, in most cases, not decreasing but rather increasing its distortion at the end of a half-period, (Fig. 6c).

Oscillograms, shown in Fig. 7, illustrate a complete operation of the network, with a twofold arc restriking and voltage recovering. These oscillograms were recorded during tests of an air circuit-breaker for 110 kV, having a double break per phase and isolating nozzle. Before the contacts leave the nozzles the circuit-breaker does not disconnect the arc at full voltage, but breaks the arc in the low voltage circuit, because, due to a clearance between the contacts and the nozzle a certain blast occurs even before the contacts leave the nozzle. Without arc restriking circuits for a current of 4-4.5 kA and a voltage of the circuit of the current at cut-off of 8.5 kV, the network ensures a time of arcing within the limits of 0.008-0.018 sec. At this current the circuit breaker safely interrupts the full recovery voltage (71 kV for each break of the circuit-breaker), at a rate of voltage recovery 700 V/μ sec, only if the time of arcing is not less than 0.025-0.027 sec. Therefore, in the tests with an artificial network, without arc restriking circuits, the arc extinction did not as a rule occur at full voltage.

By using two restriking circuits the time of arcing was increased to 0.025-0.035 sec.

The oscillogram shown in Fig. 4, illustrates the operation of a complete network during the tests of an oil circuit-breaker for 110 kV. The value of the interrupted current was 1.2 kA. By using one restriking circuit the time of arcing was brought up to 0.023 sec. During the process of arc extinction the voltage of 71 kV_{max} was applied to the connexion between two extinction devices of the same phase of a circuit-breaker; the frequency of recovery of this voltage was 17 kc/sec. The circuit-breaker did not extinguish the arc, and through it a current of an increased frequency and slowly diminishing flowed from the circuit of the recovery voltage. During the tests of one phase of this circuit-breaker in a network for a current of 10-12 kA and voltage 148 kV_{max} (two extinction devices), of which the frequency of recovery was less than 1 kc/sec, the circuit-breaker interrupted the arc in 0.017-0.024 sec, and for the low voltage the arc extinction took 0.010-0.015 sec, which predetermined the necessity of using a restriking circuit for tests of the circuit-breaker in an artificial network.

The use of the network for the testing of rectifiers

For the testing of rectifiers a network designed on the same principle as that for testing circuit-breakers may be used. As a separation device, P, it is necessary to use two rectifiers connected in parallel opposing one another. The circuit in the network of the testing current should ensure the same shape of the curve of

the current flowing through the rectifiers, as that of the current in the natural network. For this purpose it is advisable to use in the lower voltage network full-wave Fig. 8 or multiphase rectification.

The voltage of the transformer, inductance of the commutation network and parameters of other circuits should be so chosen as to ensure the required shape of the current curve, particularly during the commutation process. In the circuit of the testing current a half-wave rectification may also be used (Fig. 10), which makes this part of the installation somewhat cheaper. For full-wave and multiphase rectification the shape of the current curve in the rectifier on test is well reproduced in Fig.11b. For half-wave rectification the correct reproduction of the conditions

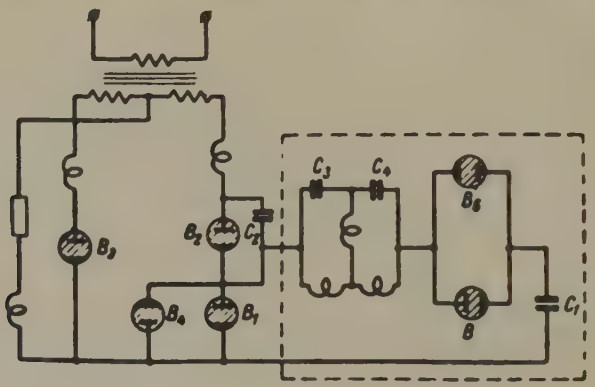

FIG.8 Full-wave network for the testing of ionic rectifiers.

of operation under natural conditions is impossible (Fig. 11a). By a proper choice of the inductance and total voltage in the commutation circuit (voltages across arcs of rectifiers B_1, B_2, B_3), we may even in this arrangement reproduce correctly the shape of the current curve during the commutation process, but we cannot achieve this during the whole time of arcing.

It is necessary to point out that the major part of the installation cost is the cost of the high voltage circuit, therefore, a certain increase in the cost of the low voltage circuit does not substantially increase the price of the whole testing installation.

The recovery voltage appears as a reverse for the rectifier on test and direct for the protective rectifier. The peak inverse anode voltage, as a rule, recovers more quickly than the direct strength. Therefore, in testing rectifiers it is necessary to use this network by connecting the high voltage circuit before the current in the rectifier on test dies out and with the subsequent recharging of the capacitance C_1, because in this case the current in the protective rectifier stops flowing earlier than in the rectifier on test.

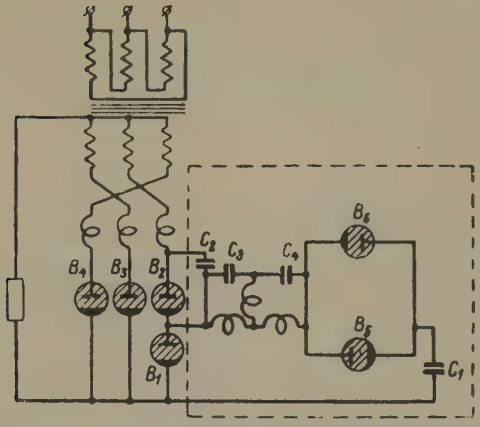

FIG.9 Multiphase network for testing ionic rectifiers.

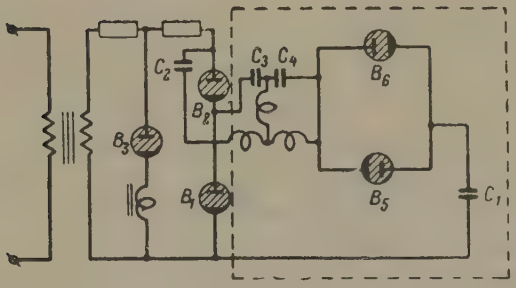

FIG.10 Half-wave network for testing ionic rectifiers.

For the operation of a rectifier in the usual multiphase conversion network the inductance of the commutation circuit differs from the inductance of the recovery voltage circuit, which is also under the influence of the third phase of the transformer, this phase being connected during the process of the voltage recovery with the rectifier through the capacitances of the network [1]. By connecting into the network of the high voltage circuit an inductance, equal to the phase inductance, we obtain a network, which fully reproduces the real conditions of rectifier operation.

The overwhelming majority of rectifiers normally operate at small ignition angles (large commutation angles) and a peak of reverse voltage not greater than 50-60 per cent of its amplitude value. Since the arc extinction in rectifiers occurs periodically 50 times per second, therefore, for normal operation a rectifier should have a great reserve in arc extinction capacity. Because of that the inductance of the high voltage circuit may be chosen a little smaller than the inductance of the real network, allowing at the same time a somewhat increased rate of change of the

current in the circuit. In this case we may tolerate a certain increase in the angle of advance in the arc extinction in the auxiliary rectifier at the expense of an increase of a few per cent in the rate of change of the current near to its zero value. Under these conditions the capacitance C_1 may be of a moderate value for a sufficiently accurate reproduction of the rectifier operation under normal conditions.

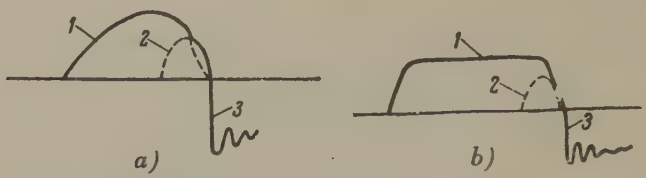

FIG.11 Current in the rectifier on test and its recovery voltage 1 - current of the low voltage circuit; 2 - current of the high voltage circuit; 3 - recovery voltage in the extinguished rectifier.

Insofar as the majority of rectifiers, and particularly high voltage power rectifiers, operate very seldom at large ignition angles and, so in these working conditions we may tolerate a certain distortion of the shape of the current curve, and during tests we may shift the moment of connecting the high voltage circuit. This enables us to ensure the necessary time of advance in the arc extinction in the auxiliary rectifier without increasing the capacitance C_1. Obviously in this case there will be no exact reproduction of conditions of the rectifier operation. The further slow increase in voltage in the rectifier (after a jump) may be ensured by a low power auxiliary transformer. When it is necessary to test a rectifier in reproducing exactly the shape of the current curve for operation at a large ignition angle, then the voltage jump, and consequently, the voltage across capacitance C_1 increases 1.7-2 times, and the cost of the capacitance C_1 increases 3-4 times. Moreover, to ensure the reliable operation of the protective rectifier B_1, for the increased rate of change of the current and under conditions without distortion in the shape of the current curve during the commutation process, it may be necessary to increase the capacitance C_1. Thus, to ensure entirely accurate testing of rectifiers for large ignition angles as well, it may be necessary to increase several times the cost of the installation this cost for high power being mainly determined by the cost of the capacitance C_1.

The addition into the network of the rectifier B_4 (Fig.8) ensures a considerable decrease in the value of the capacitance C_1, and consequently reduces the cost of the whole installation for a given advance in the arc extinction in the protective rectifier. The presence of the rectifier B_4 enables us to eliminate the influence of the current of the high voltage circuit on the shape of the curve of the current, which flows through the rectifier on test during the process of commutation, since, from the moment, when the value of the current of the high voltage circuit exceeds the instantaneous value of the low voltage circuit Fig. 11, a part of the current

$i_2 - i_1$ may flow through the rectifier B_4.

Because of this the choice of the inductance of the high voltage circuit is determined solely by the conditions of reproduction of the process of the recovery of the voltage.

As a result, the time of advance of the arc extinction in the protective rectifier B_1, when the auxiliary rectifier B_4 is present, may be more than doubled, the capacitance C_1 remaining unchanged; if, moreover, the advance in the arc extinction in the protective rectifier is kept unchanged, this capacitance may be decreased several times. For the rectifier B_4 a low power full voltage rectifier may be used, since only a small current $i_2 - i_1$ flows through it during a short time $t_3 - t_2$ (Fig. 11). For a sufficiently large value of the capacitance C_1, in a network with an auxiliary rectifier B_4, we may obtain an arbitary advance in the arc extinction in the rectifier B_1. In this case no distortion of the current flowing through the rectifier on test occurs [7].

Translated by S. Szymanski

REFERENCES

1. M.M. Akodis; *Elektrichestvo* No. 6 (1950).
2. M.M. Akodis; *Elektrichestvo* No. 5 (1953).
3. M.M. Akodis; *Elektrichestvo* No. 5 (1940).
4. M.M. Akodis; *Elektrichestvo* No. 12 (1939).
5. I. Biermans; The circuit for the testing of high voltage circuit breakers with very high rupturing capacity. *Report No. 102 of the session of the CIGRE* (1954).
6. M.M. Akodis, M.V. Bril', V.M. Rudnyi and Kh. P. Khirvonen; *Elektrichestvo* No. 7 (1954).

INCREASE OF STABILITY OF A WELDING A.C. ARC *

O.G. VEGNER

Leningrad

(Received 24 September 1957)

When alternating current in a welding arc passes through a zero value the arc is extinguished and a partial deionization of the arc gap occurs. In welding a.c. installations the necessary conditions of arc restriking are ensured by the presence in the welding circuit of a reactor, due to which a phase shift of 60° and more is produced in the current and voltage in the secondary winding of the feeding transformer. Thus the moment, when current passes through its zero value, corresponds to the moment, when the instantaneous value of the secondary voltage equals to 80-90 per cent of its amplitude value. The welding reactors are usually made with an air gap in the magnetic circuit in order to avoid a certain distortion in the shape of the current curve in networks with closed magnetic circuits; this distortion manifests itself as a delay of current in passing through zero, or almost zero.

An open welding arc in air and in a medium of inert gases is very sensitive to such a shape distortion of the current curve and reacts with a sharp decrease in arcing stability. The welding arc under the flux coating is less sensitive to unfavourable distortions in the shape of current curve, but even in this case they are undesirable. The a.c. arc stability is poorer than the stability of the d.c. arc, particularly within the range of low welding currents. Nevertheless, many important branches of welding operations require the use of a.c. feeding sources, that will ensure the arc stability within a wide range of variation of welding currents, including the smallest values: 20–30 A. One of these branches is welding of aluminium in argon.

One of the main causes of the relative instability of an a.c. arc is an insufficient rate of passing of current through the zero value for sinuisoidal law of variation; this rate is still smaller for frequent distortions, which are due to the variation in the permeability of the magnetic paths of chokes, magnetic shunts and other elements, through which magnetic fluxes pass, determining the values of inductances connected in a welding circuit.

* *Elektrichestvo* No. 5, 67-70.

One of the possible ways of increasing the rate of passing of the current through zero is to increase the frequency, e.g. up to 400–500 c/s (in high-frequency welding generators). A disadvantage of this solution is the great influence of the inductance of the circuit, consisting of welding leads, and this requires the use of special conductors and rotary convertors with small power factors.

The author has found another solution in designing a static device, which ensures such a change in the current curve, that a sufficiently fast rate of passing through zero is produced. To obtain a rectangular, and in practice a trapezoidal shape of the current curve, it would be sufficient to introduce into the current circuit a reactor with a variable coefficient of self-inductance (L): very small for small current values and sharply increasing when the current reaches certain specified values.

As a reactor with an automatic variation of the coefficient of self-inductance, a saturation choke with a magnetic path, made of steel of a high permeability for a small m.m.f. and with a sharp inflection point in the magnetizing curve at saturation may be used. Such a saturation choke should be set in conditions of "forced superposed magnetization", when in the circuit of the control winding currents of higher harmonics are suppressed.

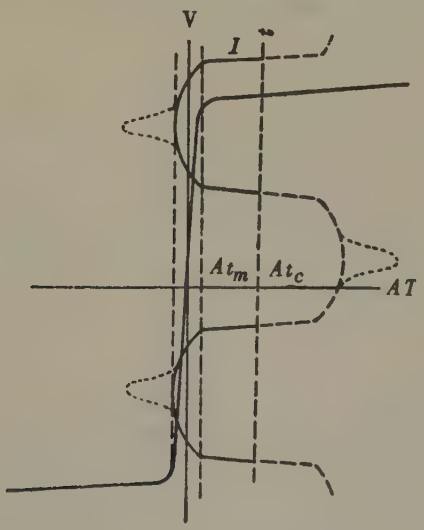

FIG. 1. Obtaining of an a.c. curve with accelerated passing through zero.

Fig. 1 shows a magnetizing curve for the steel for a magnetic path of a choke; this curve has a sharp inflection point at saturation. The control winding produces a m.m.f. At_c. The line (t), passing through the point corresponding to the m.m.f. At_c, is used as a time axis in plotting the curve of the current flowing

through the choke. It is assumed that the choke is made symmetrically; i.e. with two a.c. windings situated on separated bars of the magnetic circuit magnetized by d.c.

So long as the ampere-turns produced by the a.c. winding (At) are less than the difference $At_c - At_m$ (Fig. 1), the effective coefficient of self-inductance of the choke is comparatively small (the core is saturated) and the rate of change of current is high, but when $AT_c + At_m > At_p > At_c - At_m$, the rate of change of current is low, (the core is not saturated).

If $At_p > At_c + At_m$ then "the working point", that determines the magnetic state of the magnetic circuit of the choke, once more moves to a portion of the gentle slope of the lower branch (Fig.1) of the magnetizing curve; i.e. in the region of saturation. This manifests itself by the appearance of peaks in the current curve as shown in Fig. 1 by dotted lines.

From the above approximate and simplified discussion of the conditions of flow of the current in the choke windings, we may draw the conclusion that, in order to increase the rate of passing of the current through zero we should try to achieve the following conditions:

(a) Saturation of the magnetic circuit by the flux of the control winding should be as complete as possible; i.e. the slope of the portion of the magnetizing curve, which corresponds to the m.m.f. At_c, should be very small. From this it follows that the magnetic circuit of the choke should be made from a special steel; the following cold-rolled steels (marks in order of preference) may be used: E370, E330, E320, E310.

Experiments have shown that quite satisfactory results in obtaining a required shape of the curve of the welding circuit were obtained even without a special thermal treatment of the steel, after cutting and punching.

For a ratio of the height of the hole in the core to its width greater than two we may use the so-called wasteless punching of the core sheets, when its two legs and one yoke may be oriented along the direction of rolling of sheets, and only one yoke, which is cut together with legs, is orientated across the direction of rolling.

(b) The leakage inductance of welding transformer and of the saturation choke, which is due to magnetic fields closing through air, should be reduced to a minimum, and this should be accounted for in designing them.

It is desirable to have a welding transformer of a shell type, and the a.c. windings of the choke in a single-layer, with the smallest possible number of turns with increasing transverse dimensions of the core. Thus, in the total weight of active materials of the transformer and choke, the weight of steel should be proportionally greater, than is the case in usual welding installations.

(c) The magnitude of currents of higher harmonics, induced in the control winding of the choke, should be reduced to a minimum, by increasing, for example,

the inductance of the control circuit.

The appearance of an a.c. component of control current leads to such a situation that at the moment, when the current in the operating windings passes through zero, the current in the control winding has a much smaller value, than that, which it would have had in the absence of current in the operating windings.

A partial "demagnetization" of the choke magnetic circuit occurs at the moment, when we would like it to have its maximum saturation in order to decrease its inductance and to increase the rate at which it passes through zero.

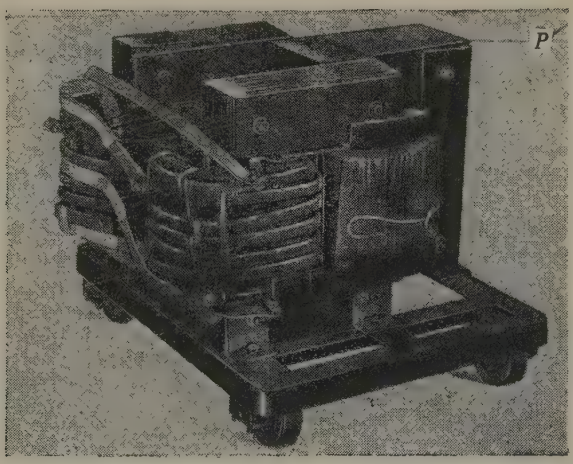

FIG. 2. A saturation choke with additional leakage stamping a/s *P*, linked with the control winding.

The author has proposed the choke design shown in Fig. 2 . It is distinguished in that the control winding surrounds not only the two cores with a.c. windings, but also an additional core, "leakage stampings" with a small air gap, which serves to increase the leakage inductance of the control winding.

A further development of this construction is the addition of an auxiliary winding, which is situated on the second, free bar of the leakage stampings and is connected in series with the control winding.

This auxiliary winding increases still more the leakage flux and the inductance of the control winding. For a relative increase of the electric strength of this arrangement it is advisable to divide the control winding and the auxiliary winding into a few sections and to connect them in pairs in series, i.e. a section of the control winding with a section of the auxiliary winding, then with the next section of the control winding and so. Then in the circuit of the control winding no voltage will appear higher than that in one of its sections.

The following design of the choke is also possible: the control winding is designed to carry a comparatively high current, but with a correspondingly reduced number of turns. The feeding of this winding may be realized by means of semi-

conductors, preferably germanium rectifiers. The suppression of higher harmonics in the control current may be done in this case by connecting into the circuit of the control winding an external choke of a sufficient inductance. Because of the small number of turns in the control winding its voltage cannot assume dangerous values.

Some results of experimental tests of saturation chokes, that ensure a quick passing of current through zero are considered below.

Fig.3a, shows an oscillogram of the current I = 84 A in a circuit comprising a transformer type STE-34 with the no-load voltage 60V, a choke, constructed according to Fig. 2 with a core made of cold rolled steel mark E 310, and a ballast rheostat with a voltage drop across it of U = 18V. The control current was equal to 0.52 A. The air gap in the magnetic circuit of the leakage stampings of the control winding was 2 mm.

The third curve in this oscillogram (not counting curves I and i_c) is the curve of the rate of change of current dI/dt. It was obtained by recording an oscillogram of the e.m.f. of the secondary winding of an instrument current transformer with an open, and, consequently, quite unsaturated magnetic circuit.

As can be seen from the oscillogram, a quite definite increase of the rate of passing of current through zero is obtained. The curve dI/dt shows the peaks at the moments when the current passes through zero. The current curve has a characteristic shape. Fig. 3b shows oscillograms of the same quantities recorded under similar conditions but for an increased gap in the magnetic circuit in the leakage stampings of the control winding; namely of from 2 to 65 mm.

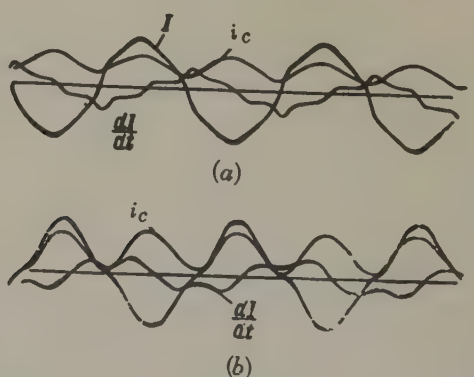

FIG. 3. Curves of the current flowing through the choke (I), of the control winding current (i_c) and of the rate of change of current dI/dt for a small gap in the leakage stampings of the control winding (curves a) and for a large gap (curves b).

The shape of curves is sharply altered: the a.c. component of the control current has so increased that at the moment of the passing of the current I through zero the instantaneous value of the magnetizing current (i_c) drops almost

to zero. The curve of the current I shows the usual distortion with delayed transition through zero. In the curve dI/dt at the moment $I = 0$ instead of peaks, which occurred in the case of a small air gap in the magnetic circuit of the leakage, troughs are present.

Further, tests were carried out in welding by chalk electrodes of 3 mm diameter for currents 120-130 A, using both a saturation choke and a choke with an air gap, type RSTE-34, of lowered voltage of no-load run of 38 V. Fig. 4 shows corresponding oscillograms.

We may note the following circumstances:

1. By using a choke type RSTE-34 and for welding at a lower voltage we have to maintain a shorter arc, than for welding by using a special saturation choke at the same voltage.

2. For the voltage of no-load run $U_0 = 38$ V welding under these conditions becomes practically impossible when using choke type RSTE-34 due to breaks of the arc even for a very small increase in its length.

3. The use of a special choke makes welding quite possible under the same conditions.

It is necessary to keep in mind that the scales of I, U, dI/dt are everywhere the same. The rate of passing of the current through zero at moments, when the voltage across the arc changes its polarity, is 2.5-3 times greater, when using the special choke, then when using the choke of the ordinary type RSTE-34. The use of the choke of the above special design proved particularly effective in an argon arc installation with a non-fusible electrode with a pulse thyratron stabilizer; this installation was designed in the VNIIESO. The improved shape of the current curve and a steeper slope of the operational portion of external characteristics allowed a quite stable process of welding with no-load running at 60V and a current of 25-30A. The accelerated passing of current through zero enables the effective use of a current pulse of very short duration produced by the thyratron stabilizer; to achieve this would be difficult when welding at low currents using an ordinary choke, which gives a nearly sinusoidal shape of the current curve. In the last case it was impossible to achieve a stable welding process with currents smaller than 50 A.

Thus, an advantage of the proposed system for a welding installation manifests itself mainly in welding with small currents. Consequently we have to expect that the main practical application of this installation will be welding with small currents in a medium of inert gases, when special conditions for a welding installation are demanded concerning the arc stability.

A disadvantage of a choke of this type is the increased expense of active materials. Nevertheless, the weight and the price of the feeding source for the arc welding are not the only important criteria, which determine its quality; the welding and exploitation properties, which affect the productivity of the welder, are more important criteria.

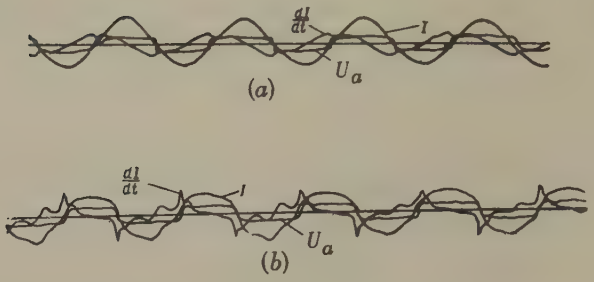

FIG. 4. Welding oscillograms for no-load running at 38 V, current 125-130A, voltage across the arc 18-20 V. Chalk electrodes of 3 mm diameter.
Curves a – when choke RSTE-34 was used;
b – when a special saturation choke was used.

The increase in the arcing stability, particularly for small currents and for such processes as the welding of aluminium, will contribute to the development of the technological uses of welding installations and to the increase in the productivity of welders work. The increased expenditure on active materials in the choke of the new construction may be justified in view of the above discussion.

Translated by S. Szymanski

PHYSICAL PROCESSES IN ELECTRICAL CERAMICS AND RATIONAL METHODS OF DEVELOPMENT *

N.P. BOGORODITSKII and I.D. FRIBERG

Leningrad

(Received 25 September 1957)

Electro-technical ceramics comprises very varied kinds of electro-technical materials: insulating, semiconductor, and magnetic materials. Common features of all ceramic materials are: the process of sintering in producing objects, and the same type of chemical bond, namely an ionic structure of crystals which form a crystalline phase of ceramics.

The division of electro-technical ceramics into three categories is not based on the physical nature of current carriers or on polarization. Technical characteristics of a material, and in the first place its conduction, serve as a criterion of classification. Many kinds of insulation ceramics with good electrical properties possess electronic conduction. Due to this physical property these materials should be classified as semiconductor . However, a sharp distinction between the insulating and semiconductor ceramics cannot be found by considering their properties, because physical processes in them often are the same.

Table 1 shows the principal categories and types of electro-technical ceramics. Later, we shall discuss the principal properties only of insulating ceramics.

Work performed during recent years has enabled us to determine the electrical properties of the most important crystalline substances which are used in modern electro-technical ceramics. From Table 2 it is seen that crystalline substances may be divided into three types on the basis of a particular way of packing the ions in the lattice [1].

The majority of compounds are characterized by close packing of the ions in the lattice and by electronic conduction. At the same time these crystalline formations are distinguished by the energy spectrum of the "forbidden" zone. The narrower the band of the forbidden zone, the greater is the influence of impurities on the electrical properties and crystalline structure, sometimes leading to their catastrophic deterioration.

* *Elektrichestvo*, No. 5, 72-78, 1958.

TABLE 1. Principal classes of electro-technical ceramics.

Category	Class of ceramic materials according to their use	Characteristic properties	Appellation of the ceramic material
Electric insulation ceramics	Ceramics for components of installations and capacitors of small capacity	Rather small permittivity ($\epsilon < 10$)	Steatite, ultra-porcelain*, celsan ceramics, corundum mullite, radio-porcelain*
	Capacitor ceramics for:	High value of permittivity ($\epsilon > 10$)	
	High-frequency circuits, including thermo-compensating and separate capacitors	High value of ϵ negative value of TC ϵ	Rutile (T_i-cond T-80) ** Perovskite (T-150)
	High-frequency thermostable capacitors	Low value of TC ϵ	Titanium-zirconium (T-40, T-20)
	Low-frequency capacitors	Very high permittivity	Strontium-bismuth titanate (S.B.T.)
	Porous ceramics for:	Insulation at high temperatures	
	Insulators for electron tubes	Low value of tan δ	Porous corundum and steatite ceramics
	Bases of wire resistors	High thermal stability	Chamotte, alundum, cordierite ceramics
	Rochelle salt and piezoceramics for:	Presence of dielectric hysteresis	
	Low-frequency capacitors	Ultra-high permittivity	
	Piezo-elements	High value of piezo-electric modulus	SM-1, T-7500, T-1700, (Variconds***) Solid solutions of titanates, zirconates, stannates
	Non-linear elements	Sharp dependence of permittivity on field intensity	
Semiconductor ceramics	Semiconductor ceramics for:	High electronic conduction	
	High power radio resistors, waveguide loads, high temperature heaters	Little dependence of resistance on temperature and voltage	Ceramics on the silicon carbide base, and also containing graphite (silit† Reraks).
	Non-linear elements	Strong dependence of resistance on voltage	Ceramics with a silicon carbide base (vilit,†† NPS)
	Thermo-resistors	Strong dependence of resistance on voltage	Ceramics based on copper and cobalt-manganese reverse spinels
Magnetic ceramics	Magnetic ceramics:	High permeability with high resistivity	
	Magnetic-soft	Low value of coercive force	Nickel-zinc, manganese-zinc, magnesium and other ferrites

TABLE 1. Principal classes of electro-technical ceramics *(continued)*

Category			
Magnetic ceramics	Magnetic hard	High value of coercive force	Barium ferrites

EDITOR'S NOTES:

* Basic porcelain with barium oxide and alkali glass.

** An abbreviation for "titanium condenser".

*** An abbreviation for "variable condenser".

† *Silit* : Semiconductor heater element; a ceramic material based on heat-resistant carborundum SiC with the addition of pure silicon and carbon. Withstands temperatures up to 1500°C in electric furnaces; used for 220 V and 20 A.

†† *Vilit* : Non-linear resistances, ceramic material based on carborundum, consists of SiC with the addition of clay and carbon (graphite).

For further details see B. M. Tareev; *Elektrotekhnicheskie Materialy*, Gosenergoizdat (1955).

In our previous works mullite was included in the group of materials characterized by increased dielectric losses. Kirillova's investigations [2] have shown that an absolutely pure mullite, obtained artificially from the purest components, is characterized by high electrical properties and has its ions closely packed. Thus, it was made clear that the increased dielectric losses in mullite, which were observed earlier, are due to the presence in it of normal alkaline impurities, which contribute to the formation of alkaline aluminosilicate glass. According to the data given by Odelevska and Verebyeichik [3] this glass is distinguished by its high dielectric losses.

Cordierite and beryl are characterized by an open structure, and due to this both its own ions and those of the impurity can participate in conduction and relaxation polarization.

In experimental investigations into the conduction of ceramics we often observe a decrease in current with time, even in those cases when the applied voltage and temperature remain strictly constant. Previously the current-time relationship was expressed by the formula

$$i_\tau = \frac{U - P_\tau}{r},$$

where i_τ is the current at time τ after application of voltage to the specimen;

U is the applied voltage;

P_τ is the "inverse e.m.f. of polarization";

r is a conventional real impedance.

The expression given above was based on the assumption that in dielectrics as well as in metals volume resistance should be independent of time. Therefore,

TABLE 2. Classification of crystalline phases of electro-technical ceramics

Type of the crystalline phase	Character of ion packing; peculiarity of the atomic bond	Name of the material	Chemical formula	Character of electric conduction	Refractive index	tan δ at radio frequencies	Volume resistance (Ω cm)
						$t = 20^0$C	
I. Crystals: dielectrics with a small refractive index	Open structure (non-corresponding to conditions of a close packing, large anion numbers for small cation charges)	Cordierite Beryl β – aluminium	$2MgO.2Al_2O_3.5SiO_2$ $Al_2O_3.3BeO.6SiO_2$ $Na_2O.11Al_2O_3$	Appreciable ionic conduction	1.537 1.560 1.668	≤ 0.01	10^{15}. . .10^{16}
	Close packing	Wollastonite Clinoenstatite Mullite	$CaSiO_3$ $MgSiO_3$ $3Al_2O_3.2SiO_2$		1.631 1.655 1.648	≤ 0.0005	$\sim 10^{18}$
II. Crystals: dielectrics with medium and high refractive index	High transition energy of a cation into another valency state	Periclase Spinel Corundum	MgO $MgAl_2O_4$ Al_2O_3	Appreciable or high ionic conduction	1.736 1.718 1.768	≤ 0.0003	$\sim 10^{18}$
	Small transition energy of a cation into another valency state	Rutile – Type of wurzite	TiO_2 Nb_2O_5 ZnO		2.616 – 2.004	Sharp dependence on impurities	10^6. . .10^{14}
III. Crystals: Rochelle salt type	Blast furnace * structure	Type of perovskite Type of perovskite Type of pyrochlore	$BaTiO_3$ $KTaO_3$ $Cd_2Nb_2O_7$	Electronic conduction	2.40 – –	≤ 0.01	10^{13}. . .10^{14}

* *EDITOR'S NOTE:* Blast-furnace possibly refers to the shape of the crystal structure.

in order to avoid such a dependence, the "real impedance" was related not to the total thickness of the specimen, but only to a certain portion of it (after deduction for a thin layer of the high resistance).

In actual conditions, an initially homogeneous dielectric, due to the redistribution of electric charges at a constant voltage, is transformed into a two-layer or three-layer one, with different resistances of layer insulation. However, it is hardly expedient to consider the resistance of the insulation of these layers separately.

The real impedance of a specimen of dielectric, which determines the magnitude of the true current after the completion of electronic and ionic polarization, may be calculated by the formula

$$r_{thr} = \frac{U}{I - \Sigma I_p},$$

where ΣI_p is the sum of the currents for a retarded polarization.

In view of the fact that the determination of the polarization currents presents considerable difficulties, the resistance is in practice calculated regardless of these currents, as a quotient of the voltage divided by the current, which is measured a long time after the application of the voltage when we can neglect the polarization currents.

It is possible to indicate five mechanisms of the through conduction of the ionic dielectrics, including electrical ceramics:

(1) Cation-cution conduction. The ions of one sign are mobile, namely cations. They are deposited at the cathode, are neutralized and become atoms of the substance(sometimes dendrites). However, it is possible, when the anode is made of a metal such as silver, that its ions diffuse into the dielectrics and replace the dielectric cations, which are transformed into atoms. In their turn silver ions in many cases participate in through-conduction and are also neutralized at the cathode, being simultaneously replaced by ions from the electrode.

(2) Electronic-cation conduction. Ions of one sign are mobile, namely cations, and these are separated from the electrode (anode). At the cathode the electron in its turn enters the dielectric and reforms its cation. This mechanism takes place in dielectrics with cations of a variable valency. Thus, for instance, in ceramics containing titanium, along with a purely electronic current, a process of electric reduction of titanium dioxide takes place according to the reaction

$$Ti^{+4} \rightarrow Ti^{+3} + Ag^{+1}$$

first of all silver ions migrate along the surface and imperfections of the ceramics.

(3) Electronic-anion conduction. Ions of one sign are mobile, namely anions. They are deposited on the anode, are neutralized and become atoms of the substance. However, this can occur when electrons from the cathode enter the dielectric, thus leading to the formation of F-type centres. For example, in the

ceramics containing titanium, along with the purely electronic current, the process of electric reduction of titanium dioxide occurs according to the reaction

$$Ti^{+4} + \bar{e} \rightarrow Ti^{+3}$$

(4) Cation-anion conduction. Both positive and negative ions are mobile. They are deposited on the cathode and anode respectively, are neutralized and become atoms of the substance.

(5) Purely electronic conduction. This kind of conduction is characteristic for a series of oxides of high-valency metals.

The types of conduction discussed above are often superimposed one on another. Let us remark that ionic conduction necessarily brings about irreversible changes in the substance.

In certain types of ceramics, for example in rutile, perovskite and others, ionic conduction is negligibly small in comparison with the electronic one; nevertheless it is sufficiently high, so that after a certain time, at an increased temperature and with silver electrodes, electro-chemical "ageing" of the material takes place. Electro-chemical ageing is an irreversible change in the electrical properties at a certain intensity of a constant field, which depends on the operational temperature.

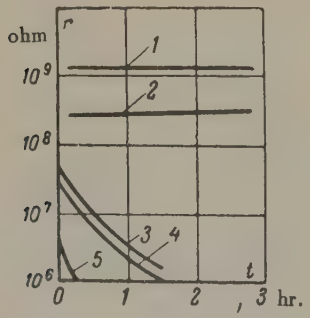

FIG. 1. Insulation resistance of disk capacitors with silver electrodes as a function of the time of application of direct voltage. θ = 400°C; U = 1000 V; thickness of the capacitor plate 0.7 mm.

(1) zirconnate ceramics; (2) stannate ceramics; (3) calcium titanate; (4) nickel titanate; (5) rutile ceramics.

As a result of the progressive decrease of the insulation resistance at increased temperatures tan δ in the ceramic material increases and breakdown occurs. The electro-chemical ageing of ceramics containing titanium is explained by the processes of reduction of titanium dioxide to the lower oxidation state under the influence of the electric field, due to the polyvalency of titanium. The electro-chemical ageing of aluminosilicate ceramics, porcelain, steatite and others possessing high ionic conduction, at increased temperatures and when silver electrodes are used, is due to the formation of dendrites, particularly of silver.

Fig. 1. shows how the resistance of the ceramics containing titanium for capacitors and certain new types of capacitor ceramics depends on the time of voltage application. From these graphs it follows that materials containing free

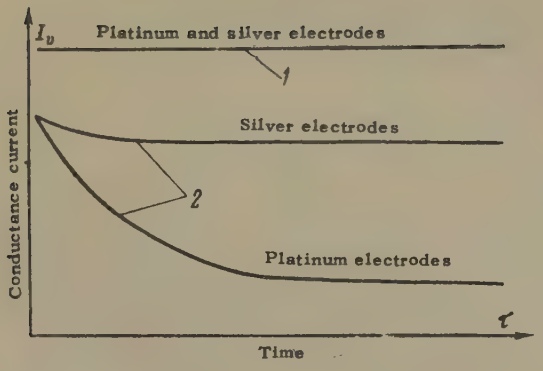

FIG. 2. Conduction current as a function of time for a constant voltage. (1) electronic conduction; (2) ionic conduction.

titanium dioxide, for example the rutile ceramics, are particularly unsuitable for use at increased temperatures. Ceramics based on chemical compounds of titanium dioxide exhibit slightly better characteristics. From this point of view, the titaniumless ceramics (e.g. zirconnate, stannate) represent another class of materials, in which the process of electro-chemical ageing is much less pronounced.

The nature of electric conduction of ceramic materials – whether electronic or ionic – has been usually determined for many years by the "Tuband" method, which requires weighing of the tested specimen and electrodes. This method is sufficiently complicated: our investigations have shown that the character of the electric conduction of ceramics can be determined much more simply by comparing experimentally-obtained relationships between current and time, when using silver, platinum or gold electrodes. This method is based on the fact that, with silver electrodes, the diffusion of silver into ceramics is observed, whereas with platinum electrodes this phenomenon is almost completely absent. Ionic conduction is present if, in the case of platinum electrodes, the current sharply drops with time; and in the case of silver electrodes, when the mechanism of electric conduction corresponds to points 1 and 2 of the above classification, the absorption is almost undetectable. The constancy of current with time with platinum and silver electrodes permits the conclusion that a purely electronic conduction is present.

Fig. 2 shows the character of the dependence of the conductance current on time at a constant voltage for ceramics with electronic and ionic conduction.

This relationship has been observed by Plashchinski on a number of ceramic materials.

The most important property of insulation ceramics is dielectric losses. We can subdivide them into three groups: losses due to polarization, losses due to the through conduction and losses caused by a heterogeneous structure.

Losses due to polarization are most important; they characterize the physical nature of the material. They may be of three kinds: of the ionic-and electronic-relaxation type, losses due to spontaneous polarization and losses at resonance

TABLE 3. Classification of dielectric losses in electro-ceramics

Basic mechanism of losses	Kind of losses	Conditions under which this kind of loss: occurs
I. Dielectric losses in polarization	Ionic relaxation	1. In crystal: individual chemical compounds with an open lattice (cordierite, beryl) 2. In crystal, solid solutions of subtraction type (oxide systems $MgO-ZrO_2$; $CaO-ZrO_2$), solid solutions of the addition type, ($Si^{+4} = Al^{+3} + R^{+1}$) and in solid solutions in a state of breakdown. 3. In a vitreous phase, particularly in the presence of alkaline oxides and in the absence of alkali-earth oxides of a large ionic radius.
	Electronic relaxation	In crystals: electronic semiconductors with a disturbance of the stoichiometric composition (TiO_2, ZnO, Nb_2O5)
	Spontaneous polarization.	In crystals: of the Rochelle salt type, at temperatures below Curie-point ($BaTiO_3$, $PbTi_2O_3$, $NaNbO_3$)
	Resonance	In crystal and glasses at frequencies above 10^{10} c/s.
II. Dielectric losses due to through conduction	Losses due to the surface conduction	Contaminated surface of the object, high air humidity
	Losses due to volume conduction	High temperature of heating of the substance, capillary hygroscopicity
III. Dielectric losses due to heterogeneous structure	Ionization losses in the substance volume	In presence of enclosed porosity and at high field intensities
	Losses due to polarization and the through conduction owing to impurities	Presence of the adsorbed and absorbed humidity at open porosity, presence of semi-conducting impurities and others

in the region of ultra-high frequencies.

Fig. 3 shows the permittivity and the dielectric power factor as functions of frequency for relaxation and resonance losses according to data given by Birks [4].

The dependence of tan δ on temperature for a great majority of electro-ceramic materials is expressed by an exponential function.

TABLE 4. Permittivity temperature coefficient of crystalline compounds which are used as components of electro-technical ceramics for capacitors.

Group	Name of the compound	Chemical formula	Permittivity	Permittivity temperature coefficient, within the temperature range		Type of structure
				from – 60°C to + 20°C	from + 20°C to + 80°C	
I. Positive TCϵ	Calcium Stannate	$CaOSnO_2$	16	+ 100	+ 115	Perovskite
	Magnesium orthotitanate	$2MgOTiO_2$	16	– 10	+ 40	Spinel
	Zinc orthotitanate	$2ZnOTiO_2$	16	+ 170	+ 180	Spinel
	Nickel titanate	$NiOTiO_2$	18	+ 40	+ 70	Ilmenite
	Calcium zirconate	$CaOZrO_2$	28	+ 50	+ 65	Perovskite
	Strontium	$SrOZrO_2$	30	+ 60	+ 60	Perovskite
II. Negative TCϵ	Barium stannate	$BaOSnO_2$	~ 20	– 80	– 40	Perovskite
	Barium zirconate	$BaOZrO_2$	~ 40	– 900	– 500	Perovskite
	Zirconium titanate	ZrO_2TiO_2	~ 40	– 120	– 90	–
	Barium tetratinate	$BaO4TiO_2$	~ 40	~ 0	~ 0	–
	Titanium dioxide	TiC_2	~ 100	– 1000	– 850	Rutile
	Calcium titanite	$CaOTiO_2$	~ 150	– 2300	– 1500	Perovskite

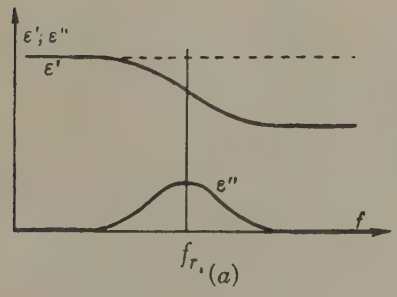

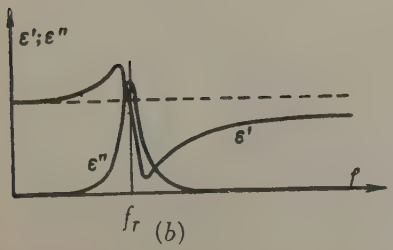

FIG. 3. Permittivity ϵ' and dielectric power factor ϵ'' as functions of temperature. (a) relaxation losses; (b) resonance losses.

TABLE 5. Ceramic materials according to GOST 5458-57.

Type of	Class	Group	Permittivity at + 20° ± 5°C	Temperature coefficient of capacity (degree^{-1} x 10^{-6})	Tangent of the dielectric loss angle, not more than				Volume resistivity (Ω) at temperature + 100± 5, not less than	Electric strength (kV/mm) not less than	Limit strength for static bending (kg/cm^2) not less than	Linear coefficient of expansion (degree^{-1} x 10^{-6}) not more than	Recommended field of application
					at temperature, (°C)			after damping					
					+20± 5	+80± 5	+100±5						
High frequency materials of permittivity more than 12	I	a	130 . . . 190	– (1.300 ± ± 200)	0.0006	0.0008	0.001	0.0008	10^{11}	6	800	12	For circuit and separation capacitors, not affecting frequency stability
		b	65 . . . 100	– (700 ± ± 100)	0.0006	0.0008	0.0012	0.0008	10^{11}	8	800	8	For the circuit, thermo-compensation and separation capacitors
	II	a	31 . . . 50	– (80 ± 30)	0.0006	0.0008	0.0010	0.0008	10^{11}	8	700	8	For capacitors of high stability
		b	17 . . . 30	– (50 ± 20)	0.0006	0.0008	0.0012	0.0008					
	III	–	12 . . . 30	+ (30 ± 20)	0.0006	0.0008	0.0012	0.0008	10^{11}	8	700	8	
High frequency materials of permittivity less than 9	IV	a	Not more than 7.5	+(110±30)	0.001	0.0012	Not standarized	0.0012	10^{12}	20	1.400	8	For small (a) and large (b) installation components
		b	Not more than 8		0.002	0.003		0.0022	10^{12}	20	1.400	8	
		c	Not more than 7.5	+(60±20)	0.0006	0.0008		0.0008	10^{12}	20	800	3	For high stability induction coils and high-frequency capacitors

(Continued Table 5.)

	V	—	Not more than 9	+(110±30)	0.0012	0.0018		0.0015	10^{12}	20	2.000	6	For small and medium size components with high mechanical strength and thermostability
	VI	—		Not standarized			0.0012 +300°C	Not standardized	10^{12} (300°C)	Not standarized	600	6	For insulators used inside vacuum apparatus
	VII	—	Not more than 7.5	+(200±100)	0.005	0.007	Not standarized	0.006	10^{11}	18	600	6	For installation components not affecting the apparatus stability
Low frequency materials of permittivity more than 1000	VIII	a	Not less than 2.800	Not standardized	0.04	0.05	Not standarized	0.07	10^{10}	2	500	12	For low frequency and d.c. capacitors
		b**	Not more than 2.000	Not standardized	0.04	0.05		0.10	10^{10}	3	500	12	For piezo-electric converters++/and low frequency capacitors
		c	Not more than 1.000	*	0.005	0.005		0.007	10^{11}	6	500	12	For low-frequency and d.c. capacitors

* Variation of permittivity of the materials of the group c, class VIII, within the range from — 60 to + 100°C, should be not more than ± 35 per cent of the permittivity at temperature + 20 ± 5°C.

** For the materials group b, class VIII, in the case when they are used in producing converters, the piezo-electric modulus d_{31} is measures, the value of which should not be less than 1.5×10^{-6}.

However, consider these dielectric losses from the point of view of the relaxation phenomena. The absence of the usual maximum of tan δ as a function of temperature can be explained by the increased number of relaxation ions with increased temperature. This was not taken into account by earlier theories of relaxation losses. On the contrary, in the relationship tan δ-frequency at a constant temperature, when the number of relaxation particles remains constant, a maximum of tan δ is possible at a certain frequency.

Table 3 gives the classification of dielectric losses in electrical engineering ceramics.

It has been said earlier that one of the important groups of insulation ceramics is that used for capacitors. In the construction of capacitors those types of ceramics are mainly used, which have a crystalline phase which exhibits electronic conduction. The high permittivity of these ceramics is explained by the presence of a strong internal electric field.

Table 4 gives characteristics of crystalline structures which are components of the crystalline phase of the capacitor ceramics.

Not long ago production of electro-ceramics materials was based mainly on experimental investigations. Theoretical conceptions have since been accumulated and allow us to establish certain laws on the basis of which electro-chemical ceramics are now developed. However, in spite of the necessity for continuously improving the electrical standards of ceramics, it is also necessary to consider the technological properties of the materials and the costs of production.

In the new specifications, GOST 5458-57, is given a sufficiently comprehensive list of ceramic materials which possess the required electrical properties and which have been tested in production. Table 5 shows the main standards for ceramic materials approved by the GOST 5458-57 specifications.

Translated by S. Szymanski

REFERENCES

1. N.P. Bogoroditskii; Dielektricheskiye poteri v radiokeramike (Dielectric losses in radio ceramics), *Dokl. nauch.-tekh. soveshchaniia po radiokeramike*, Leningrad (1955)
2. G.K. Kirollova; Elektricheskiye svoistvo mullita (Electrical properties of mullite) Zh. tekh. fiz. (1957).
3. V.I. Odelevskii and N.M. Verebyeichik; Relaksatsionnye dielektricheskiye poteri v neorganicheskikh silivatnykh steklakh (Relaxation dielectric losses in inorganic silicate glasses) *Trudy. soveshchaniia po tverdym dielektrikam.* Tomsk (1955).
4. J.B. Birks; Magnetic spectra, *J. Inst. Elect. Engng.* October (1956).

AUTOMATICALLY CONTROLLED SERIES EXCITATION FOR GENERATORS*

G.I. POLIAK

Leningrad

(Received 6 May 1957)

In automatically controlled generator excitation systems used at present, exciters with the shunt and separate excitation are used †. As far as series excitation is concerned, it is naturally useless in its pure form. Nevertheless, if it is used in conjunction with separate excitation or in special circuits, which are discussed below, it can bring about a substantial increase of stability and accuracy of control. Moreover, special circuits are extremely simple and allow us in many cases to dispense with the use of automatic voltage regulators.

Series excitation was very exhaustively investigated in 1934 by N.N. Shchedrin in the Smurov Laboratory [1]. The investigations showed that the series connexion of the series and shunt exciters of a synchronous generator is effective.

In 1943 P.S. Zhdanov [2] proposed a circuit in which the exciter of the synchronous generator is provided with two windings. One of them is series wound. The other is a separate one, fed by the difference of the standard and of the automatically controlled voltage. Such a method of excitation possesses the property of self-regulation and replaces a special automatic voltage regulator.

In 1944-1945, descriptions of electrical machine regulators acting as exciters were published; they were called rototrols. In these devices the control effect is achieved by a proper combination of series and separate excitation windings the exciter, [3-5].

In this article the properties and advantages of series excitation for automatic voltage control are discussed.

Before discussing automatic control with series excitation let us consider a d.c. generator with a direct automatic control according to the voltage deviation.

†Ionic excitation can be considered as separate excitation.

**Elektrichestvo* No. 6, 10-15, 1958.

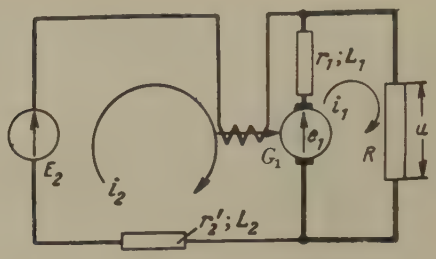

FIG. 1. Circuit of the direct automatic control according to the voltage deviation.

This automatic control circuit is shown in Fig. 1 and is characterized by the following equations (the list of notations is given at the end of this article):

$$\left.\begin{aligned}(r_1+R+pL_1)\,i_1-(r_1+pL_1)\,i_2=e_1;\\ -(r_1+pL_1)\,i_1+[r_1+r_2'+\\ +p\,(L_1+L_2)]\,i_2=E_2-e_1,\end{aligned}\right\} \qquad (1)$$

where $e_1 = c_1\, i_1$; c_1 is the coefficient of proportionality;

$$i_1 = \frac{u}{R}\,.$$

In the case of a non-linear magnetic characteristic of the generator coefficient c_1 is a variable quantity.

For steady-state conditions, the generator voltage found from equation (1) is equal to:

$$u = \frac{(r_1 + c_1)\,E_2}{\dfrac{r_1 r_2'}{R} + r_1 + c_1 + r_2'}\,. \qquad (2)$$

This expression shows that the generator voltage for constant parameters is determined by the setting voltage E_2 and by the load resistance R.

In this form the control circuit is unsuitable due to high quiescence and the non-linear magnetic characteristic of the generator. However, by assigning to the $r_1\, r_2/R$ various appropriate positive and negative values, we may obtain the required static characteristics with a positive or negative quiescence). We may also get an astatic characteristic.

The condition imposed, $r_1\, r_2/R \gtrless 0$, can be satisfied, if the co-factors r_1 and r_2' are expressed in the form of differences $r_1 = (r_1' - c_2) \gtrless 0$ or $r_2' = (r_2 - c_3) \gtrless 0$. Obviously coefficients c_2 and c_3 represent negative resistances, which may be produced by connecting into the network of series generators with resistances r_1' and r_2.

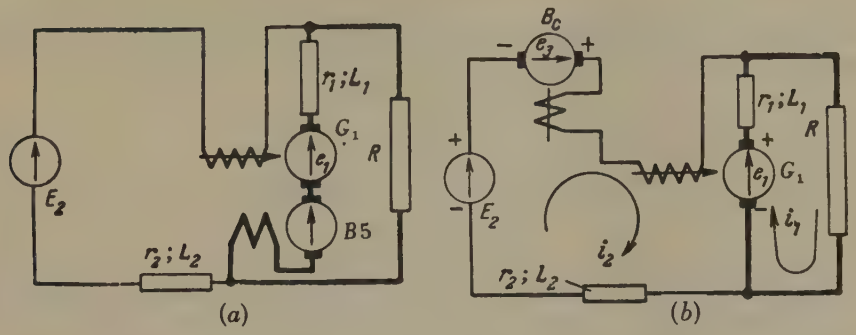

FIG. 2. Circuit of the voltage automatic control with compounding of the load current (a) and of the excitation current (b).

If the series generator B_s is connected into the armature circuit Fig. 2a then compounding of the armature current occurs which is usually performed by a series winding of the generator G_1. We shall not discuss this method of compounding as it is already well known. If a series generator B_s is connected into the excitation circuit, we then get a circuit which can be called by analogy a "circuit with compounding of the field current". This circuit, which will be called henceforth the automatically controlled series excitation circuit, is the subject of the following discussion.

For compounding of the field current, expression (2), after substitution $r_2' = r_2 - c_3$ assumes this form:

$$u = \frac{(r_1 + c_1) E_2}{\frac{r_1 (r_2 - c_3)}{R} + r_1 + c_1 + r_2 - c_3}. \tag{3}$$

Obviously, this expression can also be obtained by solving equations for the network shown in Fig. 2b.

$$\left.\begin{aligned} (r_1 + R + pL_1) i_1 - (r_1 + c_1 + pL_1) i_2 = 0; \\ -(r_1 + pL_1) i_1 + [r_1 + c_1 + r_2 - c_3 + \\ + p(L_1 + L_2)] i_2 = E_2. \end{aligned}\right\} \tag{4}$$

In establishing the equations, we expressed the e.m.f. of the generator and series exciter by means of currents: i.e. it was assumed that:

$$e_1 = c_1 i_2 \text{ and } e_3 = c_3 i_2 .$$

Static properties of this control are determined by a fractional term in the denominator of equation (3).

When $(r_2 - c_3) = 0$ the control becomes astatic. When $(r_2 - c_3) > 0$ the quiescence

control characteristic will be positive, but when $r_2 - c_3 < 0$, it will be negative.

The problem of stability of automatically controlled series excitation can be explained by solving the characteristic equation of the set of equations (4):

$$\begin{aligned} L_1 L_2 p^2 + [(r_2 - c_3) L_1 + R L_1 + \\ + (r_1 + R) L_2] p + [(r_2 - c_3)(R + r_1) + \\ + R(r_1 + c_1)] = 0. \end{aligned} \tag{5}$$

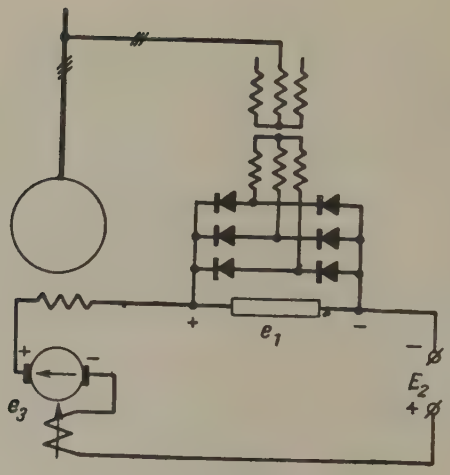

(a)

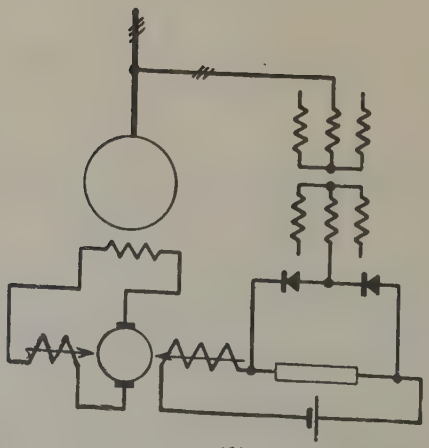

(b)

FIG. 3. Circuits of the voltage automatic control with the automatic series excitation.

The control is stable if the coefficients of equation (5) are positive, which is possible if the following conditions are satisfied:

$$\left.\begin{aligned} \frac{RL_1+(r_1+R)L_2}{L_1} &> -(r_2-c_3);\\ \frac{R(r_1+c_1)}{r_1+R} &> (r_2-c_3). \end{aligned}\right\} \tag{6}$$

The analysis of conditions (6) shows that control stability is ensured even for such high values of negative quiescence as are not encountered in practice.

Automatically controlled series excitation of synchronous generators can be realized in the circuit in Fig.3a.The voltages acting in the excitation circuit are added directly Fig. 3a. Other circuits are also possible in which instead of voltages, magnetic fluxes are added, which are proportional to the voltages, or a combined system can be used with the summation of both voltages and fluxes. As an example of these systems, the circuit proposed by P.S. Zharnov, mentioned above can be given (Fig. 3b).

We shall discuss the automatically controlled series excitation on the example given in [6, p. 310] for a case of ordinary non-inertial control.

Let us write the set of the Gorev-Park equations adding to it the equation which relates the voltage under control e_s to the remaining variables. We neglect in this case the active impedances of the stator circuits.

$$pu_d + u_q + pe_d = e_n \sin\vartheta; \tag{7a}$$

$$-u_d + pu_q - e_d = -e_n \cos\vartheta; \tag{7b}$$

$$\mu p u_d + (\rho_r + p)\, e_d = \rho_r e_r; \tag{7c}$$

$$Kps + u_q e_d = xM_m; \tag{7d}$$

$$(e_d + hu_d)^2 + h^2 u_q^2 = e_s^2. \tag{7e}$$

In the presence of series excitation, the voltage acting in the rotor circuit is equal to:

$$e_r = k_c (E_2 - e_s) + e_c; \tag{8}$$

where k_c – is the regulation factor.

The voltage of the series exciter, when expressed in relative units, can be written in this form:

$$e_c = c_r e_d. \tag{9}$$

Let us assume that the series exciter B_s is not saturated, and, consequently, coefficient C_r, which is equal in relative units to the degree of compensation of the resistance of the rotor circuit, is constant.

Taking into account (8) and (9) we find that the equation of the rotor circuit (7c) assumes this form:

$$\mu p u_d + (\alpha \rho_r + p)\, e_d = \rho_r k_c (E_2 - e_s), \tag{10}$$

Where $\alpha = 1\ c_r$.

Static characteristics of voltage control can be obtained from equations (7) for steady-state conditions:

$$u_q = e_n \sin\theta; \tag{11a}$$

$$u_d + e_d = e_n \cos\theta; \tag{11b}$$

$$\alpha e_d = k_c (E_2 - e_s); \tag{11c}$$

$$(e_d + h u_d)^2 + h^2 u_q^2 = e_s^2. \tag{11d}$$

From equation (11c) we find:

$$e_s = E_2 - \frac{\alpha}{k_c} e_d. \tag{12}$$

From the expression obtained, it follows that when $\alpha = 0$, i.e. in the presence of full compensation of the resistance of the rotor circuit by series excitation, the voltage control is astatic and depends neither on the magnitude and character of the load of a synchonous machine nor on the parameters of the stator circuit.

From (12) it follows further that, for considerable values of the factor k_c the influence of the instability of quantity α, which is possible due to the temperature variation of the field winding resistances, becomes less important.

When $\alpha \neq 0$, it follows from equations (11) that:

$$e_s^2 - 2\,\frac{k_c (1-h)^2 E_2 + \alpha k_c (1-h)\, e_n \cos\theta}{k_c^2 (1-h)^2 - \alpha^2}\, e + \\ + \frac{[\alpha e_n \cos\theta + k_c (1-h)\, E_2]^2 + (\alpha h e_n \sin\theta)^2}{k_c^2 (1-h)^2 - \alpha^2} = 0. \tag{13}$$

From the equation obtained, the relationship $e_s = f(\alpha)$ is plotted in Fig. 4 when $\theta = 0$ and $\theta = 90°$. In this case, the normal voltage E_2 was determined from the conditions, that, when $\theta = 0$, the quantity e_s is equal to unity for all values of α. As follows from the graphs, the values of α within the limits of from -0.05 to $+0.1$ are important in practice. For other values of α, the error in control is excessively large, therefore, a special voltage corrector would be required. In plotting the curves shown in Fig. 4, the regulation factor was assumed to be $k_c = 3.5$.

To evaluate the influence of automatically controlled series excitation on static stability, we have to change from equations (7) to equations of small

disturbances, neglecting transients in the stator:

$$\left.\begin{aligned} \Delta u_q - e_n \cos \vartheta_0 \Delta\vartheta = 0; \\ -\Delta u_d - \Delta e_d - e_n \sin \vartheta_0 \Delta\vartheta = 0; \\ \mu p \Delta u_d + (\alpha\rho_r + p)\,\Delta e_d - \rho_r k_c \Delta e_s = 0; \\ e_{d0}\Delta u_q + u_{q0}\Delta e_d + Kp^2\Delta\vartheta = 0; \\ \Delta e_s = -\frac{(e_{d_0} + hu_{d_0})(\Delta e_d + h\Delta u_d) + h^2 u_{q_0}\Delta u_q}{e_{s0}}. \end{aligned}\right\} \qquad (14)$$

In the presence of non-inertial voltage control according to the law $\Delta e_r = k\,\Delta e_s$, we have to put in the set of equations (14) $\alpha = 1$ and $k_c = k$.

From the four of the stability conditions given by Hurvitz, which follow from the characteristic equation of the set of equations (14), the dominant condition is:

$$a_3 = \rho_r e_{d0} e_n \left\{ \alpha \cos \vartheta_0 + \frac{k_c}{e_{s0}} (1 - h)\,[he_n + \right.$$
$$\left. + (1 - h)\, e_{d0} \cos \vartheta_0 \right\} > 0. \qquad (15)$$

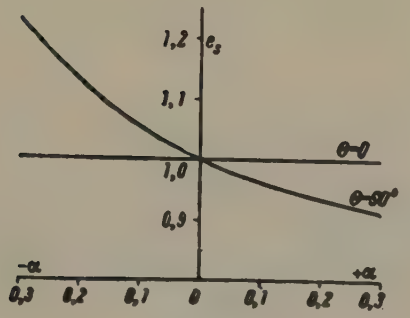

FIG. 4. Accuracy of automatic control as a function of factor α.

Fig. 5 shows curves of relationships for ordinary control ($\alpha = 1$) and automatically controlled series excitation:

$$A_3 = \frac{a_3}{\rho_r e_{d0} e_n} = \alpha \cos \vartheta_0 + \frac{k_c}{e_{s0}} (1 - h)\,[he_n + $$
$$+ (1 - h)\, e_{d0} \cos \vartheta_0.$$

The example given in [6] is reproduced here as a case of the ordinary control ($a = 1$).

The influence of series excitation on dynamic stability can be estimated by the extent to which the field flux of a synchronous machine can be maintained and even increased in emergency processes.

Since the greatest decrease in flux is possible in the presence of a generator short-circuit, this case of emergency, in analogy to [1], is discussed below.

In investigating series excitation, Shchedrin comes to the conclusion that "the connexion of an unsaturated series exciter in series with a shunt exciter can produce an extremely powerful effect in sustaining the magnetic flux of a synchronous machine. This effect is equivalent to a ten-fold increase in the time constant of the generator excitation circuit" * [1].

Riudenberg also points out the use of series excitation in order to increase stability, [7].

To evaluate the efficiency of automatically controlled series excitation, the variation of the aperiodic component of the excitation current in the presence of the generator short-circuit was investigated [see 1].

Such an analysis permitting a simplification of the problem, is at the same time very instructive since the largest drop in flux is possible at short-circuit. So far as the character of the flux variation is concerned it is represented by the aperiodic component of the synchronous e.m.f.

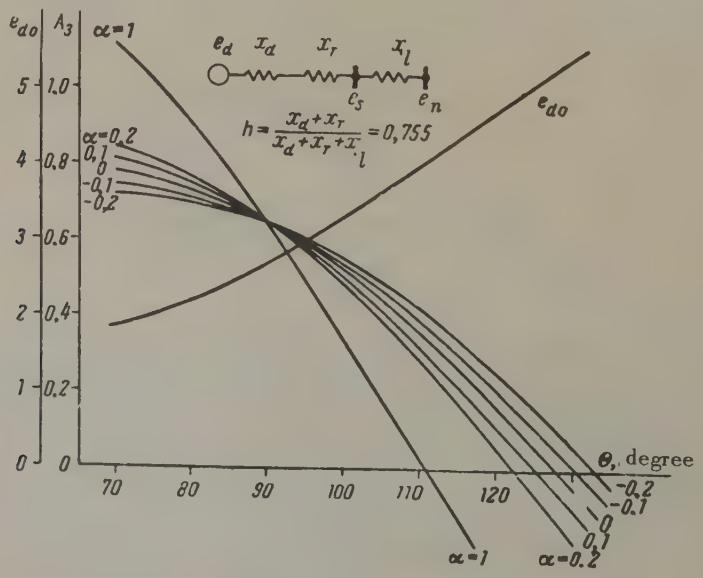

FIG. 5. Curves to determine the limiting angles.

*In the case, when the series excitation ensures 90 per cent of the rated value of the m.m.f.

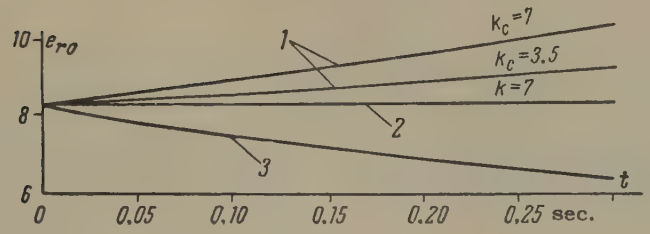

FIG. 6. The aperiodic component of the excitation current for different kinds of automatic control of excitation.
1. automatically controlled series excitation;
2. forced excitation;
3. no automatic control.

The e.m.f. e_d is determined by solving equations (7). In this case the right hand sides of equations (7a) and (7b) are made equal to zero, but the right-hand side of equation (7c) is $\rho_r - e_{ro}$ in the absence of the excitation control, and $\rho_r\, k e_{ro}$ if the non-inertial regulator is used. Here k is the regulation factor, which in this case is equal to the multiplicity of the ceiling excitation.

In the presence of automatically controlled series excitation, $e_s = 0$ and, consequently, the right hand side of equation (10) is $\rho_r\, k_c\, E_2$. The solution of equations (7) for the short-circuit of a generator on no load, i.e. for initial conditions $t = 0$, $u_{d0} = 0$, $U_{q0} = 0$, $e_d = e_{r0}$, gives the operator solutions for e_d and for the aperiodic component of its original function. See the following table with the notations:

$$\sigma = 1 - \mu = \frac{x'_d}{x_d};\quad T'_d = 2\pi f \frac{\sigma}{\rho_r}.$$

Fig. 6 shows curves plotted from the formulae given in the table. These curves were constructed for the circuit shown in Fig. 3b in this case, the excitation ceiling relating to the no-load excitation was taken as seven.

Certain of the above assumptions have been verified under laboratory conditions on d.c. and a.c. generators. In particular, experiments which have been carried out have confirmed control stability not only for small and zero quiescence but also for negative quiescence.

The circuit of the automatically controlled series excitation was tested on a model turbo-generator of the electro-dynamical d.c. NII class when an asynchronous motor of comparable power was connected. In this case, the sources of the normal and controlled voltage E_n and e_s were connected to the separate field windings of the balancing exciter, which was series connected to the armature of the series exciter. In the latter instead of series winding ordinary shunt winding was used, which was connected in parallel to the rotor winding.

Oscillograms of the starting of the motor are shown in Fig. 7.

TABLE 1.

Type of the excitation control	Operator solution $e_d(p)$	Aperiodic component e_{da}
No control	$e_{r0}\dfrac{p^3+\frac{\rho_r}{\sigma}p^2+\frac{1}{\sigma}p+\frac{\rho_r}{\sigma}}{\left(p+\frac{\rho_r}{\sigma}\right)(p^2+1)}$	$e_{r0}\left[\dfrac{x_d}{x'_d}e^{-\frac{t}{T'_d}}+\left(1-e^{-\frac{t}{T'_d}}\right)\right]$
For $\alpha=1$	$e_{r0}\dfrac{p^3+\frac{k\rho_r}{\sigma}p^2+\frac{1}{\sigma}p+k\frac{\rho_r}{\sigma}}{\left(p+\frac{\rho_r}{\sigma}\right)(p^2+1)}$	$e_{r0}\left[\dfrac{x_d}{x'_d}e^{-\frac{t}{T'_d}}+k\left(1-e^{-\frac{t}{T'_d}}\right)\right]$
With automatically controlled series excitation for $\alpha\neq 0$	$\dfrac{\rho_r k_c E_2(p^2+1)+\sigma e_{d0}\,p\left(p^2+\frac{1}{\sigma}\right)}{\sigma\left(p+\alpha\frac{\rho_r}{\sigma}\right)(p^2+1)}$	$e_{r0}\dfrac{x_d}{x'_d}e^{-\alpha\frac{t}{T'_d}}+\dfrac{k_c}{\alpha}E_2\left(1-e^{-\alpha\frac{t}{T'_d}}\right)$
With automatically controlled series excitation for $\alpha=0$		$e_{r0}\dfrac{x_d}{x'_d}+k_c E_2\dfrac{t}{T'_d}$

The oscillogram (Fig. 7a) is an example of the control with positive quiescence.

$$\delta = \frac{u_{xx} - u_n}{u_{xx}} = \frac{1-0.94}{1} = 0{,}06.$$

In this case, factor $k_c = 1$; currents in the windings of the balancing exciter are equal to the excitation currents on no-load when the exciter is used in the ordinary circuit of the shunt exciter.

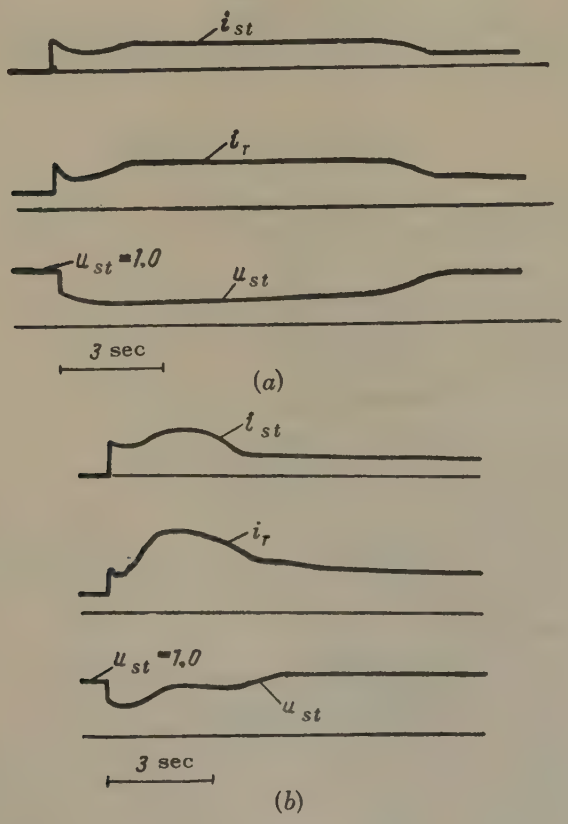

FIG. 7. Oscillograms of the starting of an asynchronous motor..

The oscillograms in (Fig. 7b) are examples of the control with negative quiescence.

$$\delta = \frac{u_{xx} - u_n}{u_{xx}} = \frac{1 - 1.1}{1} = -0.1.$$

Negative quiescence is obtained by decreasing the resistance in the excitation circuit. In this experiment $k_c \approx 2$.

These oscillograms confirm the stability and effectiveness of the control system discussed both for the positive and negative quiescence.

As can be seen from the oscillograms, the excitation current "follows" the stator current and can be maintained equal to or greater than the initial value of the aperiodic component. The decrease of the excitation current at the beginning of the process is explained mainly by the inductance of the shunt winding, which plays the role of the "series" winding of the exciter B_s.

The considerations given above permit the conclusion that the automatically controlled series excitation of synchronous machines is a very simple excitation automatic control system and allow us to obtain a considerably greater effect in preserving static and dynamic stability than does the use of automatic regulators acting on the shunt or separate excitation.

LIST OF LETTER NOTATIONS

R – the load resistance of a d.c. generator;
r'_1, r_1 – resistances of the armature circuit;
L_1 – inductance of the armature circuit;
r_2, r'_2 – resistances of the excitation circuit;
L_2 – inductance of the excitation circuit;
i_1 – load current of a d.c. generator;
i_2 – current of the excitation circuit of a d.c. generator;
e_1 – e.m.f. of a d.c. generator;
e_3 – e.m.f. of the series exciter of a d.c. generator
E_2 – standard voltage of a d.c. generator.
u – terminal voltage of a d.c. generator.
U_d, U_q – axial and cross components of the voltage drop in the stator circuit.
e_d – e.m.f. in the axial circuit;
e_r – excitation voltage;
e_s – terminal voltage of a generator;
e_n – voltage at the receiving end of a transmission line;
θ – angle between e.m.f. e_d and voltage e_s;
ρ_r – decrement of the rotor circuit;
i_r – rotor current;
e_c – voltage of a series exciter.

Translated by S. Szymanski

REFERENCES

1. N.N. Shchedrin; *Vliianiye reguliatora Tirrillia na perekhodnoye i ustanovivsheyessia dvizheniye sinkhronnoi mashiny i nekotoryye voprosy kinetiki vozbuzhdeniia. Otchet po nauchno-issledovatelskoi rabote laboratorii vysokikh napriazhenii im Smurova (Influence of the Tirrill regulator on the transient and steady state motion of a synchronous machine and certain problems of excitation kinetics. Report on the scientific and research work of the Smurov H.T. laboratory)* (1935).
2. P.S. Zhdanov; Kompoundiravannyye skhemy vozbuzhdeniia sinkhronnykh mashin. (Compound excitation circuits of synchronous machines) *VEP*, No. 9 (1943).

3. E.L. Harder; G.E. Valentine *Trans. Amer. Inst. Elect. Engrs.* Vol. 64, 601 (1945).
4. W. Harris; *Elect. Engng.* Vol. 65, 118, No. 3 (1946).
5. A.B. Cheliustkin; Rototrol i ego primeneniye (Rototrol and its application), *Amerikanskaia tekhnika i promyshlennost,* No. 7 (1944).
6. A.A. Gorev; *Perekhodnye protsessy sinkhronnoi mashiny (Transients in a synchronous machine),* Gosenergoizdat (1950).
7. P. Ruidberg; *Perekhodnye protsessy v elektroenergeticheskikh sistemakh (Transients in electrical power systems),* Izd. Inostrannoi literatury (1955).

NEGATIVE SEQUENCE FILTERS WITH INDEPENDENT ARMS *

A.B. VITANOV

Bulgaria, Sofia

(Received 30 April 1957)

Symmetrical component filters are now being used very widely. The most common are negative sequence filters almost all are filters with independent arms. These filters are subdivided into many classes, groups etc. and to each subdivision there are appropriate formulae. However, these classes and groups do not cover the infinite variety of filters with independent arms.

In this article an attempt is made to lay down the foundation of a single theory for all filters with independent arms and to give general formulae, the analysis of which should enable us to choose the optimum variants of filters.

Filters of negative sequence voltage

In its general form a device for distinguishing any one voltage symmetrical component consists of a voltage converter and a filter (Fig. 1).

In the voltage converter, the applied voltages $\dot{U}_{AB}$ and $\dot{U}_{BC}$ are converted into those required:

$$\left.\begin{aligned} \dot{U}_m &= k\dot{U}_{AB} + k_2\dot{U}_{BC}\ ; \\ \dot{U}_n &= k_3\dot{U}_{AB} + k_4\dot{U}_{BC}\ . \end{aligned}\right\} \qquad (1)$$

In a particular case, a device may be used without a converter in this case it consists only of a filter, to which voltages are applied:

$$\dot{U}_m = \dot{U}_{AB} \text{ and } \dot{U}_n = \dot{U}_{BC}\ .$$

Filters with independent arms may have two arms (Fig. 2) or one arm (Fig.3); single-arm filters are a special case of two arm filters.

* *Elektrichestvo*, No. 6, 29-32, 1958.

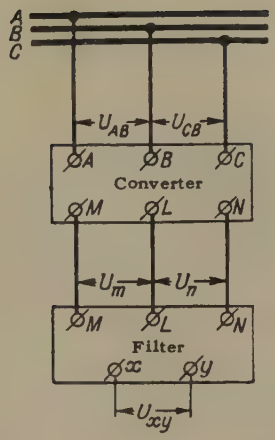

FIG. 1. Block diagram of a device for distinguishing voltage symmetrical components.

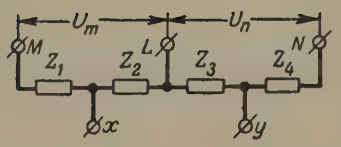

FIG. 2. A two-arm voltage filter.

Two arm filters.

In order that the circuit shown in Fig. 2 should be a filter of negative sequence voltage, it is necessary and sufficient that, when the voltage of the positive sequence U_1 is applied to the voltage converter, the potentials of the points x and y should be equal; i.e.

$$\dot{U}_x = \dot{U}_y \,. \tag{2}$$

Assuming $U_M = 0$ we get:

$$\left.\begin{aligned} \dot{U}_x &= -\frac{Z_1}{Z_1+Z_2}\dot{U}_m; \\ \dot{U}_y &= -\dot{U}_m - \frac{Z_3}{Z_3+Z_4}\dot{U}_n. \end{aligned}\right\} \tag{3}$$

Assuming in equation (1) that $\dot{U}_{AB}$ and $\dot{U}_{BC}$ are voltages of the positive sequence $\dot{U}_{AB} = U_1$ and $\dot{U}_{BC} = a^2 U_1$, we find:

$$\left.\begin{aligned} \dot{U}_{m1} &= U_1(k_1 + a^2 k_2); \\ \dot{U}_{n1} &= U_1(k_3 + a^2 k_4). \end{aligned}\right\} \tag{4}$$

Let us introduce the following substitutions:

$$\left.\begin{aligned} \xi &= \frac{Z_2}{Z_1}; \quad \eta = \frac{Z_4}{Z_3}; \\ n &= \frac{Z_3+Z_4}{Z_1+Z_2}; \quad p = \frac{k_1 + a^2 k_2}{k_3 + a^2 k_4}. \end{aligned}\right\} \tag{5}$$

Using the relationships obtained, after a number of transformations, we get:

$$\eta = -1 - \frac{1+\xi}{\xi} \cdot \frac{1}{p}. \tag{6}$$

Parameters of the negative sequence voltage filter should satisfy this condition; it is assumed below that this condition is always satisfied.

On applying to the circuit the negative sequence voltage U_2, we get at the terminals x, y the no-load voltage U_{xy}:

$$\dot{U}_{xy} = \dot{U}_{x2} - \dot{U}_{y2}. \tag{7}$$

In this case $\dot{U}_{AB} = U_2$, $\dot{U}_{BC} = aU_2$, and therefore:

$$\left.\begin{aligned} \dot{U}_{m2} &= U_2(k_1 + ak_2); \\ \dot{U}_{n2} &= U_2(k_3 + ak_4). \end{aligned}\right\} \tag{8}$$

Substituting (8) into (3) and afterwards into (7) we get:

$$\dot{U}_{xy} = j\sqrt{3}\,\frac{U_2\xi}{1+\xi}\,\frac{k_2k_3 - k_1k_4}{k_3 + a^2k_4}. \tag{9}$$

The ratio of no-load running m is defined as the ratio of the no-load voltage to the negative sequence voltage U_2:

$$m = \frac{\dot{U}_{xy}}{U_2} = j\sqrt{3}\,\frac{\xi}{1+\xi}\,\frac{k_2k_3 - k_1k_4}{k_3 + a^2k_4}. \tag{10}$$

The total impedance of the filter short-circuit Z_{sf} is the impedance measured on the secondary terminals when the primary ones are short-circuited, [1].

From the circuit shown in Fig. 2 it is seen that

$$Z_{s.f} = \frac{Z_1Z_2}{Z_1 + Z_2} + \frac{Z_3Z_4}{Z_3 + Z_4}. \tag{11}$$

Substituting (5) into (11) and taking into consideration (6) we get:

$$Z_{s.f} = \frac{\xi Z_1}{1+\xi}[1 - n\xi p^2 - n(1+\xi)p]. \tag{12}$$

If a relay is connected at the point x and y (Fig. 2), then its current, voltage and power are determined by expressions [1 and 2]:

$$\dot{I}_p = \frac{\dot{U}_{xy}}{Z_p + Z_{s.f}}; \tag{13}$$

$$\dot{U}_p = \frac{\dot{U}_{xy} Z_p}{Z_p + Z_{s.f}}; \tag{14}$$

$$\dot{S}_p = \hat{U}_p \dot{I}_p = \left| \frac{\dot{U}_{xy}}{Z_p + Z_{s.f}} \right| Z_p^*. \tag{15}$$

Here and below the conjugate values of the quantities, which are not functions of time, are denoted by a superscript *.

When U_2 = const, the relay gives maximum power when $|Z_p| = |Z_{s.f}|$. Since this corresponds to the maximum sensitivity of the filter-relay circuit, this condition is nearly always satisfied by the rewinding of the relay.

Assuming that the condition $|Z_p| = |Z_{s.f}|$ is satisfied and denoting $\phi = \phi_p - \phi_{s.f}$, where ϕ_p and $\phi_{s.f}$ are respectively angles of impedances, from (13), (14), and (15) we get the following formulae:

$$\dot{I}_p = \frac{j\sqrt{3}U_2}{Z_1(1+e^{j\varphi})} \frac{1}{1+np(1+\xi-\xi p)} \frac{k_2k_3 - k_1k_4}{k_3 + a^2k_4}; \tag{16}$$

$$\dot{U}_p = \frac{j\sqrt{3}U_2}{1+e^{-j\varphi}} \frac{\xi}{1+\xi} \frac{k_2k_3 - k_1k_4}{k_3 + a^2k_4}; \tag{17}$$

$$\dot{S}_p = \frac{3U_2^2}{Z_1(1+e^{j\varphi})^2} \frac{1}{\left(1+\frac{1}{\xi^*}\right)[1+np(1+\xi-\xi p)]} \frac{(k_2k_3 - k_1k_4)^2}{k_3^2 - k_3k_4 + k_4^2}. \tag{18}$$

In determining the power consumed by the filter, we shall only take into account the power which is due to the voltage of the positive sequence [1, p. 24].

$$\dot{S}_f = \frac{\dot{U}_{m1}^2}{Z_1 + Z_2} + \frac{\dot{U}_{n1}^2}{Z_3 + Z_4}.$$

Taking into account (4), (5) and (6) we get:

$$\dot{S}_f = \frac{U_1^2}{Z_1(1+\xi)} \left[k_1^2 - k_1k_2 + k_2^2 + \right.$$
$$\left. + \frac{1}{n}(k_3^2 - k_3k_4 + k_4^2) \right]. \tag{19}$$

It is quite sufficient to use the following filter characteristics:

(1). Ratio of the maximum power on the relay to the power consumed when $U_1 = U_2$:

$$\alpha = \left(\frac{\dot{S}_p}{\dot{S}_\phi}\right)_{U_1=U_2} = \tag{20}$$

$$= \frac{3(k_2k_3 - k_1k_4)^2}{(1+e^{j\tau})(k_3^2 - k_3k_4 + k_4^2)\left[k_1^2 - k_1k_2 + k_2^2 + \frac{1}{n}(k_3^2 - k_3k_4 + k_4^2)\right][1+np(1+\xi-\xi p)]}.$$

(2). The ratio of the relative unbalanced voltage, caused by the frequency deviation to the relative frequency variation:

$$\gamma_f = \frac{d\dot{U}_{nb}}{mU_1} : \frac{df}{f_0} = \frac{d\dot{U}_{nb}}{df}\frac{f_0}{mU_1}, \tag{21}$$

where $\dot{U}_{nb} = \dot{U}_{xy_1} = \dot{U}_{x1} - \dot{U}_{y1}$
From (3), (4) and (5) we get:

$$\dot{U}_{nb} = U_1\left[\frac{\xi}{1+\xi}(k_1 + a^2k_2) + \frac{1}{1+\eta}(k_3 + a^2k_4)\right].$$

Differentiating this equation for f:

$$\frac{d\dot{U}_{nb}}{df} = U_1\left[\frac{1}{(1+\xi)^2}\frac{d\xi}{df}(k_1 + a^2k_2) - \right.$$
$$\left. - \frac{1}{(1+\eta)^2}\frac{d\eta}{df}(k_3 + a^2k_4)\right].$$

Substituting the value of this derivative into (21) and taking into account (6) and (10) we find:

$$\gamma_f = \frac{-j}{\sqrt{3}}\left(\frac{1}{\xi}\frac{d\xi}{df} - \xi\frac{d\eta}{df}p\right)\frac{1}{1+\xi} \times$$
$$\times f_0\frac{(k_1 + a^2k_2)(k_3 + a^2k_4)}{k_2k_3 - k_1k_4}, \tag{22}$$

where the values of derivatives and quantity ξ are calculated for $f = f_0$.

The derivatives which appear in expression (22) are calculated by the formulae:

$$\left(\frac{d\xi}{df}\right)_{f=f_0} = \frac{j}{f_0}\,\frac{|X_2|\,Z_1 - |X_1|\,Z_2}{Z_1^2}\,; \tag{23}$$

$$\left(\frac{d\eta}{df}\right)_{f=f_0} = \frac{j}{f_0}\,\frac{|X_4|\,Z_3 - |X_3|\cdot Z_4}{Z_3^2}\,. \tag{24}$$

Substituting (23) and (24) into (22) and taking into consideration (5) and (6) we get:

$$\gamma_f = \frac{1}{Z_1(1+\xi)}\left[-|X_1| + \frac{|X_2|}{\xi} + \right.$$
$$\left. + \frac{|X_3|}{n}\left(1 + \frac{1}{p} + \frac{1}{\xi p}\right) + \frac{|X_4|}{n}\right]\frac{(k_1 + a^2 k_2)(k_3 + a^2 k_4)}{\sqrt{3}\,(k_2 k_3 - k_1 k_4)}\,. \tag{25}$$

Single arm filters.

The single arm filters are a particular case of the two-arm negative sequence filters; for the single-arm filters $Z = \infty$, $Z_4 = 0$. In this case ξ and η assume the following values:

$$\eta = \frac{Z_4}{Z_3} = 0; \quad \xi = -\frac{1}{1+p}\,. \tag{26}$$

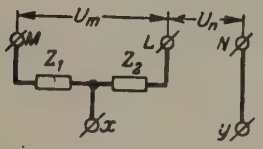

FIG. 3. A single-arm voltage filter.

For the single-arm filters $n = \infty$. If we repeat the deduction of all formulae obtained above with respect to the single-arm filters, we find that they can be obtained by the formal removing of all terms containing n (these terms are characteristic for the presence of the second arm).

Removing from expressions (10), (12), (16), (17), (18), (19), (20) and (25) all terms containing n and substituting into these expressions the quantity ξ from (25), we get for the single-arm filters the following expressions:

$$m = -j\sqrt{3}\,\frac{k_3 k_2 - k_1 k_4}{k_1 - a^2 k_2}\,; \tag{27}$$

$$Z_{s.f} = -\frac{Z_1}{p}; \tag{28}$$

$$I_p = \frac{j\sqrt{3}U_2}{Z_1(1+e^{j\varphi})} \frac{k_2k_3 - k_1k_4}{k_3 + a^2k_4}, \tag{29}$$

$$\dot{U}_p = \frac{-j\sqrt{3}U_2}{1+e^{-j\varphi}} \frac{k_3k_2 - k_1k_4}{k_1 + a^2k_2}; \tag{30}$$

$$\dot{S}_p = -\frac{3U_2^2}{Z_1(1+e^{j\varphi})^2} \frac{(k_3k_2 - k_1k_4)^2}{(k_1 + ak_2)(k_3 + a^2k_4)}; \tag{31}$$

$$\dot{S}_\phi = \frac{U_1^2}{Z_1}(k_1 + ak_2)(k_1 + a^2k_2 + k_3 + a^2k_4); \tag{32}$$

$$a = \frac{-3(k_3k_2 - k_1k_4)^2}{(1+e^{j\varphi})^2(k_1 + ak_2)^2(k_3 + a^2k_4)[k_1 + k_3 + a^2(k_2 + k_4)]}; \tag{33}$$

$$\gamma_f = jf_0\frac{d\xi}{df}\frac{[k_1 + k_3 + a^2(k_2 + k_4)]^2}{\sqrt{3}(k_2k_3 - k_1k_4)} =$$

$$= -\frac{1}{Z_1}[X_1 + X_2(1+p)]\frac{(k_3 + a^2k_4)(k_1 + a^2k_2 + k_3 + a^2k_1)}{\sqrt{3}(k_2k_3 - k_1k_4)}. \tag{34}$$

Negative sequence current filters

In the general form a filter for distinguishing any current symmetrical component (Fig. 4) is similar to a filter for distinguishing voltage symmetrical components and consists of the same parts.

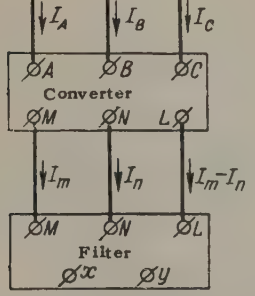

FIG. 4. Block diagram for distinguishing current symmetrical components.

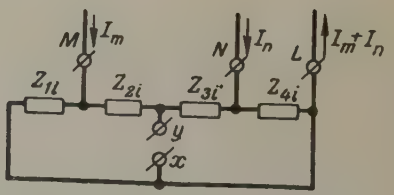

FIG. 5. A two-arm current filter.

As it known, the circuit of every current filter can be obtained from the circuit of the voltage filter by arranging a binary circuit with conjugate elements.

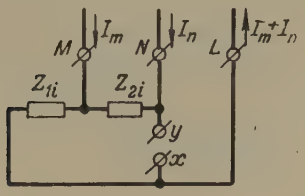

FIG. 6. A single-arm current filter.

In this way, the circuits shown in Figs 2 and 3 can be converted into general circuits of two-arm and single-arm negative sequence current filters.
In this case:

$$\left.\begin{aligned} \dot{I}_m &= (k_1 + ak_2)\,\dot{I}_A; \\ \dot{I}_n &= (k_3 + ak_4)\,\dot{I}_A \end{aligned}\right\} \tag{35}$$

and

$$Z_i = \frac{1}{Z^*}, \tag{36}$$

where Z_i is the impedance of the current filter corresponding to the impedance Z of the voltage filter.

All the expressions deduced for the voltage filters therefore remain valid for the current filters, if we introduce into these expressions the following parameters:

$$Z_1 = \frac{1}{Z^*_{1i}}; \tag{37}$$

$$\xi = \frac{Z^*_{1i}}{Z^*_{2i}}; \tag{38}$$

$$n = \frac{Z^*_{1i}\,Z^*_{2i}}{Z^*_{3i}\,Z^*_{4i}}\,\frac{Z^*_{3i} + Z^*_{4i}}{Z^*_{1i} + Z^*_{2i}} \tag{39}$$

and substitute everywhere instead of U_1 the current of the positive sequence I_1, and instead of U_2 the current of the negative sequence I_2.

In analysing the results obtained we have to take into consideration the following.

For current filters:

$$m = \frac{I_{xy}}{I_2}, \tag{40}$$

where $I_{x\gamma}$ is the short-circuit current flowing between the short-circuited terminals x and γ when negative sequence currents I_2 enter the filter.

To the short-circuit impedance of the voltage filter $Z_{s.f}$ there corresponds in the current filter, a no-load impedance $Z_{s.c}$, which is measured on secondary terminals, when the primary terminals are open:

$$Z_{c.s} = \frac{1}{Z^*_{s.f}}. \tag{41}$$

For current filters, formulae (16), (17), (18), (20) or (29), (30), (31), (33) give conjugate values of the sought quantities; i.e.

$$I_{pi} = \hat{I}_p,\ \dot{U}_{pi} = \hat{U}_p,\ \dot{S}_{pi} = \hat{S}_p,\ a_i = a^*.$$

When total impedances, which are the result of the series connexion of resistances and reactances, are present in filters, then formulae (25) and (34) for γ are not correct since the value of the derivatives $d\xi/df$ and $d\eta/df$ is changed. The new values of the derivatives are:

$$\left(\frac{d\xi_i}{df}\right)_{f=f_0} = \frac{j}{f_0}\,\frac{|X_{2i}|\,Z^*_{1i} - |X_{1i}|\,Z^*_{2i}}{Z^{*2}_{2i}}; \tag{42}$$

$$\left(\frac{d\eta_i}{df}\right)_{f=f_0} = \frac{j}{f_0}\,\frac{|X_{4i}|\,Z^*_{3i} - |X_{3i}|\,Z^*_{4i}}{Z^{*2}_{4i}}. \tag{43}$$

Substituting (42) and (43) into (22) and (34) and taking into consideration (36) and (38), after transformation we get:

for the two-arm current filter of negative sequence,

$$\gamma_{fi} = \frac{Z_1}{1+\xi}\{\xi|X_{2i}| - |X_{1i}| + \\ + n(\xi_p + \xi - 1)[|X_{4i}|(\xi p + \xi + 1) + |X_{3i}|\xi p]\} \times \\ \times \frac{(k_1 + a^2k_2)(k_3 + a^2k_4)}{\sqrt{3}(k_2k_3 - k_1k_4)};$$

for the single-arm current filter of negative sequence,

$$\gamma_{fi} = -Z_1[|X_{1i}|(1+p) + |X_{2i}|]\,\frac{(k_3 + a^2k_4)^2}{\sqrt{3}(k_2k_3 - k_1k_4)}$$

The formulae obtained can be used to determine the characteristics of any filter with independent arms and the filter parameters and to choose the optimum filter.

Translated by S. Szymanski

REFERENCES

1. V.L. Fabrikant; *Filtry simmetricheskikh sostavliaiushchikh (Symmetrical components Filters)*, Gosenergoizdat (1950).
2. A.M. Fedoseyev; *Releinaia zashchita elektricheskikh sistem (The relay protection of electrical systems)*, Gosenergoizdat (1952).

CALCULATION OF THE CHARACTERISTICS OF AN ELECTRIC DRIVE WITH FREQUENCY CONTROL BY THE EQUIVALENT RESISTANCE METHOD*

V.V. ARTAMONOV

Krasnoiarsk Polytechnic Institute

(Received 3 February 1958)

The analytical method of calculating the characteristics of an electric drive with frequency control [3] is based on the equivalent circuit of an asynchronous motor, (Fig. 1). This method is discussed in [1 and 2]. It is cumbrous and not sufficiently accurate. This is due to the complexity of the calculations of magnetic circuit saturation and of the current displacement in the rotor. In most cases this compels us to assume that the parameters of the equivalent circuit are constant.

A method is proposed which permits us to obtain more accurate results, if in calculating we take as a basis the motor characteristics given for the rated frequency of the supply.

The equivalent circuit of an asynchronous motor for variable frequency.

The equivalent circuit shown in Fig. 1 can be represented in the form of two parts; one of them reproduces only the influence of the supply current frequency, the other - only of the load.

For this purpose let us separate the resistance of the stator winding from the resistance r_1 / α .

$$\frac{r_1}{\alpha} = r_1 \frac{1-\alpha}{\alpha} + r_1. \tag{1}$$

In this case, the equivalent circuit of an asynchronous motor for any frequency can be represented as a series connexion of an additional resistance::

$$r_d = r_1 \frac{1-\alpha}{\alpha} \tag{2}$$

with an ordinary standard equivalent circuit (Fig. 2).
The "internal" voltage of this equivalent circuit, we shall in the following call the rated voltage.

* *Elektrichestvo* No. 6, 66-69, 1958.

$$\dot{U}_{r.p.} = \frac{\dot{U}_{1p}}{a} - \dot{I}_1 r_d \tag{3}$$

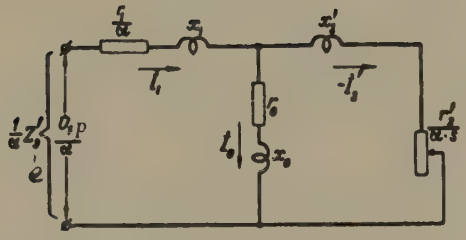

FIG. 1.

Equivalent circuit of an asynchronous motor for the supply variable frequency $U_{1.p.}$ Complex phase voltage across the stator winding at the nominal frequency; $a = f/f_n$ - current frequency parameter in the stator winding;
Z'_e – the motor equivalent impedance at a supply variable frequency; $s = \dfrac{a\omega_c - \omega}{a\omega_c}$ – the rotor slip;

I_1, I_2, I_0 – currents in the corresponding arms of the equivalent circuit;

$r_1, r_2, r_0, X_1, X_2, X_0$ – resistances of the arms of the equivalent circuit.

Its influence on the motor properties for a frequency differing from the normal is analogous to the influence of the voltage U_1 on the stator terminals of the motor, for the nominal frequency. Thus, for example, assuming that the parameters of the equivalent circuit are constant, we get for the driving torque of the rotor the following formula:

$$M = M_k \left(\frac{U_p}{U_n}\right)^2 \frac{2 + as_k}{\frac{\beta}{s_k} + \frac{s_k}{\beta} + as_k}, \tag{4}$$

where M_k and s_k are the critical torque and slip of the natural mechanical characteristics respectively.

Thus, the motor mechanical characteristic can be easily obtained for any supply frequency by using the known relationship between the rated voltage and the load parameter β by simple recalculation of the natural mechanical characteristic.

The latter can be given analytically or graphically.

The equivalent impedance of this part of the equivalent circuit, which remains after the separation of the resistance r_d, when expressed as a function of the parameter β, represents an ordinary equivalent impedance of the motor, which corresponds to the nominal frequency:

$$Z_e = R_e + jX_e. \tag{5}$$

In this case the equivalent impedance, which also accounts for the influence of the supply frequency, is obtained on the basis of the equivalent circuit, shown in Fig. 2.

$$\frac{1}{\alpha} Z'_e = Z_e + r_d. \tag{6}$$

Equality (6) gives the relationship between the motor characteristics, which correspond to various frequencies.

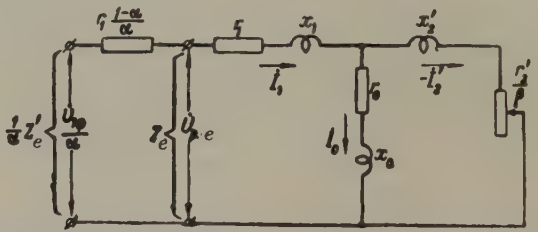

Equivalent circuit of an asynchronous motor for the supply variable frequency reduced to the nominal frequency.

$U_{r.p.}$ – rated phase voltage across the stator winding;

$\beta = f/f_n$ – parameter of the current frequency in the rotor (load parameter);

Z_e – equivalent impedance of the motor for the supply nominal frequency.

I_1, I_2, I_0 – currents in the corresponding arms of the equivalent circuit;

$r_1, r_2, r_0, X_1, X_2, X_0$ – resistances of the arms of the equivalent circuit.

Active R_e and reactive X_e components of the motor equivalent impedance, corresponding to the nominal frequency, are usually determined by means of the known parameters of the equivalent circuit:

$$R_e = r_1 + \frac{\beta^2 r_0 x_2'^2 + \beta z_0^2 r_2' + r_0 r_2'^2}{\beta^2 (z_0^2 + x_2'^2 + 2x_0 x_2') + \beta \cdot 2 r_0 r_2' + r_2'^2}; \tag{7}$$

$$X_e = x_1 + \frac{\beta^2 (z_0^2 x_2' + x_0 x_2'^2) + x_0 r_2'^2}{\beta^2 (z_0^2 + x_2'^2 + 2x_0 x_2') + \beta 2 r_0 r_2' + r_2'^2}. \tag{8}$$

However, if we find the equivalent impedance in this way, the method of calculation discussed now has no advantage in comparison with the existing one so far as

the accuracy and volume of calculations are concerned.

At shown above, to determine the motor properties for an arbitrary frequency it is sufficient to know the dependence of the equivalent impedance on the slip and the natural mechanical characteristic, which can be obtained experimentally. Therefore, the field of the most effective application of the method discussed is not the calculation of characteristics for an arbitrary frequency on the basis of given parameters of the equivalent circuit, but the re-evaluation of characteristics, appropriate to the nominal frequency, for any other arbitrary frequencies.

Calculation of operating characteristics

Under steady-state conditions the properties of an electric drive are determined by the families of: mechanical characteristics, characteristics of the current fed to the motors under control by the frequency converter, curves of efficiency, cos ϕ and the torque developed by the machine frequency converter. It is most convenient to represent all the above characteristics as functions of the load parameter β.

The main stage in calculating characteristics by the method discussed is the determination of the rated voltage as a function of the load parameter, when the dependence of the voltage of the supply source on the frequency is known. In spite of the fact that the rated voltage is a complicated function of the slip, frequency and stator voltage, its determination by means of the equivalent impedance is comparatively simple and, for the arbitrary values of the frequency and load parameters α and β is performed in the same way, independently of the presence or absence of the frequency converter.

In a general case, when the power of the converter is comparable to the power of the connected motors, we have:

$$U_p = \frac{E_{f.c.}}{\alpha} \left| \frac{Z_e}{Z_e + Z_d} \right|, \tag{9}$$

where $E_{\text{f.c}}$ = the e.m.f. of the frequency converter, which is known for any arbitrary value of the frequency;

$Z_d = R_d + jX_d$ is the additional impedance including all resistances of the stator circuit of the motor:

$$R_d = \frac{1}{\alpha}(r_{f.c.} + r_l) + r_d; \tag{10}$$

$$X_d = x_{f.c.} + x_l, \tag{11}$$

where $r_{\text{f.c.}}$ and $X_{\text{f.c.}}$ are components of the frequency converter impedance;

r_1 and X_1 are corresponding components of the connecting loads:

If we can neglect the impedance of the variable frequency source and assume that the motor is connected to a grid of infinite power, then formula (9) assumes this form:

$$U_p = \frac{U_1}{\alpha} \left| \frac{Z_e}{Z_e + r_d} \right|, \tag{12}$$

where U_1 is the voltage at the stator terminals for the nominal frequency.
After determinating the rated voltage, it is easy to find the remaining characteristics.
The stator current of the motor:

$$I = \frac{U_p}{\sqrt{3} z_e} = \frac{E f.c.}{\sqrt{3} z_\Sigma}, \tag{13}$$

where

$$z_\Sigma = \sqrt{(R_e + R_d)^2 + (X_e + X_d)^2}$$

and

$$z_e = \sqrt{R_e^2 + X_e^2}.$$

The active power taken in by the motor from the frequency converter is:

$$P_{1d} = 3I^2 (R_e + r_d), \tag{14}$$

The total power of the frequency converter, neglecting steel losses and mechanical losses in the converter:

$$P_{1\Sigma} = 3I^2 (R_e + R_d). \tag{15}$$

The useful power on the motor shaft:

$$P_{2d} = \frac{M\omega}{9{,}81} = M \frac{\omega_c}{9{,}81} (\alpha - \beta) \tag{16}$$

Efficiences of the motor and converter:

$$\eta_d = \frac{P_{2d}}{P_{1d}} \quad \text{и} \quad \eta_{f.c.} = \frac{P_{1d}}{P_{1\Sigma}}. \tag{17}$$

The reactive power consumed and the efficiency of the motor-converter circuit are determined in the usual way.

The calculation ends by determining the electro-magnetic torque developed by the frequency converter:

(a) for a synchronous generator:

$$M = \frac{I^2 p}{1026} (R_e + R_d) \quad [\text{kgm}]; \tag{18}$$

(b) for an asynchronous frequency converter:

$$M = \frac{I^2 p}{1\,026}\left(R_e + R_d - \frac{r_1'}{c}\right) \text{ [kgm]}, \tag{19}$$

where p is the number of pole pairs of the machine;

r_1' is the active resistance of the primary winding of the asynchronous converter reduced to the secondary (load) winding; and

$c \approx 1 + \frac{X_1}{X_m}$ is the reduction factor of the asynchronous converter.

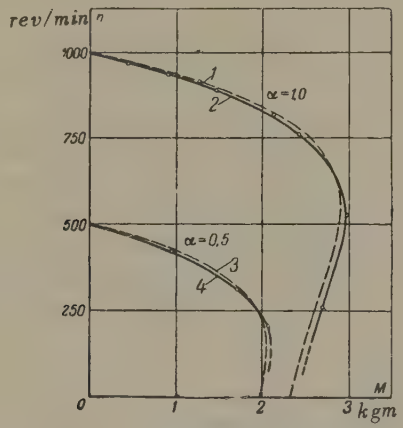

Rated (1, 3) and experimental (2, 4) mechanical characteristics of the MTK — 12-6 motor when fed by an asynchronous frequency converter of the AMK — 75 type, (Maker — AEG).

Using the method discussed the mechanical characteristics of the MTK-12-6 motor for 3.5 KW and 1000 rev/min were calculated when fed by an asynchronous frequency converter. The equivalent impedances were calculated by formulae (7) and (8). The parameters of the equivalent circuit were determined from no-load and short-circuit experiments. The natural mechanical characteristic was plotted on the basis of the catalogue data. The results of the calculations and experiments are shown in Fig. 3.

The determination of the law of the voltage variation of the frequency converter

Let us determine a law of the voltage variation of the frequency converter such that the constancy of the absolute slip of the motor rotor is ensured regardless of the variation of the supply frequency and load.

In the simplest case when the load torque is independent of the speed of rotation and is equal, for example, to the nominal torque, the above conditions of

the frequency control are ensured if $U_p = U_n = \text{const}$. In this case for all frequencies $\beta = S_n$.

Consequently by formulae (9) and (12) we get:

$$U_1 = \alpha U_n \left| 1 + \frac{r_d}{Z_{e.n.}} \right|; \tag{20}$$

$$E'_{n.\varkappa} = \alpha U_n \left| 1 + \frac{Z_d}{Z_{e.n}} \right|, \tag{21}$$

where $Z_{e.n} = \text{const.}$ is the motor equivalent impedance corresponding to the rated slip.

If the load torque varies with the frequency then, to ensure the conditions discussed of the frequency control, the following additional condition should be satisfied [4].

$$\frac{\Phi}{\Phi_n} = \sqrt{\frac{M}{M_n}}. \tag{22}$$

Since for $\beta = \text{const.}$, $U_p = \Phi$, from (22) we get:

$$U_p = U_n \sqrt{\frac{M}{M_n}}. \tag{23}$$

Thus, in a general case:

$$U_1 = \alpha U_n \sqrt{\frac{M}{M_n}} \left| 1 + \frac{r_d}{Z_{e.n}} \right|; \tag{24}$$

$$E_{f.c.} = \alpha U_n \sqrt{\frac{M}{M_n}} \left| 1 + \frac{Z_d}{Z_{e.n}} \right|. \tag{25}$$

In formulae (22) – (25), M is the torque developed by the motor for a speed of rotation corresponding to the value of the frequency in question.

Calculating the starting torque of the motor

Let us find the relationship between the starting torque of the motor and the frequency of the feed current: For the stalled rotor, $\alpha = \beta$. Consequently, the starting torque of the motor can be calculated on the basis of the natural mechanical characteristic of the motor taking into account the voltage drop in the additional resistances of the stator circuit.

Thus, for example, if the motor mechanical characteristic can be expressed by equation (4) then the equation for calculating the starting torque assumes this form:

$$M_n = M_\varkappa \left(\frac{U_p}{U_n} \right)^2 \frac{2 + a s_\varkappa}{\frac{\alpha}{s_\varkappa} + \frac{s_\varkappa}{\alpha} + a s_\varkappa}. \tag{26}$$

The rated voltage is determined, as in the general case, by formulae (9) and (12), and the equivalent and additional impedances by formulae (7), (8), (10) and (11), In this case we have to replace β in formulae (7) and (8) by α.

If the natural mechanical characteristic is given in the form of a graph, as, for example, for motors with an increased starting torque, then the equivalent impedance should be determined taking into account the saturation of the magnetic system and the current displacement in the rotor.

Translated by S. Szymanski.

REFERENCES

1. A.A. Bulgakov; *Chastotnoye upravleniye asinkhronnymi elektrodvigatelyami (Frequency control of asynchronous motors).* Izd. Akad. Nauk SSSR (1955).
2. A.A. Bulgakov; *Asinkhronnyi dvigatel' pri peremennoi chastote (Asynchronous motor at a variable frequency), Trudy VEI,* 46, Gosenergoizdat, (1941).
3. V.T. Kas'yanov; *Elektrichestvo,* No. 2 (1949).
4. M.P. Kostenko; *Elektricheskie mashiny. "Spetsialnaya chast'" (Electric machines. "Special part")* Gosenergoizdat (1949).

PROPERTIES AND DESIGN OF A MULTI-MOTOR DRIVE SYSTEM WITH A MECHANICAL DIFFERENTIAL*

B.M. SHKOLNIKOV and I.I. SUD

Giproneftemash Gosplana RSFSR

(Received 27 December 1957)

For many operating machines a reversible drive is needed which allows a smooth and continuous variation of the mechanism speed of rotation within a practically unlimited range. Usually the upper speed of the direct and reverse sense of rotation is given, and within the range from this maximum speed to the minimum speed, which is very near to zero, a continuous sequence of steady rotation speeds should be possible.

This kind of drive is particularly useful in mechanisms for boring oil holes [1].

In installations of this type an intermediate gear with a variable gear ratio is inserted between the driven mechanism and the driving motor. An asynchronous squirrel-cage motor can be used as a driving motor in such installations. The gear ratio can be changed either by steps, remaining constant at each step, or smoothly.

Due to operational requirements, for mechanisms driving the cutting tool a gear with a continuously varying gear ratio (from the output shaft to the driving motor) is needed, this ratio varying from zero to a certain maximum value for various directions of the output shaft.

In practice this problem can be solved by using a gear, which consists of a differential speed reducer, of which one driving shaft is driven by a controlled d.c. motor, and the other by an asynchronous squirrel-cage motor. Such a system of drive is used in the drilling automatic regulator type BAR 1-150 and is a particular case of a system, consisting of two controlled electric machines, which drive a common load; static and dynamic conditions of this system are discussed in detail in the works of Golovan and Gudkov [2-4].

The purpose of this article is to discuss the method of calculating and choosing the gear ratios of speed reducers and electrical machines for the drive shown in Fig. 1 , in addition, a comparison of this electric drive with other known

* *Elektrichestvo* No.6, 69-74, 1958.

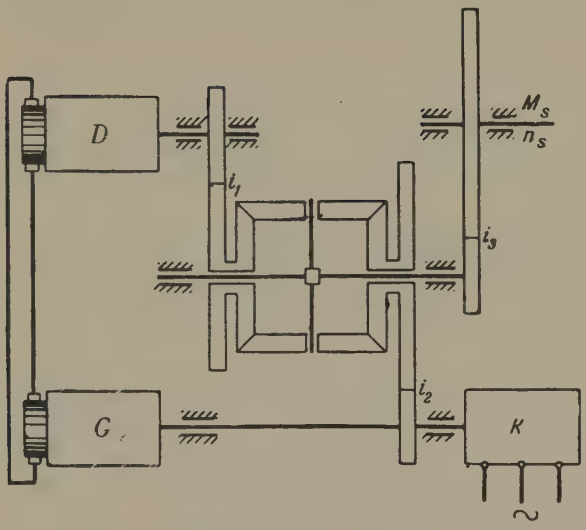

FIG.1. Kinematic diagram of an electrical differential drive.

systems is given on the basis of operating experience.

In the above diagram an asynchronous motor with a squirrel-cage rotor K and a d.c. machine D drive two driving shafts of a speed reducer. At the same time, motor K drives another d.c. machine G. Machines G and D are connected as a generator-motor system. They are both separately excited. Machine K is fed from the a.c. gird.

Similar drive systems are used abroad. For example the firm "Speed Control" (U.S.A.) produces for the textile and metal machining industries many commercial types of similar mechanisms [5].

Choice of gear ratios

Let us introduce the following notations M_S, M_K, M_D - load torques on the speed reducer shaft and on shafts of machines K and D respectively; n'_S, n''_S - maximum and minimum speeds of the output shaft of the speed reducer for direct and reverse sence of rotation; i_1 - gear ratio from planet gears to machine B; i_2 - gear ratio from planet gears to machine K; i_3 - gear ratio from the output shaft to the differential shaft; n'_D and n''_D - maximum and minimum speed of rotation of machine D; Taking into account possible signs of speeds, equation $n_S = f(n_D, n_K)$ assumes this form:

$$n_S = \pm \frac{n_D}{2i_1 i_3} \mp \frac{n_K}{2i_2 i_3} . \qquad \text{A}$$

However this form of the equation makes a general solution more difficult, therefore, in the following discussion we shall write this equation in the following form:

$$n_S = \frac{n_D}{2i_1 i_3} - \frac{n_K}{2i_2 i_3}, \tag{1}$$

which is valid for the opposite sense of rotation of machines K and D under the condition that $n_D > o$. Particular cases may be accounted for by a proper choice of signs n_S, n_D and n_K.

Assuming n_K = const., we get the expression for $n_S = f(n_D,)$ which represents the equation of a straight line, passing through the given points of the co-ordinates (n_D'', n_S'') and (n_D', n_S'):

$$n_s = \frac{n_s'' - n_s'}{n_D'' - n_D'} n_D - \frac{n_s'' - n_s'}{n_D'' - n_D'} n_D' - n_s' \tag{2}$$

From (1) and (2) it follows:

$$i_1 i_3 = \frac{n_D'' - n_D'}{2(n_s'' - n_s')} \tag{3}$$

and

$$\frac{n_K}{2i_2 i_3} = \frac{n_s'' - n_s'}{n_D'' - n_D'} n_D' + n_s'. \tag{4}$$

If we neglect the efficiencies of mechanical gears, then the torques on the shafts of machines K and D can be determined from the following expressions:

$$M_K = \frac{M_S}{2i_2 i_3}; \quad M_D = \frac{M_S}{2i_1 i_3}. \tag{5}$$

In this way, for a given M_S, we can by the gradient of this line evaluate approximately the value of M_D, which determines the weight, size and cost of the machine D.

In a similar way the segment cut by this straight line on the axis n_S characterizes the power of the machine K.

In Fig. 2 relationships $n_S = f(n_D)$ are shown for the case, when the maximum speed of the output shaft is achieved for the upper (straight line 1) and for the lower (straight line 2) limits of the speed control of the machine D. The size of the machines D in both cases will be the same. In the second case, the power of the machine K (oa_2) will be greater than in the first case. We can decrease the size of the machine by decreasing the speed limits of the machine under control (straight line 3).

The choice of this or another alternative is made on the basis of the graph of

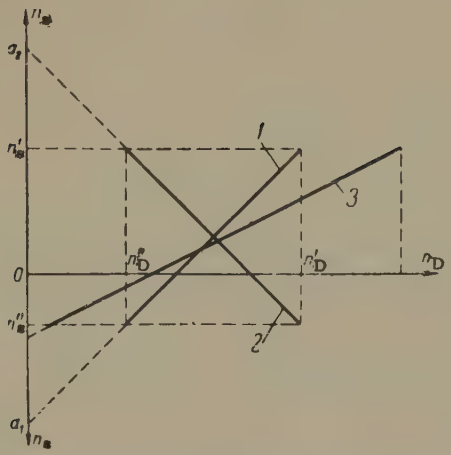

FIG.2. Speed characteristics of an electrical differential drive.

the speed variation with time of the reducer output shaft and the character of the load torque. The sense of rotation of the machine D should coincide with the operational sense of rotation of the reducer output shaft.

In the automatic drilling regulator BAR 1-150 the direct sense of rotation of the output shaft is in the direction of the lowering of the drilling column, consequently the machine D rotates in the same direction. Accordingly the motor K rotates in the direction of the raising of the column.

From the given conditions we can determine $i_1 i_3$ and $n_K / i_2 i_3$ [equations (3) and (4)]; thus, the choice of two out of the four of these quantities is arbitrary. Usually we choose n_K and i_3.

The choice of i_3 depends on considerations of design. In choosing a nominal speed of rotation of machine, that is not regulated, we have to take into account the necessity of ensuring the operation of the machine G under rated conditions and also the fact that the decrease in size of the machine K leads to the increase of the gear ratio i_2.

Reduction factor for the moments of inertia and the load torques

The usual formula for expressing the moments of inertia about one axis of rotation (2) with respect to the other axis (1) has the form:

$$J_{r\,1} = J_2 \left(\frac{\omega_2}{\omega_1}\right)^2 = J_2 \frac{1}{k_r^2}. \qquad (6)$$

For the differential mechanism:

$$k_r = \frac{\omega_1}{\omega_2} = \frac{n_1}{n_2} \neq \text{const.} \tag{7}$$

In fact, from (1) we get:

$$\frac{n_1}{n_2} = \frac{n_D}{n_S} = 2i_1 i_3 + \frac{n_K}{n_S}\frac{i_1}{i_2}. \tag{8}$$

The ratio n_K/n_S varies within very wide limits and, in particular for $n_S = o$ it tends towards infinity. However, in spite of the fact that $k_1 \neq$ const., no change in the moments of inertia takes place in this case. For a differential mechanism, expression (6) is not valid.

Since a differential reducer represents a system with two degrees of freedom, the Lagrange equations of the second order, which relate to this mechanism, will have the following form:

$$\left.\begin{aligned} \frac{d}{dt}\frac{\partial A}{\partial \dot{\omega}_D^*} - \frac{\partial A}{\partial \dot{\varphi}_D^*} &= Q_D^*; \\ \frac{d}{dt}\frac{\partial A}{\partial \dot{\omega}_K^*} - \frac{\partial A}{\partial \dot{\varphi}_K^*} &= Q_K^*, \end{aligned}\right\} \tag{9}$$

where A is the kinetic energy stores in the system; Q_D^* and Q_K^* are generalized forces reduced to the differential driving pinions; ϕ_D^* and ϕ_K^* are angles of rotation of the shafts of machines D and K, reduced to the differential driving pinions; ω_D^* and ω_K^* are angular speeds of machines D and K reduced to the differential driving pinions.

If we neglect the rotation of the planet gears about their own axes, the amount of kinetic energy stored in the system is equal to:

$$A = \frac{1}{2} J_S^* (\omega_S^*)^2 + \frac{1}{2} J_D^* (\omega_D^*)^2 + \frac{1}{2} J_K^* (\omega_K^*)^2, \tag{10}$$

where J_S^*, J_D^*, J_K^* are total moments of inertia reduced to the appropriate differential shafts.

It is easy to show that the generalized forces are equal respectively to:

$$\left.\begin{aligned} Q_D^* &= \frac{1}{2} M_S^* - M_D^*; \\ Q_K^* &= -\frac{1}{2} M_S^* - M_K^*, \end{aligned}\right\} \tag{11}$$

where M_S^*, M_D^*, M_K^* are torques reduced respectively to the corresponding differential shafts.

Substituting (10) and (11) into (9), we get:

$$\left.\begin{aligned} J_D^* \frac{d\omega_D^*}{dt} - \frac{1}{4} J_s^* \frac{d\omega_K^*}{dt} = \\ = \frac{1}{2} M_s^* - M_D^* = M_{dynD}^* \\ J_K^* \frac{d\omega_K^*}{dt} - \frac{1}{4} J_s^* \frac{d\omega_K^*}{dt} = \\ = M_K^* - \frac{1}{2} M_s^* = M_{dyn\,K}^* \end{aligned}\right\} \qquad (12)$$

where $\overline{J}_D^* = \frac{1}{4} J_s^* + J_D^*$;

$\overline{J}_K^* = \frac{1}{4} J_s^* + J_K^*$.

Since the angular speed ω_K^* varies little, (2-3 per cent), then $\frac{d\omega_K^*}{dt} = O$. Thus, the first of equations (12) can be written in this form †:

$$\overline{J}_D^* \frac{d\omega_D^*}{dt} = \left(\frac{1}{4} J_s^* + J_D^*\right) \frac{d\omega_D^*}{dt} = M_{dynD}^* \qquad (13)$$

Thus, the moments of inertia reduced to the differential shaft are reduced to its driving pinions by dividing by the constant factor $k_r^2 = 4$. In the steady state conditions $\frac{d\omega_D^*}{dt} = O$. Therefore, $|M_D^*| = |M_K^*| = \frac{1}{2} M_s^*$, i.e. the load torques are reduced by the same reduction factor $k_r = 2$.

Choice of machine

When choosing a machine we make use of the functional block diagram of the drive shown in Fig. 3 where single lines represent mechanical connexions and double lines - electrical connexions.

Depending on the character of the load torque and the sense of rotation, machines K and D can work either as motors or as generators. When the load torque has the properties of reactance, then, with the change of the sense of rotation of the reducer output shaft, the operational character of a d.c. machine changes. Machine K, which is non-regulated always works as a motor. In the case of the potential load torque when the sense of rotation of the reducer output shaft changes, the operational conditions of a machine, that worked as a generator,

† Equation (13) was deduced independently of the authors by A.I. Driakhlov.

do not change. Machine K, which worked as a motor begins working as a generator, if a power regeneration system is provided; when working without regeneration it continues to work as a motor.

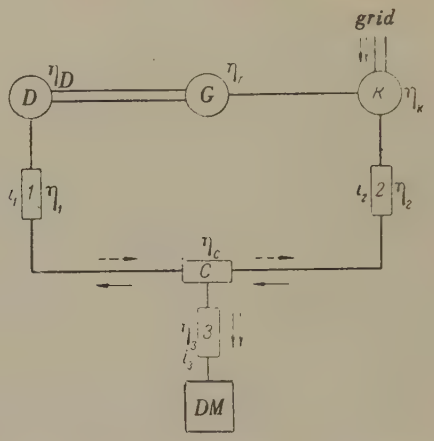

FIG.3. Functional block diagram of an electrical differential drive. K, D and G. - electrical machines. 1 transmission from planet gears to machine D; 2 - transmission from planet gears to machine K; 3 - transmission from the output shaft to the differential shaft; C - planet gear assembly; DM - driven mechanism; η_1, η_2, η_3, η_C, η_G, η_D, η_K. - values of the efficiencies of the links on rated load.

In designing the drive mechanism we assume its normal operational conditions. In particular, in the BAR 1-150 the sense of rotation of machine D, which rotates in the sense of the lowering of the tool, coincides with the sense of the load torque, and consequently, whether the load goes up or down, this machine works as a generator. Machine K, which rotates in the sense of raising the load, can work both as a motor (forced lowering) or as a generator (regeneration) when the load goes down.

In Fig. 3, the sense of the power transfer is shown by continuous arrows for the case, when machine K works as a motor and machine D as a generator; dotted arrows indicate that both machines K and D work as motors. Formulae for calculating the torques of the machines are given in table 1.

For choosing a machine we assume in these formulae values of efficiencies, and of n_D and n_K for nominal conditions. Obviously, the second alternative of the operational conditions of machines offers a less advantageous solution from the point of view of weight and size and consequently, the price of a d.c. machine. Other possible operational conditions of drives are calculated in a similar way according to the direction of the power transfer.

Mechanical characteristic of a drive

We assume that a mechanical characteristic of machine D is linear within the

TABLE 1.

Conditions of the machine operation	Formulae for calculating torques of the machines		
	machine K	machine D	machine G
Machine K as a motor Machine D as a generator	$\frac{M_S}{2i_1i_2i_3\eta_2\eta_3\eta_C}\left(i_1 - i_2\eta_1\eta_2\eta_G\eta_D\eta_C^2\frac{n_D}{n_K}\right)$	$\frac{M_S\eta_1\eta_C}{2i_1i_3\eta_3}$	$\frac{M_S\eta_1\eta_C\eta_G\eta_D}{2i_1i_3\eta_3}\frac{n_D}{n_K}$
Machine K — as a motor Machine D — as a motor	$\frac{M_S}{2i_1i_2i_3\eta_1\eta_2\eta_3\eta_C\eta_D\eta_G}\left(i_2\frac{n_D}{n_K} - i_1\eta_1\eta_2\eta_C^2\eta_G\eta_D\right)$	$\frac{M_S}{2i_1i_3\eta_1\eta_3\eta_C}$	$\frac{M_S}{2i_1i_3\eta_1\eta_3\eta_C\eta_G\eta_D}\frac{n_D}{n_K}$

operational limits and that the speed of rotation of machine K is constant, i.e.

$$n_D = a_1 + b_1M_D \text{ and } n_k = a_2 = \text{const.} \tag{14}$$

In this case the equation of the mechanical characteristic of drive assumes this form:

$$n_S = A + BM_S. \tag{15}$$

The values of coefficients A and B for various operational conditions are given in table 2. Neglecting the variation of the efficiencies of the individual links of the system, we may assume that the drive mechanical characteristic is linear.

Speed control

Speed control of the reducer output shaft is realized, as in a usual generator-motor circuit, by varying the excitation of machines G or D. However, taking into account the presence of a.c. in the system of the non-regulated machine, in both cases the speed control can be exerted only at a constant torque. Equation 1 can be represented in this form:

$$n_Si_3 = 0.5\left(\frac{n_D}{i_1} - \frac{n_K}{i_2}\right)$$

or

$$n_S^* = 0.5\,(n_D^* - n_K^*),$$

where n_s^*, n_D^*, n_K^* - are respectively the speeds of rotation reduced to the shaft and driving gears of the differential.

If $n_D^* > n_K^*$ then $n_s^* > 0$; if $n_D^* < n_K^*$ then $n_s^* < 0$; and $n_s^* = 0$ if $n_D^* = n_K^*$. Varying the magnitude of n_D^* we can get a speed of rotation of the drive output shaft, which is variable in magnitude and direction. The direct and reverse sense of rotation of the output shaft is realized without reversing the sense of rotation of the driving motor.

Efficiency

In a general case

$$\eta_g = \frac{\text{useful power}}{\text{power taken from the grid}} = \frac{M_s \cdot n_s}{M_K \cdot n_K} \eta_K$$

where η_K - efficiency of motor K.

Substituting the values of M_K and n_D we get

$$\eta_g = \frac{an_s}{\beta n_K - \gamma - \delta M_s} \tag{16}$$

(the values of a, β, γ and δ for the conditions under consideration are given in table 2).

The efficiency of the transmission gear is proportional to n_s; the control is uneconomical and involves losses. From this point of view the control in the drive is analogous to the control of electrical machines, when the speed on no-load running remains constant.

The power N_{grid}, taken by motor K from the grid, when the load torque is applied to the gear output shaft and for a speed of rotation of the shaft equal to zero is:

$$N_{grid} = \frac{M_K n_K}{\eta_K}.$$

The values of M_K are taken from table 1, putting $\frac{n_D}{i_1} = \frac{n_K}{i_2}$

Thus, the advantages of the drive system described above are:

(1) the possibility of obtaining a speed of rotation of the driven shaft as small as we like, without decreasing the speed of rotation of the driving shaft to a value, that is undesirable from the point of view of the cooling of the motor.

(2) the possibility of reversing the sense of rotation of the driven shaft, when

TABLE 2

Machine operational conditions	Coefficients in formulae (15) and (16) for different operational conditions of the electrical machines of the drive					
	A	B	α	β	γ	δ
Machine D - as a generator Machine K - as a motor	$\frac{a_1 i_2 - a_2 i_1}{2 i_1 i_2 i_3}$	$\frac{b_1 \eta_1 \eta_C}{4 i_1^2 i_3^2 \eta_3}$	$2 i_1 i_2 i_3 \eta_2 \eta_3 \eta_C \eta_K$	i_1	$i_2 a_1 \eta_1 \eta_2 \eta_C^2 \eta_D \eta_G$	$\frac{b_1 i_2}{2 i_1 i_3 \eta_2 \eta_C \eta_G \eta_D}$
Machines D and K as motors	$\frac{a_1 i_2 - a_2 i_1}{2 i_1 i_2 i_3}$	$\frac{b_1}{4 i_1^2 i_3^2 \eta_1 \eta_3 \eta_C}$	$2 i_1 i_2 i_3 \eta_1 \eta_3 \eta_C \eta_D \eta_G \eta_K$	$- i_1 \eta_1 \eta_2 \eta_C^2 \eta_D \eta_K$	$- i_2 a_1$	$\frac{b_1 i_2}{2 i_1 i_3 \eta_1 \eta_3 \eta_C}$

the sense of rotation of electrical machines remains unaltered;

(3) the possibility of obtaining wide limits of speed variation of the driven shaft for relatively narrow limits of speed control of electrical machines.

The disadvantages of drives of this kind are: low efficiency when operating under the conditions of the control characteristics, and the comparatively complicated construction of the reducer.

Conclusions

(1) The method proposed makes it possible to choose correctly, by means of simple calculations, the proper gear ratios and electrical machines of the generator-motor system with a differential reducer.

(2) The properties discussed enable the field of rational application of this system to be determined.

Translated by S. Szymanski

REFERENCES

1. B.M. Shkolnikov and I.I. Sud; Burovoi avtomaticheskii reguliator tipa BAR 150 (Automatic boring regulator type BAR - 150) *Energeticheskii biulleten* No. 7 (1954).
2. A.T. Golovan; Rabota dvukh elektricheskikh mashint cherez mekhanicheskii differentsial, (Operation of two electric machines by a mechanical differential) *VEP*, Nos. 7-8 (1942).
3. A.T. Golovan; *Elektroprivod (Electrical drive)* Gosenergoizdat (1948).
4. V.S. Gudkov; *Elektrichestvo* No. 10 (1956).
5. Electrical differential speed drive *Machinery*, 56, No. 2 (1949).

ELEKTRICHESTVO

ELECTRIC TECHNOLOGY, U.S.S.R.

1959 VOLUME 2 APRIL

CONTENTS

Made and printed in Great Britain by The Campfield Press, St. Albans